



UNIVERSITÉ DE LILLE
École doctorale Biologie Santé de Lille
Année : 2021

THÈSE DE SCIENCE

**BH3 profiling allows to functionally characterize T-cell
prolymphocytic leukemia and to identify innovative
therapeutic options**

Présentée et soutenue publiquement le 01/12/2021 à 15h00
Au Pôle Formation
Par **Charles Herbaux**

JURY

Rapporteur et Présidente :

Madame le Professeur Martine AMIOT

Rapporteur :

Monsieur le Docteur Bertrand NADEL

Directeur de Thèse :

Madame le Professeur Stéphanie POULAIN

Co-Directeur de Thèse :

Monsieur le Docteur Matthew S. DAVIDS

1. Table of content

1.	TABLE OF CONTENT	2
2.	RESUME DE LA THESE EN FRANÇAIS	4
3.	RESUME DE LA THESE EN ANGLAIS	6
4.	RESUME DE THESE VULGARISE POUR LE GRAND PUBLIC EN FRANÇAIS	8
5.	RESUME DE THESE VULGARISE POUR LE GRAND PUBLIC EN ANGLAIS	9
6.	INTRODUCTION	10
6.1.	T-CELL PROLYMPHOCYTIC LEUKEMIA	10
6.1.1.	Overview	10
6.1.2.	Pathophysiology	11
6.1.3.	Generalities on T-PLL diagnosis	14
6.1.4.	Blood and bone marrow	17
6.1.5.	Immunophenotype	18
6.1.6.	Genetics	18
6.1.7.	Serum markers	20
6.1.8.	Inactive phase and progression	21
6.1.9.	Current treatment of T-PLL	21
6.1.10.	Innovative therapeutic approach for T-PLL	22
6.2.	APOPTOSIS AND BCL2 FAMILY PROTEINS	23
6.2.1.	Overview	23
6.2.2.	BCL-2 family biology	25
6.2.3.	Activation of the apoptotic pathway	26
6.2.4.	Targeting the intrinsic apoptotic pathway in the clinic	28
6.3.	ASSAYS TO EVALUATE BCL-2 FAMILY PROTEINS FUNCTION	30
6.3.1.	BH3 profiling	30
6.3.2.	Dynamic BH3 profiling	31
6.3.3.	BH3-mimetic toolkit	32
6.3.4.	Choice	33
6.4.	AIM OF THE PRESENT WORK	33
7.	MATERIAL AND METHODS	36
7.1.	STUDY DESIGN AND PATIENT SAMPLES	36
7.2.	INITIAL DRUG SCREENING	36
7.3.	OTHER PRIMARY CELLS, CO-CULTURE AND TREATMENT EX VIVO	37
7.4.	DNA SEQUENCING	38
7.5.	BH3 PROFILING	39
7.6.	IMMUNOBLOTTING	41
7.7.	REAGENTS AND ANTIBODIES	41
7.8.	STATISTICAL ANALYSIS	42
8.	RESULTS	43
8.1.	COMBINATORIAL DRUG SCREENING SHOWS POSSIBLE SYNERGY WITH VENETOCLAX	43
8.2.	CO-TREATMENT OF TWO PATIENTS WITH VENETOCLAX AND IBRUTINIB	46
8.3.	IBRUTINIB IS REDUCING ITK ACTIVITY AND ENHANCING BCL2 DEPENDENCY IN VIVO	48
8.4.	T-PLL CELLS ARE RELATIVELY UNPRIMED FOR APOPTOSIS AND HAVE HETEROGENEOUS DEPENDENCE ON BCL-2 AND MCL-1	50
8.5.	STROMAL SUPPORT PROMOTES SURVIVAL AND REDUCES OVERALL MITOCHONDRIAL PRIMING IN VITRO	59
8.6.	PHARMACOLOGICAL INHIBITION OF BCL-2 AND MCL-1 INDUCES CELL DEATH	60
8.7.	BELINOSTAT AND RUXOLITINIB SELECTIVELY INCREASE BCL-2 DEPENDENCE	63

8.8.	PRIMARY CELLS FROM JAK/STAT PATHWAY MUTATED T-PLL ARE MORE SENSITIVE TO INHIBITION OF JAK1 THAN OF ITK	69
8.9.	VENETOCLAX PLUS RUXOLITINIB WAS EFFECTIVE FOR TWO DIFFERENT REFRACTORY T-PLL PATIENTS	73
8.10.	VENETOCLAX PLUS ROMIDEPSIN WAS EFFECTIVE FOR ONE REFRACTORY T-PLL PATIENT	78
9.	DISCUSSION.....	80
10.	PERSPECTIVE.....	86
11.	ACKNOWLEDGEMENTS.....	89
12.	PUBLICATIONS AND CO-AUTHORS	90
13.	REFERENCES.....	91

2. Résumé de la thèse en français

Les thérapies conventionnelles pour les patients atteints de leucémie prolymphocytaire à cellules T (T-PLL), telles que la chimiothérapie cytotoxique et l'alemtuzumab, ont une efficacité limitée et une toxicité importante. Plusieurs nouvelles classes thérapeutiques ont démontré une activité préclinique dans la T-PLL, notamment des inhibiteurs de la voie JAK/STAT et les inhibiteurs du récepteur des cellules T, ainsi que des inhibiteurs d'histone désacétylase (HDAC). Récemment, le venetoclax, un inhibiteur de BCL-2, a également montré une certaine activité clinique dans le traitement de la T-PLL.

Une première étape a consisté à effectuer un screening classique des médicaments avec une mesure du métabolisme des cellules par CTG (CellTiter-Glo). Le venetoclax a été utilisé en combinaison par paires avec 25 médicaments sélectionnés. Ce test a révélé que l'ibrutinib était le partenaire le plus efficace dans les échantillons primaires de T-PLL. Deux patients ont été traités avec cette combinaison, avec seulement une réponse transitoire au traitement.

Nous avons ensuite cherché à caractériser les dépendances apoptotiques fonctionnelles dans la T-PLL afin d'identifier de nouvelles combinaisons thérapeutiques dans cette maladie. Vingt-quatre échantillons primaires de patients atteints de T-PLL ont été étudiés en utilisant le profilage BH3, un test fonctionnel permettant d'évaluer la propension d'une cellule à subir le mécanisme d'apoptose (niveau de priming apoptotique). Cette

technique permet aussi d'évaluer la dépendance relative d'une cellule à l'égard des différentes protéines antiapoptotiques.

Les cellules primaires de T-PLL présentaient un niveau relativement faible de priming apoptotique et dépendaient principalement des protéines BCL-2 et MCL-1 pour leur survie. L'inhibition pharmacologique sélective de BCL-2 ou de MCL-1 a provoqué la mort des cellules primaires de T-PLL. Le ciblage de la voie JAK/STAT avec le ruxolitinib, un inhibiteur de JAK1/2, ou des HDAC avec le bélinostat a augmenté la dépendance à l'égard de BCL-2 mais pas de MCL-1, sensibilisant ainsi les cellules de T-PLL au venetoclax. Sur la base de ces résultats, 2 patients atteints de T-PLL réfractaires ont été traités avec une combinaison de venetoclax et de ruxolitinib. Nous avons observé une réponse profonde pour le patient avec une T-PLL mutée sur JAK3 et une stabilisation de la maladie chez la patiente avec une T-PLL non mutée sur les protéines de la voie JAK/STAT.

Notre approche fonctionnelle, basée sur la médecine de précision, a permis d'identifier les inhibiteurs d'HDAC et de la voie JAK/STAT comme des partenaires prometteurs du venetoclax, ce qui justifie une exploration clinique plus aboutie de ces combinaisons dans la T-PLL.

3. Résumé de la thèse en anglais

Conventional therapies for patients with T-cell prolymphocytic leukemia (T-PLL), such as cytotoxic chemotherapy and alemtuzumab, have limited efficacy and considerable toxicity. Several novel agent classes have demonstrated preclinical activity in T-PLL, including inhibitors of the JAK/STAT and T-cell receptor pathways, as well as histone deacetylase (HDAC) inhibitors. Recently, the BCL-2 inhibitor venetoclax also showed some clinical activity in T-PLL.

A first step was to perform a conventional drug screening with a measure of the metabolism of the cells with CTG (CellTiter-Glo). Venetoclax was used in pairwise combination with 25 selected drugs. This assay revealed ibrutinib as the most potent partner in primary T-PLL samples. Two patients were treated with this combination, with only a transient response to therapy.

Then we sought to characterize functional apoptotic dependencies in T-PLL to identify a novel combination therapy in this disease. Twenty-four samples from patients with primary T-PLL were studied by using BH3 profiling, a functional assay to assess the propensity of a cell to undergo apoptosis (priming) and the relative dependence of a cell on different antiapoptotic proteins.

Primary T-PLL cells had a relatively low level of priming for apoptosis and predominantly depended on BCL-2 and MCL-1 proteins for survival. Selective pharmacologic inhibition of BCL-2 or MCL-1 induced cell death in primary T-PLL cells. Targeting the JAK/STAT

pathway with the JAK1/2 inhibitor ruxolitinib or HDAC with belinostat both independently increased dependence on BCL-2 but not MCL-1, thereby sensitizing T-PLL cells to venetoclax. Based on these results, we treated 2 patients with refractory T-PLL with a combination of venetoclax and ruxolitinib. We observed a deep response in JAK3-mutated T-PLL and a stabilization of the nonmutated disease.

Our functional, precision-medicine–based approach identified inhibitors of HDAC and the JAK/STAT pathway as promising combination partners for venetoclax, warranting a clinical exploration of such combinations in T-PLL.

4. Résumé de thèse vulgarisé pour le grand public en français

Les thérapies conventionnelles pour les patients atteints de leucémie prolymphocytaire à cellules T (T-PLL), telles que la chimiothérapie cytotoxique et l'anticorps monoclonal alemtuzumab, ont une efficacité limitée et une toxicité importante. Plusieurs nouvelles classes thérapeutiques ont démontré une activité préclinique dans la T-PLL, mais aucune n'est suffisamment efficace en monothérapie.

Notre étude a consisté à mieux comprendre les mécanismes de mort cellulaire programmée dans cette maladie, pour trouver une ou plusieurs combinaisons thérapeutiques efficaces dans cette maladie.

Nous avons ainsi trouvé que la survie des cellules de T-PLL dépendait principalement de deux protéines mitochondriales : BCL2 et MCL1. Nous avons aussi observé que l'inhibition de deux voies de signalisation en particulier (JAK/STAT et HDAC) augmentait encore la dépendance des cellules malades à BCL2.

Sur la base de ces résultats, 2 patients atteints de T-PLL réfractaires aux médicaments classiques ont été traités avec une combinaison de venetoclax (inhibiteur de BCL2) et de ruxolitinib (inhibiteur de JAK/STAT), avec une efficacité significative.

5. Résumé de thèse vulgarisé pour le grand public en anglais

Conventional therapies for patients with T-cell prolymphocytic leukemia (T-PLL), such as cytotoxic chemotherapy and the monoclonal antibody alemtuzumab, have limited efficacy and significant toxicity. Several new therapeutic classes have demonstrated preclinical activity in T-PLL, but none are sufficiently effective as a single agent.

Our study consisted in better understanding the mechanisms of programmed cell death in this disease, in order to find one or more effective therapeutic combinations in this disease.

We found that the survival of T-PLL cells was mainly dependent on two mitochondrial proteins: BCL2 and MCL1. We also observed that inhibition of two signaling pathways in particular (JAK/STAT and HDAC) further increased the dependence of diseased cells on BCL2.

Based on these results, 2 patients with T-PLL refractory to conventional drugs were treated with a combination of venetoclax (BCL2 inhibitor) and ruxolitinib (JAK/STAT inhibitor), with significant efficacy.

6. Introduction

6.1. T-cell prolymphocytic leukemia

6.1.1. Overview

T-Prolymphocytic Leukemia (T-PLL) had been recognized in 1973 as distinct from chronic lymphocytic leukemia (CLL) by its particular clinical presentation, the morphological characteristic of tumor lymphoid cells, and the extremely poor clinical outcome. (Catovsky *et al.*, 1973) T-PLL is a rare and usually aggressive T-lymphoid malignancy with a cytogenetic distinctive characteristic of $inv(14)(q11q32)$ or $t(14;14)(q11;q32)$ involving the T-cell receptor (TCR) alpha/delta gene locus at 14q11 and the *TCL1A* gene cluster at 14q32.1. (Staber *et al.*, 2019) Recently, gain-of-function (activating) mutations in JAK/STAT pathway genes, including theoretical loss of negative regulators of STAT5B, have been identified in approximately 90% of T-PLL cases, suggesting that this pathway is another distinctive characteristic of T-PLL's pathophysiology. (Wahnschaffe *et al.*, 2019) Cytotoxic chemotherapy rarely provides deep and durable remission for T-PLL patients. (Herbaux *et al.*, 2015) Alemtuzumab, the monoclonal anti-CD52 antibody, is the standard of care in first therapeutical line, and provides responses observed in about 90% of patients. (Dearden *et al.*, 2001, 2011) However, severe leukopenia and severe infectious complications are common with alemtuzumab, and responses are usually short, with a median disease-free interval of 7 months. As such, for T-PLL patients able to achieve response, allogeneic hematopoietic stem cell transplantation is the only possible hope for long term survival. (Wiktor-Jedrzejczak *et al.*, 2019; Yamasaki *et al.*, 2019) Despite

these therapeutic options, the median overall survival is only about 20 months.(Cross *et al.*, 2019) Modern oncology has discovered an increasing number of new effective anticancer drugs; however, so far, they have limited benefit for patients suffering of T-PLL. With an overall incidence of 0.6 to 1.2 / million in the general population, T-PLL is a very rare disease.(Matutes *et al.*, 1991; Herling *et al.*, 2004) Because of the very rapid progressing clinical course and sometimes uncertain diagnosis, it has been a difficult disease to study systematically. Case reports, single-center retrospective studies, and small trials are of course difficult to compare because of imprecise defined and inconsistent diagnostic criteria as well as response evaluation.(Gandhi *et al.*, 2008; Dearden *et al.*, 2011; Hopfinger *et al.*, 2013; Herbaux *et al.*, 2015; Boidol, Kornauth, van der Kouwe, *et al.*, 2017; Pflug *et al.*, 2019) To date, T-PLL has been evaluated according to criteria for chronic lymphocytic leukemia (CLL), as described by the international workshop on CLL (IWCLL).(Cheson *et al.*, 1988, 1996; Hallek *et al.*, 2008, 2018) As we are describing below, T-PLL is biologically and clinically very different from CLL, and the IWCLL criteria seem rarely appropriate. Furthermore, modifications of the IWCLL criteria adopted by investigators have not been uniform. Thus, the T-PLL International Study Group (TPLL-ISG) recently published consensus criteria for diagnosis, staging, and treatment response assessment of T-PLL.(Staber *et al.*, 2019)

6.1.2. Pathophysiology

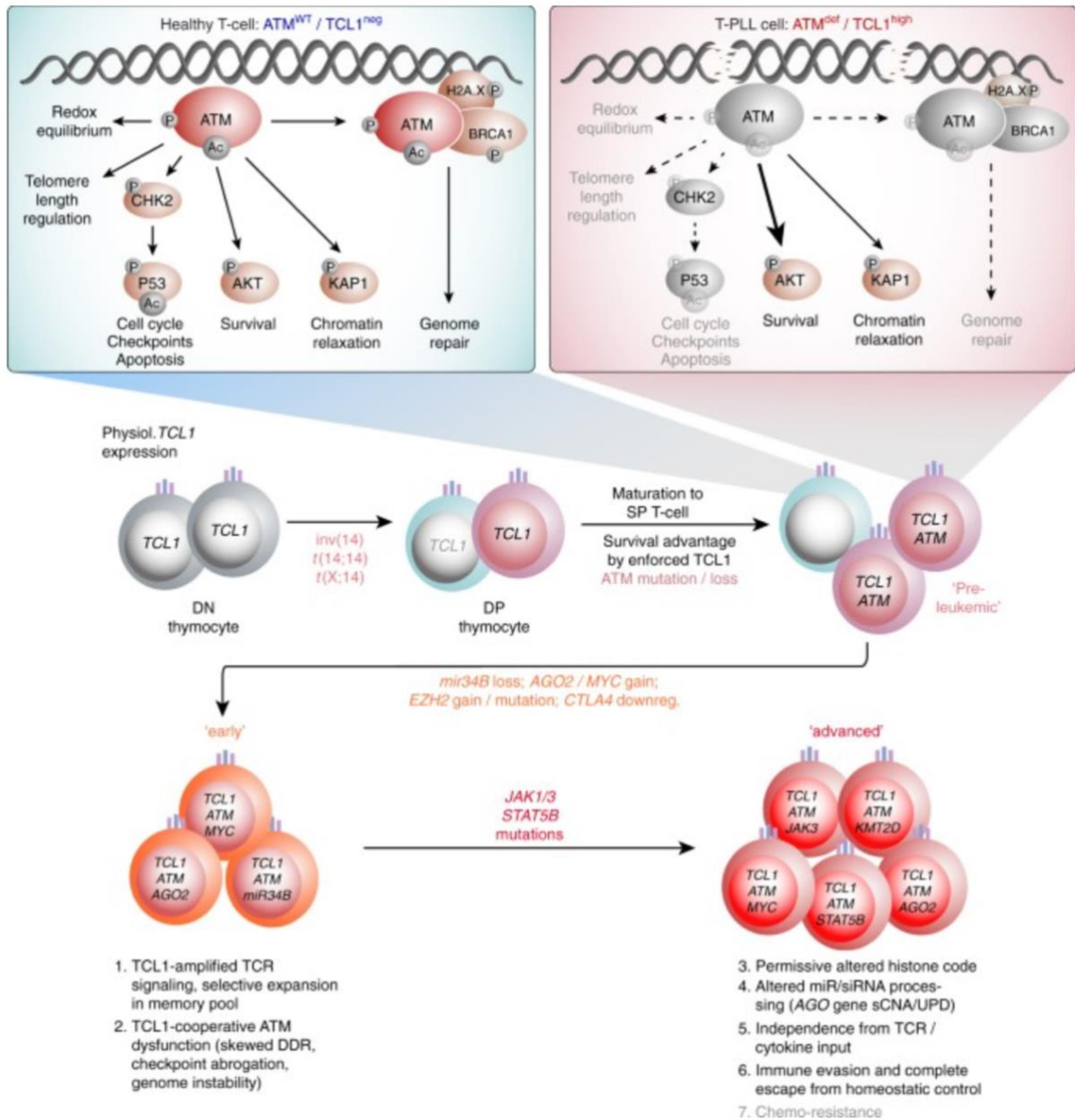
The pathophysiology of this disease is not fully understood. The most frequent cytogenetic features in T-PLL are recurrent changes involving chromosome 14, the most common are *inv(14) (q11q32)* and *t(14;14) (q11;q32)*. These alterations lead to the activation and overexpression of the proto-oncogene *TCL-1*(Matutes *et al.*, 1991) which plays an

important role in the pathogenesis of T-PLL. *TCL1A* was first observed and isolated by Croce C.M. et.al. in 1985, showing its abnormal activation in T cell malignancies.(Croce *et al.*, 1985) In subsequent studies, the *TCL1A* gene family, which consists of 5 members *MTCP1*, *TCL1A*, *TCL1B*, *TNG1* and *TNG2*, was described and found to be located at chromosome 14q32.1 and chromosome Xq28 in humans.(Hallas *et al.*, 1999) In healthy T cells, TCL1 is expressed early in T cell differentiation, in CD4-/CD8- cells but not at later stages of differentiation. TCL1 proteins are able to promote cell proliferation through activation of the protein kinase B (AKT).(Pekarsky *et al.*, 2000) Moreover, it is a cofactor of AKT1 function, enhances AKT1 kinase activity, and promotes the nuclear transport of this protein. Genomic alterations of the tumor suppressor ATM (ataxia telangiectasia mutated) are also found in more than 85% of cases(Stilgenbauer *et al.*, 1997), as well as activating mutations on the JAK/STAT pathway.(Wahnschaffe *et al.*, 2019) The overall cytogenetic and mutational spectrum of T-PLL is mainly annotated to axes of DNA damage responses, T-cell receptor/cytokine signaling, and histone modulation. A multi-dimensional model of T-PLL pathogenesis has been recently formulated,(Schrader *et al.*, 2018a) centered on a unique combination of TCL1 overexpression with ATM aberrations as initiating core lesions. The effects imposed by TCL1 cooperate with disrupted ATM toward a leukemogenic phenotype of severe impairment of DNA damage processing. The dysfunctional ATM is then ineffective in mitigating high redox burdens and telomere attrition, resulting in a p53-dependent apoptotic response to genotoxic insults (Figure 1).(Schrader *et al.*, 2018a)

Figure 1: Proposed model of T-PLL development.(Schrader et al., 2018)

Top: Cellular mechanisms of a normal thymic lymphocyte (left) compared to the functioning of a post-thymic T-PLL precursor (right box) with overexpression of TCL1 and disruption of ATM. Effects of this assumed initiating lesion of $TCL1^{up}/ATM^{dis}$ on the main signaling pathways and functions of ATM are shown by differential arrows. It includes modifications on some of ATM's essential tasks by TCL1, resulting in inhibition of apoptosis. The 'TCL1'-lesion can refer to the disruption of any of the TCL1 family members. $TCL1^{up}/ATM^{dis}$ simultaneously confer a functional signature with inefficiency of ATM in correcting oxidative damage, to support genome and telomere integrity, and to activate protection of p53 programs.

Timeline: Chronology is based on identified frequencies in sCNA data and tumor fractions in sequencing data. Constitutive TCL1 expression and loss-of-negative regulators cause amplifications of TCR-derived survival signals. In the context of dysfunctional ATM this entertains ROS accumulation and genomic instability, which in turn entails further alterations of oncogenes like MYC, of epigenetic modifiers, and of miR processing. Overt-stage autonomous proliferation, including escape from niche-defined homeostatic control relies on independence from milieu input, as potentially conveyed by JAK/STAT mutations. Emerging data on the impact of JAK/STAT signaling on non-canonical functions of histone modulators like EZH2 indicate yet unrecognized cross-talks between the affected functional branches.



6.1.3. Generalities on T-PLL diagnosis

T-PLL has been defined by the 2017 World Health Organization classification as an aggressive T-cell leukemia, constitute of highly proliferating small to medium-sized T-lymphocytic cells. Despite their post-thymic provenance and their mature phenotype, those cells are called T-prolymphocytes. (Catovsky *et al.*, 1973; Swerdlow *et al.*, 2016) The formerly

used category of T-cell Chronic Lymphocytic Leukemia (CLL) is now include in the T-PLL spectrum. T-PLL represents approximatively 2% of mature leukemias in adults.(Matutes *et al.*, 1991; Herling *et al.*, 2004) To date, the largest studies describing the clinical and biological abnormal features at diagnostic included between 38 and 119 patients, thus indicating that cohorts with more than 50 T-PLL cases can be considered to be significant.(Jain *et al.*, 2017; Schrader *et al.*, 2018a)

At the time of diagnosis, patients can present B-symptoms, hepatomegaly, splenomegaly, and frequently excessive lymphocytosis above $100 \times 10^9/L$. Lymph nodes can also be involved, as well as other organs including skin, pleural or peritoneal effusions (approximately 25% of patients), and central nervous system (< 10% of patients).(Matutes *et al.*, 1991; Swerdlow *et al.*, 2016) Some edema can also be present in patients with T-PLL: periorbital, conjunctival and peripheral edema.(Matutes *et al.*, 1991) T-PLL has to be discriminated from other T cell malignancies, which is possible on clinical, molecular and cytogenetic specificities. Some other leukemic T-cell neoplasia have overlapping features, like adult T-cell lymphocytic leukemia (ATLL), Sézary syndrome, T-cell large granular lymphocytic leukemia, or T cell lymphomas with circulating tumor cells. To establish an accurate diagnosis, several parameters have to be evaluated: peripheral blood smear, lymphocyte immunophenotyping, and cytogenetic features. However, in many cases the diagnosis can be highly suspected on peripheral blood lymphocytes morphology and immunophenotype. Bone marrow evaluation is usually not useful in T-PLL, but it can be required for confirmation of a remission.

The recently published consensus criteria proposed 3 major diagnostic criteria and 4 minor criteria. T-PLL diagnostic is made if all 3 major criteria are met, or if the first 2 major criteria in addition to 1 minor criterion are present.(Staber *et al.*, 2019) The first 2 major criteria are critical in defining the diagnosis, the third major criterion, alterations of TCL1 family protein, is present in more than 90% of cases. In the remaining 10% of cases, at least 1 of the other common genetic features or an involvement of a T-PLL typical site has to be present.(Herling *et al.*, 2004)

Table 1: Requirements to establish the diagnosis of T-PLL.

Major criteria	Minor criteria (at least 1 required)
<ul style="list-style-type: none"> • $>5 \times 10^9/L$ cells of T-PLL phenotype in peripheral blood or bone marrow • T-cell clonality (by PCR for TRB/TRG, or by flow cytometry) • Abnormalities of 14q32 or Xq28 OR expression of TCL1A/B, or MTCP1* 	<ul style="list-style-type: none"> • Abnormalities involving chromosome 11 (11q22.3; ATM) • Abnormalities in chromosome 8: idic(8)(p11), t(8;8), trisomy 8q • Abnormalities in chromosome 5, 12, 13, 22, or complex karyotype • Involvement of T-PLL specific site

*Cases without TCL1A, TCL1B, or MTCP1 rearrangement or their respective overexpression are collected as TCL1-family negative T-PLL.

6.1.4. Blood and bone marrow

The diagnosis of T-PLL requires the presence of clonal T cells with a prolymphocytic morphology in the peripheral blood (more rarely in the bone marrow). Three main morphologic variants can be seen (Ravandi and O'Brien, 2005; Kotrova *et al.*, 2018): in 75% of cases, the cells are medium-sized with a moderately condensed chromatin, a single visible nucleolus, high nuclear/cytoplasmic ratio, and a slightly basophilic cytoplasm, typically showing protrusions (blebs), without granules. In 20% of cases, tumor cells present as a smaller variant with condensed chromatin; and in around 5% of cases, malignant cells demonstrate irregular nuclei similar to Sézary cells of mycosis fungoides, with a cerebriform nuclei. An ongoing project of our team aims to find an association between these morphological variants and distinct clinical presentations, outcomes or molecular abnormalities.

The clonality of these T lymphocytes can be confirmed by molecular assays (polymerase chain reaction [PCR]; or next-generation sequencing [NGS]) of the clonal rearrangement of T-cell receptor genes (TCR β and TCR γ) or by flow cytometry. (Kotrova *et al.*, 2018) Immunophenotyping is more frequently used, given the complexity and expensive nature of molecular biology analysis. Moreover, lymphocytosis is often major, therefore, cases where phenotyping is not sufficient are rare. Serologic or PCR-based testing for HTLV (human T lymphotropic virus) type 1 is negative. In case of positive HTLV1, an adult T-cell lymphocytic leukemia (ATLL) has to be discussed. Infrequently, asymptomatic patients are diagnosed as part of the evaluation of an abnormal laboratory test result.

The diagnosis of T-Prolymphocytic Leukemia can be established without bone marrow examination; however, it could be useful in etiological assessment of ambiguous cytopenias. It is possible to discuss the evaluation of the bone marrow (mostly aspirate, or biopsy) to confirm a complete remission and define remission with incomplete recovery. But usually, clinical response and normalization of lymphocytosis are sufficient.

6.1.5. Immunophenotype

T-PLL cells are post-thymic T cells that coexpress mature T-lymphoid markers and demonstrate cytoplasmatic expression of TCL1 oncogenes as a frequent hallmark. T-PLL are most commonly CD4+, with just over half of these cases coexpressing CD8 (CD4+/CD8+) and just under half expressing CD4 without CD8 (CD4+/CD8-). CD4-/CD8+ populations are less frequent, and a CD4-/CD8- immunophenotype are possible but rare. The percentage of patients with T-PLL expressing specific markers are: cyTCL1+ (>90%), CD4+(60%), CD8+(15%), CD4+CD8+(25%), CD5+ (100%), CD7+ (>90%), CD3+ (>80%).(Herling *et al.*, 2004)

6.1.6. Genetics

In T-PLL cells, the T-cell receptor genes (TCR β or TCR γ) are clonally rearranged, which can be confirmed (by PCR/ NGS), but this is usually not performed. Cytogenetic analysis of T-PLL cells commonly show complex karyotypes (in 71%-82%). Recurrent genetic features are key arguments to make the diagnosis.(Pekarsky, Hallas and Croce, 2001; Dürig *et al.*, 2007; Herling *et al.*, 2008) Therefore, T-PLL can be distinguish from other T-lymphoproliferative and leukemic malignancies with the help of chromosome banding analysis and fluorescence in situ

hybridization (FISH). Rearrangements involving TCL1 (T-cell leukemia/lymphoma1) family genes are relatively specific for T-PLL and are present in more than 90% of cases. Involved genes in descending order of frequency are TCL1A, MTCP1 (mature T-cell proliferation), and TCL1B (alias TCL1/MTCP1-like 1 [TML1]). Likewise, the more frequent cytogenetic abnormalities are inv(14)(q11q32), t(14;14)(q11;q32) (involving TCL1A or TCL1B), or t(X;14)(q28;q11) (involving MTCP1). Detection of aberrant TCL1 protein expression via immunophenotyping or immunohistochemistry can represent another diagnostic hallmark. It is more sensitive than cytogenetics but the intracytoplasmic staining is technically difficult and less commonly use in hematology laboratories.(Herling *et al.*, 2008, p. 1; Sun *et al.*, 2018, p. 1) Few cases are observed in which neither a rearrangement nor an overexpression of TCL1A, TCL1B, or MTCP1 is detected, but which otherwise carry typical clinical, cytomorphological, and molecular criteria of T-PLL (clonal expansion of cells with a prolymphocytic T-cell phenotype). These cases called “TCL1-family negative T-PLL” should be collected for a comprehensive scientific analysis.

Deletions of or missense mutations at ATM (ataxia telangiectasia mutated) locus at 11q23 are found in up to 80% to 90% of T-PLL cases.(Stilgenbauer *et al.*, 1997; Vorechovský *et al.*, 1997) An increased risk of developing T-PLL is known in patients who harbor ATM germ line mutations, namely patients suffering of “ataxia telangiectasia” disease.(Stilgenbauer *et al.*, 1997; Vorechovský *et al.*, 1997) Other chromosomal alterations of sporadic T-PLL include chromosome 8 abnormalities (idic(8)p11), t(8;8)(p11-12;q12), and trisomy 8q), deletion in 12p, and alterations in chromosome 6.(Stengel *et al.*, 2016, p. 3) At diagnostic, deletions of the *TP53* gene are observed in 31% of cases, and *TP53* mutations in 14% of cases.

NGS has recently identified additional recurrent genomic abnormalities, the more frequent are involving JAK/STAT signaling (up to 75% of cases).(Kiel *et al.*, 2014a) In a single study, *JAK3* mutations showed a negative impact on prognosis.(Stengel *et al.*, 2016) Further work is needed to confirm this putative prognostic significance in T-PLL. Other common genetic lesions, but that are not specific for T-PLL, are haploinsufficiency for the tumor suppressor gene *CDKN1B* (50%(Bellanger *et al.*, 2014)) and mutations in the epigenetic regulators *EZH2* (deletions, 18%; mutations, 13%), *TET2* (17%), and *BCOR* (9%). Genetic sequencing is currently not a diagnostic requirement; however, it may provide information to target new therapeutic options (for example JAK inhibitors or HDAC inhibitors). Of course, those genomic assays are important to continue to decipher underlying pathogenesis of T-PLL and might find mutations with a prognostic significance.

6.1.7. Serum markers

Similar to other lymphoproliferative malignancies, serum lactate dehydrogenase (LDH) and β 2 microglobulin (β 2MG) are reflecting disease burden in T-PLL. LDH higher than 1668 U/L and β 2MG higher than 8 mg/L were found to be associated with inferior overall survival in a retrospective study including 119 patients with T-PLL.(Jain *et al.*, 2017) High LDH levels were also associated with a shorter overall survival in multivariate analysis. Lymphadenopathy, organomegaly and elevated β 2MG were suggestive of bulky disease. These serum markers are not routinely used at this time, because the prognosis of the disease is so poor and relapses so frequent that they do not seem to have any real practical significance.

6.1.8. Inactive phase and progression

A vast majority of patients with T-PLL present with a major lymphocytosis (usually $> 100 \times 10^9/L$), poor performance status, generalized lymphadenopathy, splenomegaly and/or hepatomegaly.(Dearden, 2015) However, 20% to 30% of patients demonstrate initially stable or slowly progressive disease, with few or no clinical signs.(Garand *et al.*, 1998) These 2 different disease states are relevant for the clinical management of patients and may help to understand T-PLL pathophysiology. Criteria for initiating treatment in a clinical trial and in general practice are the same as those that define active disease. Because there is no evidence that asymptomatic patients (“inactive T-PLL”) would benefit from immediate treatment, it should be restricted to patients with active or symptomatic disease (“active T-PLL”). This principle is very well documented in CLL and can reasonably be applied to T-PLL. However, within 1 to 2 years, nearly all inactive T-PLL convert into active disease. During the observation period, a clinical examination has to be performed every 3 months, along with blood counts at monthly intervals.

6.1.9. Current treatment of T-PLL

Very few trials have been conducted and published on T-PLL. Initial attempts with CHOP (cyclophosphamide, doxorubicin, vincristine, and prednisone) or CHOP-like regimens have been particularly discouraging.(Catovsky, 1982) Alemtuzumab (anti-CD52) currently remains the best first line treatment for T-PLL. The IV administration has to be favored, with an overall response rate (ORR) higher than 90% and PFS between 8 and 11 months.(Pawson *et al.*, 1997; Dearden *et al.*, 2001) The safety profile of this monoclonal antibody is very

difficult, with many severe infectious adverse events. Despite this high response rate, most patients will relapse, the median duration of remission for responders is less than 2 years. That's why consolidation therapy with an allogeneic stem cell transplant should be considered for patients achieving a complete or partial remission. The therapy related mortality and relapse rates of this approach remain high, but this allows to observe around 33% of long-term survivors.(Guillaume *et al.*, 2015) A lower relapse rate has been described for patients who received conditioning with at least 6 Gy total body irradiation,(Wiktor-Jedrzejczak *et al.*, 2019) but this needs to be confirmed in future studies. Autologous stem cell transplant can be considered, particularly for patients without a compatible donor. This procedure could prolong progression free survival, but no long-term survivors are observed.(Krishnan *et al.*, 2010) There is no evidence to support any maintenance therapy.

Patients that are not eligible to alemtuzumab, or who are relapsing after this therapy, exhibit a very poor prognosis. Salvage regimens can achieve an ORR of 50% to 76%, but the durations of response are very short, and the reported overall survival is between 6 and 9 months.(Mercieca *et al.*, 1994; Herbaux *et al.*, 2015)

6.1.10. Innovative therapeutic approach for T-PLL

Given the chemoresistance of T-PLL, as well as the safety profile and broad target range of alemtuzumab, recent work focused on more targeted agents. *Ex vivo* high-throughput drug sensitivity and resistance testing platform on primary T-PLL samples(Boidol, Kornauth, Kouwe, *et al.*, 2017; Andersson *et al.*, 2018) identified the BCL-2 inhibitor venetoclax and histone deacetylase inhibitors (HDACi) as promising targeted agents. Integrated large-

scale genetic profiling assays also identified various recurrent lesions in DNA repair molecules and histone modifiers in T-PLL.(Schrader *et al.*, 2018b) Early clinical data suggest that HDACi have *ex vivo* activity in T-PLL and may partially overcome chemoresistance in T-PLL.(Hasanali *et al.*, 2015) High-throughput drug testing studies also demonstrated *in vitro* sensitivity of T-PLL cells to JAK inhibitors (JAKi). Additionally, a modest activity was reported with the combination of tofacitinib (a pan JAK inhibitor) and ruxolitinib (a JAK 1/2 inhibitor).(Gomez-Arteaga *et al.*, 2019) Despite the promising data of novel agents in T-PLL, the early clinical data also suggest that a sustained response to these drugs is unlikely when they are given as monotherapy.(Boidol, Kornauth, Kouwe, *et al.*, 2017; Smith *et al.*, 2020) Combining different classes of drugs, such as HDACi, MDM2 inhibitors, chemotherapy and BCL-2 antagonists, is proposed to act synergistically.(Schrader, Braun and Herling, 2019; Pützer *et al.*, 2020) The Bruton tyrosine kinase (BTK) inhibitor ibrutinib was recently identified as a promising combination partner for venetoclax in T-PLL.(Kornauth *et al.*, 2019) An off-target effect of ibrutinib is inhibition of IL-2–inducible kinase (ITK), a T-cell–dominant member of the TEC-kinases family that drives proximal T-cell receptor (TCR) signaling.(Berg *et al.*, 2005) Consistent with this, *ex vivo* assays also demonstrated inhibitory activity of PRN694, a specific ITK inhibitor (ITKi), against T-PLL.(Zhong *et al.*, 2015)

6.2. Apoptosis and BCL2 family proteins

6.2.1. Overview

Apoptosis, a form of programmed cell death, differs from other forms of cellular death such as necroptosis, autophagy, ferroptosis, pyroptosis, netosis, or necrosis.(Kerr, Wyllie and

Currie, 1972) During apoptosis, morphological changes, such as the shrinkage of the nuclei and mitochondria, occur in the cell. Notably, the blebbing, *i.e.* the plasma membrane ties off cell content, is shown to continuously reduce cell size and functionality. The phagocytosing cells are able to rapidly clear these apoptotic bodies, avoiding thus a strong inflammatory response. The extrinsic death receptor pathway, regulated by the tumor necrosis factor (TNF) and first apoptosis signal death receptor super families, or the intrinsic B-cell leukemia/lymphoma-2 (BCL-2) family-regulated mitochondrial pathway, can trigger apoptosis. These two pathways merge at mitochondrial level via the protein truncated BH3-interacting domain (tBID). Recently, novel therapies on hematologic malignancies have focused on the intrinsic apoptotic pathway, and so will we in the present manuscript.(Valentin, Grabow and Davids, 2018)

Apoptosis mediated through the intrinsic pathway is one of the most extensively studied areas of cancer research since BCL-2 discovery (Cleary, Smith and Sklar, 1986). Thus, one of the major hurdles that a nascent neoplastic cell must overcome to transform into a malignant cell is apoptosis.(Hanahan and Weinberg, 2011) Historically, BCL-2 gene was discovered as the “driver” of follicular lymphoma (FL) pathogenesis because of its involvement in the t(14;18)(q32;q21) chromosomal translocation, which is the genetic hallmark of FL pathogenesis.(Tsujiimoto, Ikegaki and Croce, 1987) More recent data suggested that BCL-2 played a contributive role in the pathophysiology of chronic lymphocytic leukemia (CLL), mantle cell lymphoma (MCL), and Waldenström macroglobulinemia (WM). Indeed, in multiple myeloma (MM), another hematological malignancy, the reliance of the malignant cell on BCL-2 family proteins seem to vary.(Gomez-Bougie *et al.*, 2018) In terms of cell growth or

proliferation and unlike most oncogenic proteins, the dysregulation of BCL-2 does not confer an advantage, but rather it allows survival of cells that would normally undergo apoptosis.

Myeloid cell leukemia-1 (MCL-1), another key prosurvival protein initially described for its significant role of regulator of myeloid cell differentiation (Kozopas *et al.*, 1993), has since then been identified as a crucial survival factor in MM, diffuse large B-cell lymphoma (DLBCL), acute lymphoblastic leukemia (ALL), acute myeloid leukemia (AML), and chronic myeloid leukemia (CML). (Kaufmann *et al.*, 1998) To these two key prosurvival proteins, a third one can be added, the B-cell lymphoma-extra-large (BCL-xL), (Boise *et al.*, 1993), which is essential for megakaryocyte survival. Over more, the loss or inhibition of BCL-xL leads to thrombocytopenia. BCL-xL function impairment may also trigger the pathogenesis of several hematologic disorders such as myeloproliferative disorders, polycythemia vera included. (Silva *et al.*, 1998)

6.2.2. BCL-2 family biology

According to literature, BCL-2 family regulates intrinsic apoptotic pathway. The BCL-2 family is composed of 2 major groups of proteins: (1) the prosurvival proteins with its founding member BCL-2, MCL-1, BCL-xL, B-cell lymphoma-w (BCL-w), and BCL-2-related gene expressed in fetal liver-1 (BFL-1), all of which down-regulate cell death and (2) the proapoptotic proteins. The latter can be further divided into (a) BH3-only proteins: BCL-2-interacting mediator of cell death (BIM), p53-upregulated modulator of apoptosis (PUMA; BBC2), NOXA (phorbol-12 myristate-13-acetate-induced protein 1; PMAIP1), BCL-2-associated death promotor (BAD), BH3-interacting domain (BID), BCL-2-interacting killer

(BIK), BCL-2–modifying factor (BMF), Harakiri (HRK) and (b) the BCL-2–associated X protein (BAX

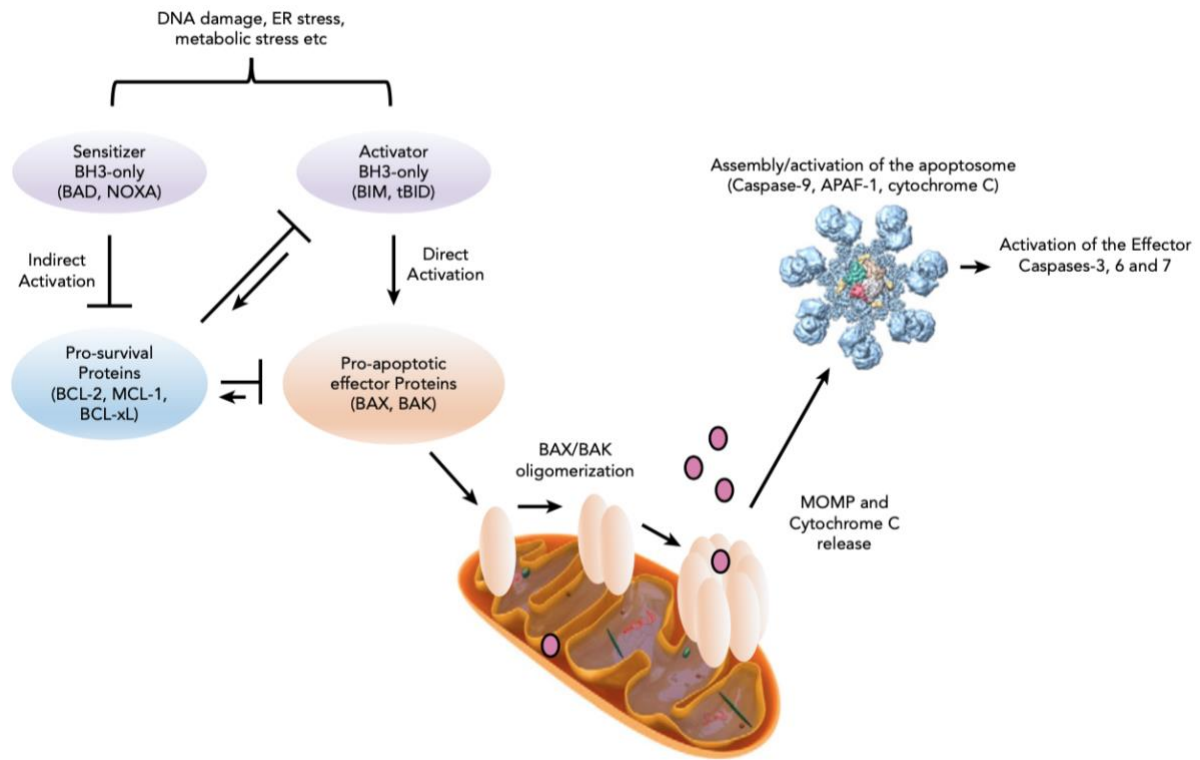
) / BCL-2 homologous antagonist killer (BAK)-like proteins. (Valentin, Grabow and Davids, 2018). A common feature is shared by the whole BCL-2 proteins family: *i.e.* the common BCL-2 homology (BH) domains based on their sequence similarity. BH3-only proteins only share the BH3 domain with the wider family. Prosurvival and BAX/BAK-like proteins hold 4 and 3 BH domains, respectively.

6.2.3. Activation of the apoptotic pathway

Apoptosis can be decomposed into 3 distinct phases: (1) initiation, (2) commitment, and (3) execution. Stress stimuli such as nutrient deprivation or DNA damage are potential inducers of this process. As a death stimulus, BH3-only proteins are activated in a cell-type-specific and a temporal manner, and relocate/activate the BAX/BAK-like proteins in the initiating step. (Willis *et al.*, 2007) During the commitment phase, BAX and BAK are able to combine so as to form homodimers and heterodimers, which further assemble to pore-like structures in the outer mitochondrial membrane, thus leading to mitochondrial outer membrane permeabilization (MOMP) (Czabotar *et al.*, 2013). The subsequent consequences are the loss of mitochondrial transmembrane potential and oxidative phosphorylation, and the relocation of cytochrome C, initially located in mitochondrial intermembrane space, to the cytoplasm. (Liu *et al.*, 1996) In the execution step, the apoptosome is formed by the combination of cytochrome C together with APAF-1 and procaspase-9, which mediates the post-translational modification of procaspase-9 to its active form caspase-9 and consequently

initiates the activation of the effector caspases-3, 6 and 7, which in turn activate DNases, thus allowing DNA degradation (Figure 2).

Figure 2: The intrinsic apoptotic pathway.(Valentin, Grabow and Davids, 2018)



It is noteworthy that the “point of no return” generally occurs at the level of BAX/BAK activation. Usually, then, the cell undergoes programmed cell death. BH3-only proteins have different affinities for particular prosurvival proteins. This affinity variation can be explained by their structural differences. Interestingly, some BH3-only proteins, *e.g.* BIM and PUMA, were found to bind all prosurvival proteins with high affinity. Other BH3-only proteins bind more selectively, such as NOXA, which binds mainly to MCL-1, and BAD, which binds BCL-2, BCL-xL and BCL-W. The induction of apoptosis can take two main forms. (1) The first one is the direct activation model. In this model, BH3-only proteins play the role of either activators (*eg*, BIM, Bid/tBid, PUMA) or sensitizers (*eg*, BAD, NOXA). Activators are able of binding both

prosurvival and BAX/BAK-like proteins, causing the integration into the outer mitochondrial membrane. Prosurvival proteins such as BCL-xL can capture BH3-only proteins, therefore impairing BAX activation. Through a direct binding to the prosurvival protein, sensitizers mediate the release of activators. (2) The second model, the indirect (displacement) model, assumes a constitutive activation of BAX and BAK, but that these two proteins are bound to prosurvival proteins to prevent apoptosis. In case of the occurrence of a death stimulus, BH3-only proteins can be able to relocate BAX and BAK. Because of BH3-only proteins binding affinities disparity for each prosurvival protein, apoptosis initiation requires the activation of several BH3-only proteins to displace sufficient amounts of BAX and BAK, with MOMP as consequence. Recent findings have suggested that these 2 models likely coexist and operate in a context-specific manner, leading to a unified model in which prosurvival proteins inhibit BAX and BAK and sequester both BH3-only proteins. In regards of hematologic malignancies, the large range of binding affinities of BH3-only proteins for each prosurvival protein enables to specifically target the prosurvival proteins with pharmacologically selective inhibitors with great therapeutic potential.(Chen *et al.*, 2005)

6.2.4. Targeting the intrinsic apoptotic pathway in the clinic

When considering different hematologic malignancies, the mechanism by which prosurvival protein dependency increases can be extremely variable. In CLL, because of the loss of repression by microRNA (miRNA) 15/16, malignant cells harboring del(13q) express high BCL-2 protein levels,(Cimmino *et al.*, 2005) whereas MCL and MM cells seem to express high BCL-2 due to dysregulation of cyclin proteins.(Touzeau *et al.*, 2016) The following DNA defect t(14;18), which juxtaposes the BCL-2 gene to the immunoglobulin heavy chain (IgH)

locus, increasing thus BCL-2 protein levels, has been observed in both FL and double-hit DLBCL. Other causes, such as microenvironmental factors, may also up-regulate BCL-xL and/or MCL-1 expression in CLL, FL, and MM.(Ghia *et al.*, 1998; Herishanu *et al.*, 2011; Punnoose *et al.*, 2016) In regards of oncogenic pathways, BCL-2 family lies downstream of tumor protein 53 (TP53), the famous genome guardian, which is by definition often dysfunctional in hematological malignancies, leading to cytotoxic chemotherapy resistance. Indeed, the BCL-2 family can be therefore an attractive therapeutic target in hematologic malignancies. This is why so many efforts were made to target the BCL-2 pathway therapeutically, including antisense oligonucleotides, peptide inhibitors, and small molecule inhibitors. It is noteworthy that the first major breakthroughs in targeting the apoptotic machinery directly consisted of the dual BCL-2/BCL-xL inhibitor ABT-73752, and its orally bioavailable equivalent ABT-263 (navitoclax).(Ashkenazi *et al.*, 2017) Unfortunately, sometimes, promising molecules in preclinical studies were disappointing when clinically tested afterwards. For instance, navitoclax was linked to the occurrence of thrombocytopenia due to inhibition of BCL-xL (an important prosurvival factor for megakaryocytes/platelets), its use generating thus a dose-limiting toxicity in the clinic.(Roberts *et al.*, 2012) However, other potentially more efficient inhibitors are currently studied, *e.g.* the first selective and highly potent BCL-2 inhibitor, venetoclax (VEN; formerly ABT-199/GDC-0199), was found to be active in preclinical testing of non-Hodgkin lymphoma (NHL) and AML cell lines, and in primary CLL samples, the mutation status of TP53 causing no impact on its activation.(Souers *et al.*, 2013) Over more, VEN was shown to significantly induce less thrombocytopenia than navitoclax, in xenograft models.

As a major development, the approval of VEN in CLL heralded a new era in targeting the intrinsic pathway of apoptosis therapeutically. This is the first step in the challenging but

hopefully powerful new approach to cancer therapeutics that spans across hematologic malignancies and even applies to some solid tumors. The hope is that, eventually, in a near future, clinicians should have access to a huge choice of specific and highly efficient inhibitors of BCL-2, MCL-1, BCL-xL and BFL-1.

6.3. Assays to evaluate BCL-2 family proteins function

Some cancer cells lie close to the apoptotic threshold but are held back from death by prosurvival BCL-2 family proteins. Others depend for survival on loss or reduction of proapoptotic proteins in the setting of increased proliferation, cell growth, and changes in dependence on the microenvironment. Both scenarios create a vulnerability in cancer cells which allows for a therapeutic window for agents targeting this pathway. Assays that aid us in better understanding resistance mechanisms and in predicting clinical response to agents targeting the BCL-2 family would be helpful to optimize therapy. Here we will describe 2 different assays to evaluate these dependences.

6.3.1. BH3 profiling

BH3 profiling is a functional assay which interrogates mitochondria to assess both their proximity to the threshold of apoptosis, and their relative dependence on anti-apoptotic BCL-2 family proteins, such as BCL-2, MCL-1 or BCL-xL. The profile determines the proximity of a cell to the apoptosis threshold, known as 'mitochondrial priming', and also identifies the specific prosurvival proteins on which a cell depends for its survival. (Ryan *et al.*, 2016) Using defined inputs in the form of peptides derived primarily from the BH3 domains of pro-

apoptotic members of the BCL2 family, BH3 profiling invokes a response in the mitochondria in the form of mitochondrial outer membrane permeabilization measured indirectly by flowcytometry on the amount of intracellular cytochrome C. BH3 profiling on blood samples from CLL patients on the phase 1 study of VEN found that pretreatment CLL cells were uniformly dependent on BCL-2, and that mitochondrial priming was associated with the depth of disease reduction in BM and PB.(Anderson *et al.*, 2016) In contrast to CLL, primary AML and MM cells are more heterogeneous, with survival related to BCL-2, BCL-xL, MCL-1, or a mixture of these, depending on the sample.

6.3.2. Dynamic BH3 profiling

A variation of this technique known as dynamic BH3 profiling (DBP) measures the early net proapoptotic signaling induced by a drug treatment. DBP takes advantage of the fact that alterations in mitochondrial priming are evident well before cancer cells undergo apoptosis in response to drug treatment.(Montero *et al.*, 2015) DBP consists in exposing the intact cells to one or more agents, and then ask whether the treatment causes an increase in apoptotic priming or specific apoptotic dependencies. In practice, we expose the cells (from a patient sample or cell line) ex vivo to treatments of interest, and after a short incubation (typically 6-24 hours) the cells are permeabilized with digitonin and exposed to BH3 peptides or mimetics. Death signaling, measured by increased priming, should be initiated only in those cells that are dependent on the particular pathway that is targeted by the peptide or inhibitor.

An important question addressed by the team who created DBP was “Does early (e.g., measured within 16 hours) death signaling predict frank cell death, even when cell death does

not occur until a few days later?”. It was initially tested in over a hundred cell line experiments, and confirmed.(Montero *et al.*, 2015) In subsequent cell lines and clinical experiments, Montero *et al* find that early drug-induced death signaling measured by DBP predicts chemotherapy response across many cancer types and many agents, including combinations of chemotherapies, showing its versatility and applicability. For example, DBP results have been found to correlate with response to treatment in patients with a variety of hematologic malignancies.(Montero *et al.*, 2015) Furthermore, DBP has proven to be a useful method for predicting promising novel agent combination regimens such as VEN plus ibrutinib in CLL.(Deng *et al.*, 2017)

6.3.3. BH3-mimetic toolkit

A BH3-mimetic toolkit can also be used to determine BCL2, BCLxL, and MCL1 dependence by ex vivo treatment of cell lines or mononuclear cells from primary samples.(Gomez-Bougie *et al.*, 2018) Dependencies were analyzed using an unbiased BH3 mimetics cell-death clustering by k-means. This study opens the way to rationally use venetoclax and/or MCL1 inhibitors for clinical evaluation in myeloma at both diagnosis and relapse. The advantage of this technique over BH3 profiling is that it assesses apoptotic function more broadly, down to the phosphatidylserine flip-flop. However, direct assessment of global priming is not possible, and this assay is limited by the choice of pharmacological inhibitors, whereas BH3 profiling also uses peptides derived primarily from the BH3 domains of pro-apoptotic members of the BCL2 family

6.3.4. Choice

Baseline and dynamic BH3 profiling are the two assays we have chosen for this project. We preferred the assay with the most comprehensive evaluation of the overall priming and of specific dependences over including an evaluation of the mechanisms taking place after cytochrome C release. Moreover, BH3 profiling is described more extensively in the literature and is performed routinely in Davids lab.

6.4. Aim of the present work

Taking into account all these data, we aimed to perform a conventional drug screening with a measure of the metabolism of the cells with CTG. We then completed the evaluation with BH3 profiling to evaluate baseline dependencies in BCL2 family proteins in T-PLL. This functional precision medicine technique provides orthogonal information that is not provided by genomics and traditional viability assays alone. For this second step, given the current accessibility of the different drugs, we decided to select 4 drug candidates in order to target 3 main pathways in T-PLL:

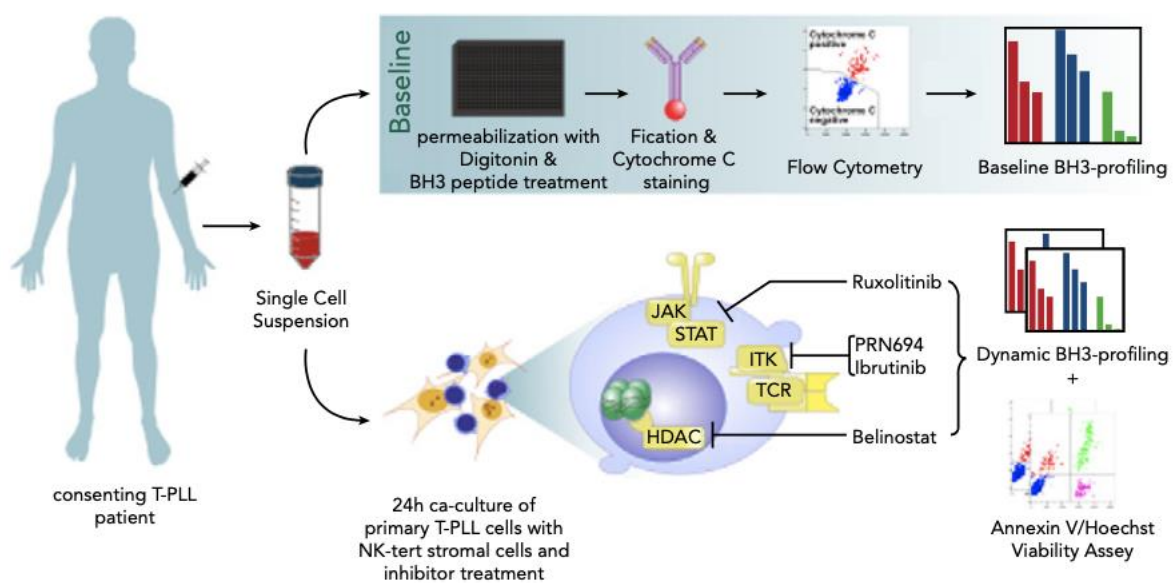
1/ belinostat, one of the most effective HDACi described in T-PLL, which is approved for peripheral T-cell lymphoma;

2/ ruxolitinib, the most effective JAKi described in T-PLL, which is approved in the treatment of myeloproliferative disorders;

3/ ibrutinib as the first potential ITKi described to be effective in T-PLL and PRN694, a highly selective ITKi (IC50: 0.3 nM versus 2.2 nM for ibrutinib).

We planned to utilize dynamic BH3 profiling (DBP), which measures early drug-induced changes in net pro-apoptotic signaling, (Montero *et al.*, 2015a) to identify optimal combination partners. We further study the mechanistic impact of these inhibitors on T-PLL biology, mitochondrial priming and drug sensitivity (Figure 3).

Figure 3: Visual abstract of the project's aim. We subjected single-cell suspensions of blood samples to baseline BH3 profiling. In parallel, we cocultured primary T-PLL cells with the stromal cell line NKtert and exposed them to ruxolitinib, PRN694, ibrutinib, belinostat, or DMSO. Then, we performed a DBP to measure early drug-induced changes in net proapoptotic signaling and examined whether the findings with DBP could be corroborated with the results of cell viability assays



7. Material and Methods

7.1. Study design and patient samples

The study was undertaken in compliance with the principles of the Helsinki Declaration, and all patients provided written informed consent. Twenty-four clinically annotated primary T-PLL patient samples were obtained from the French Innovative Leukemia Organization (FILO) network, Medical University of Vienna, and Dana-Farber Cancer Institute. Figure 1A outlines the methodology we used in this work. Primary cells from peripheral blood were viably frozen in FBS supplemented with 10% DMSO until the time of thawing. To enrich our analysis for T-PLL cells, we utilized flow cytometry to gate on CD5+CD19- T cells, which generally accounted for >90% of total cells. Patients had to fulfil current diagnostic criteria of T-PLL (Staber *et al.*, 2019). Twenty-four primary samples from treatment-naïve chronic lymphocytic leukemia (CLL) patients were utilized as a comparator for baseline BH3 profiling. *Ex vivo* drug treatments and immunoblotting by Western Blot were performed as previously described (Ten Hacken *et al.*, 2018) and are detailed in Supplemental Methods. Primary T-PLL and CLL cells were treated with venetoclax, AZD5991, S63845, A-1331852, belinostat, ruxolitinib, PRN694, ibrutinib, or the vehicle (DMSO) as a control.

7.2. Initial drug screening

We employed combinatorial drug screening to identify synergistic combination partners to enhance the efficacy of venetoclax in T-PLL patients. Twenty-four candidate

compounds were selected based on their clinical approval status, literature data, and mechanisms of drug action. Venetoclax was used in pairwise combinations in primary T-PLL samples with a mean post-thawing viability of 93% and mean purity of 94%. All patient samples (bone marrow aspirates, peripheral blood, or excised lymph node) were prepared freshly and used for drug-screening analysis within 3 hours of harvest. Resulting single-cell suspensions (in RPMI 1640 plus 10% fetal calf serum) were seeded at 1×10^5 cells per well in 384-well plates containing compound libraries with each drug in 4 concentrations in triplicate. Drug-concentration range was determined by dose-response experiments in primary cells and cancer cell lines for each compound. Drug plates were prepared with 5x5 drug combination matrices with each combination tested in triplicate (venetoclax + combination partner). Bortezomib (10 μ M) and DMSO served as positive and negative controls, respectively. Differential cell viability was determined after 72 hours with CellTiter-Glo (Promega) on an EnVision plate reader (PerkinElmer). One sample was excluded from analysis due to low overall cell viability. Bliss score deviation averaged over all combination points for each drug and individual samples was calculated as indicator of additive, synergistic, or antagonistic drug combination effects. The analysis was carried out using the SynergyFinder R package. (He *et al.*, 2018, p.)

7.3. Other primary cells, co-culture and treatment ex vivo

Human peripheral blood mononuclear cells (PBMCs) were collected from patients with T-PLL (or CLL) and isolated from whole blood by density gradient centrifugation over Ficoll-Paque (GE Healthcare), then viably frozen in FBS (Gibco) supplemented with 10% DMSO until the time of analysis. Upon thawing, cells were cultured at 10^6 cells/mL in RPMI 1640 medium

supplemented with 10% FBS, 100 U/mL penicillin, and 100 µg/mL streptomycin (Gibco) (R10) at 37°C and 5% CO₂, and samples with >80% viability were further analyzed. Given the limited number of viable T-PLL samples, we optimized an annexinV / Hoechst viability assay using as few cells as possible. Therefore, we maintained the cells in vitro in co-culture with the stromal cell line NKTert (NKT, purchased from the Riken cell bank, Tsukuba, Japan), with approximately 30,000 tumor cells per wells in a 96 wells plate, and 5,000 NKT cells per well. The NKT cells were cultured in 50µL of R10 24h before the introduction of the T-PLL cells, themselves added in 50µL of R10, for a total of 100µL per well at h0, as previously described in CLL(Kurtova *et al.*, 2009). *Ex vivo* drug treatments included: BH3 mimetics (BCL-2i: venetoclax, MedChemexpress #HY-15531; MCL-1i: AZD5991, Chemgood #C-1060 and S63845 MedChemexpress #HY-100741; BCL-xLi: A-1331852, Selleck #S7801), HDACi (belinostat Selleck #S1085), JAK/STATi (ruxolitinib, Selleck #S1378-5MG) and TCRi (PRN694 MedChemexpress #HY-12780; ibrutinib Selleck #S2680). After Annexin V/Hoechst staining, cells were fixed with 4% paraformaldehyde, neutralized with N2 buffer (1.7 M Tris, 1.25 M glycine pH 9.1) and analyzed using a BD Fortessa with 96-well HTS plate-reader. NKTert cells were excluded using FSC and SSC, and the analysis was performed on the cells in the CD5+CD19- gate. Individual analyses were performed in triplicate for all drug treatment conditions.

7.4. DNA Sequencing

DNA was extracted from isolated cells using QIAmp kit (Sigma-Aldrich, Saint-Quentin Fallavier, France). Mutational landscape was assessed using by Sanger sequencing and/or targeted next generation sequencing (NGS) to examine a panel of candidate genes. The panel

of candidate genes includes: TP53 (exon 2-11), ATM (full gene), JAK1 (exon 13-15, exon 20), JAK3 (exon 11-16; exon 18-19), STAT5B (exon 15-17), STAT3 (exon 20-21) and IL2R (exon 8). NGS was performed using the Ion Torrent PGM platform (Life Technologies, CA, USA) at mean depth coverage of 2,000 per nucleotide; at least 20 variants reads were needed to identify a mutation. Raw data were analyzed with both Torrent Browser (ThermoFisher) and SeqNext (JSI Medical System).


7.5. BH3 profiling

BH3 profiling was performed as previously described. (Montero *et al.*, 2015a) Primary cells were suspended in MEB2P buffer (150 mM mannitol, 10 mM HEPES-KOH pH 7.5, 150 mM KCl, 1 mM EGTA, 1 mM EDTA, 0.1% BSA, 5 mM succinate, 0.25% poloxamer 188) prior to analysis. Single cell suspensions were added to 384-well plates and incubated for 60 minutes with BH3-only peptides (BIM, PUMA, BAD, MS1, HRK and FS1) and venetoclax and A-133 utilized like the peptides to assess the effect of low concentrations of these drugs directly on mitochondria in the presence of 0.002% digitonin (for permeabilization of primary cells). After fixation with 4% paraformaldehyde and neutralization with N2 buffer (1.7 M Tris, 1.25 M glycine pH 9.1), cells were stained overnight with a cocktail of anti-cytochrome c–Alexa Fluor 488, anti-CD19-PE/Cy7, anti-CD5-PE, and Hoechst 33342. Prepared plates were analyzed using a BD FACS Fortessa. Flow cytometry data were analyzed using FACS Diva version 8.0.1 (BD Pharmingen). Cytochrome c (cyt c) release was used to assess the degree of mitochondrial outer membrane permeabilization in response to each BH3 peptide or tool drug, which was normalized relative to cyt c release with DMSO (0% loss, negative control) and the ion-channel forming peptide alamethicin (100% loss, positive control). Binding affinities for the BH3

peptides with respect to overall priming and specific BH3-only protein dependencies are summarized in Figure 4.

Figure 4: Interactions between BH3 proteins and tool compounds of BH3 profiling with anti-apoptotic Bcl-2 proteins. Red indicates high-affinity binding and green indicates low-affinity binding.

	Overall priming		Specific BH3-only protein dependencies				
	BIM	PUMA	BAD	VEN	HRK	MS1	FS1
BCL2	High	High	High	High	Low	Low	Low
BCLxL	High	High	High	Low	High	Low	Low
MCL1	High	High	Low	Low	Low	High	Low
BFL1	High	High	Low	Low	Low	Low	High



High affinity binding
Low affinity binding

Dynamic BH3 profiling (DBP) was performed with the same protocol, with the addition that the primary cells were treated *ex vivo* with ruxolitinib, belinostat, PRN694, ibrutinib or the vehicle (DMSO) for 24 hours prior to analysis. Individual analyses were performed in duplicate for all drug treatment conditions.

7.6. Immunoblotting

Cells were lysed on ice for 15 minutes in RIPA Buffer (MilliporeSigma) containing a phosphatase inhibitor cocktail (phosSTOP; Roche-Genentech) and a complete protease inhibitor cocktail (Roche-Genentech). Cells were then centrifuged at 11,000 g for 10 minutes at 4°C, and supernatants were collected and stored at –80°C until further use. Protein content was determined using the BCA Protein Assay Kit (Thermo Fisher Scientific), according to the manufacturer’s instructions. NuPage Sample Buffer (4x) and NuPage Sample Reducing Agent (10x) were added to twenty-five micrograms of total protein, loaded onto 4%–12% sodium dodecyl sulfate–polyacrylamide gradient gels (Invitrogen), and then transferred to nitrocellulose membranes (Thermo Fisher Scientific). Membranes were blocked for 1 hour in TBS-Tween containing 5% bovine serum albumin and incubated overnight with primary antibodies (diluted 1:1,000), followed by species-specific HRP-conjugated secondary antibodies (diluted 1:2,500 for phospho-proteins and 1:5,000 for total-proteins, except actin, diluted 1:10,000) for 90 minutes. Membranes were probed with primary antibodies. SuperSignal West Pico Chemiluminescent Substrate and Immobilon Western Chemiluminescent HRP substrate (Thermo Fisher Scientific) were used to visualize immunoreactive bands by a Chemidoc (Bio-Rad).

7.7. Reagents and antibodies

The compounds used for TCR pathway activation were: CD3 mouse antibody (BioLegend #317304), CD28 mouse antibody (eBioscience #16-0281-82) and rabbit anti-mouse IgG (H+L) cross-adsorbed secondary antibody (ThermoFisher #31190). The primary

antibodies and stain used for flow cytometry analyses were as follows: anti-cytochrome c-Alexa Fluor 488 (6H2.B4/612308, Biolegend), anti-CD19-PE/Cy7 (anti-human [H13B19/302216], BioLegend), anti-CD5-PE (anti-human [UCHT2/300608], Biolegend), Hoechst 33342 (H3570, Invitrogen) and annexin V (A13201, Life Technologies). The primary antibodies used for Western blot analyses were as follows: acetyl-histone H3 rabbit antibody (Lys627, Cell Signaling Technology, #8173T), histone H3 mouse antibody (Cell Signaling Technology, #14269S), phospho-STAT5 rabbit antibody (Tyr694, Cell Signaling Technology, #9351S), STAT5 rabbit antibody (Cell Signaling Technology, #34662), phospho-PLCy1 rabbit antibody (Tyr683, Cell Signaling Technology #14008S), PLCy1 rabbit antibody (Cell Signaling Technology #5690), β -actin mouse antibody (Santa Cruz Biotechnology, #SC-47778), anti-rabbit IgG, HRP-linked ab (Cell Signaling Technology, #7074), anti-mouse IgG, HRP-linked ab (Cell Signaling Technology, #7076S).

7.8. Statistical analysis

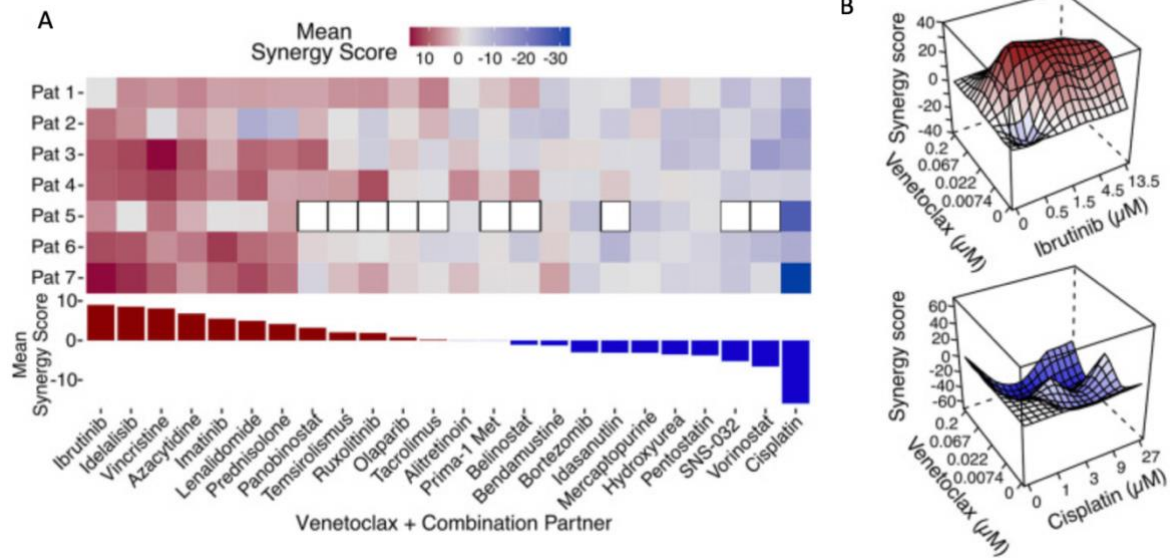
Using GraphPad Prism 8, two paired groups (same samples but different conditions) were compared by a paired t test, while unpaired groups were compared using an unpaired t test. Multiple groups were compared using an ANOVA for repeated measures. In all figures, paired samples are linked by a line. The correlation between two variables was analyzed using a simple linear regression. Two-tailed nominal $p \leq 0.05$ was considered significant. In each figure, ns (not significant) = reported p-value greater than 0.05, * = $p \leq 0.05$, ** = $p \leq 0.01$, *** = $p \leq 0.001$ and **** = $p \leq 0.0001$.

8. Results

8.1. Combinatorial Drug Screening shows possible synergy with venetoclax

To identify promising combination partners to enhance the efficacy of venetoclax in T-PLL patients, as detailed in the introduction, we first selected candidate compounds based on approval status, T-PLL biology and suggested mechanisms of drug action. Functional drug screening using venetoclax in pairwise combination with 25 selected drugs revealed ibrutinib as the most potent partner in primary T-PLL samples (Figure 5 A and B). Interestingly, ibrutinib single agent activity was very modest, analogous to previous reports. (Oberbeck *et al.*, 2020)

Figure 5: Ibrutinib synergizes with venetoclax in T-prolymphocytic leukemia in a drug screening based on CTG approach. (A) Heatmap demonstrating deviation from the Bliss independence score for each combination and individual patients (n=7). Synergy is denoted in red while antagonism is shown in blue. Clear boxes represent missing data for Patient 5 whose material was only screened for a subset of drugs due to sample availability. The bar plot in the lower half shows the synergy score as a mean over all patients. Drug synergy was calculated using the Synergy finder R package by integrating data of three independent runs. (B) A representative three-dimensional drug synergy plot (data from Patient 7) for ibrutinib and cisplatin with venetoclax.

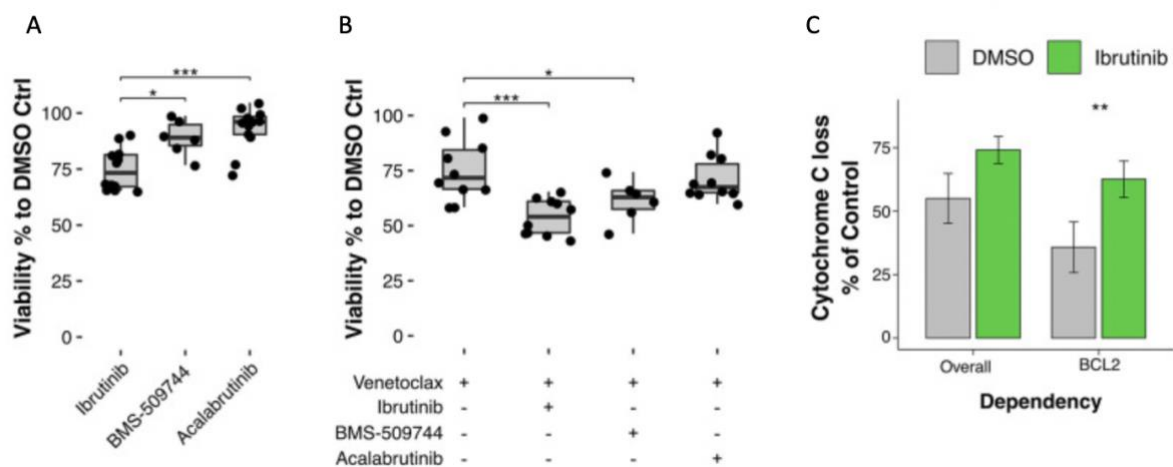


Nevertheless, single agent treatment with BMS-509744, a specific ITK inhibitor, has been demonstrated to be ineffective in primary T-PLL cells.(Dondorf, Schrader and Herling, 2015) To elucidate the mechanism of the combinatory effect, we treated primary T-PLL samples with ibrutinib, BMS-509744 or acalabrutinib (specific BTK inhibitor) alone (Figure 6 A) or in combination with venetoclax (Figure 6 B). In contrast to BTK specific inhibition, only ITK inhibitors, ibrutinib and BMS-509744 enhanced BCL2-inhibitor induced cell death. Dynamic BH3-profiling of primary T-PLL samples ex vivo demonstrated enhanced overall and BCL2 dependent apoptotic priming upon ibrutinib treatment (Figure 6 C). These data provide the first evidence that ITK-dependent apoptotic resistance in T-PLL is critical in mediating BCL2 inhibitor resistance.

*Figure 6: Ibrutinib synergizes with venetoclax via inhibition of ITK and enhances BCL2-dependent apoptotic priming. (A) Annexin V assay showing viability compared to that with a DMSO control for ibrutinib (n=12 different T-PLL patient samples), ITK-inhibitor BMS-509744 (n=6), and BTK-inhibitor acalabrutinib (n=12, Wilcoxon-Mann-Whitney test, ***P<0.001,*

* $P < 0.05$, all compounds tested at 10 μM with drug exposure for 24 h under NKtert co-culture).

(B) Annexin V assay demonstrating viability of T-PLL samples under NKtert co-culture treated with venetoclax alone ($n=10$), or in combination with ibrutinib ($n=10$), BMS-509744 ($n=6$), and acalabrutinib ($n=10$) compared to DMSO-Ctrl. (t-test, ibrutinib, acalabrutinib and BMS-509744 were used at a dose of 10 mM with drug exposure for 24 h, venetoclax was used at a dose of 100 nM with drug exposure for 4 h both as a single agent and in combination. After annexin V/Hoechst staining, cells were fixed with paraformaldehyde and analyzed using a BD Fortessa with a 96-well HTS plate-reader. NKtert cells were excluded using forward and side scatter parameters. Primary antibodies were directed against cytochrome c (Alexa Fluor 488-labeled, 6H2.B4/612308, Biolegend), CD19 (PE/Cy7-labeled, H13B19/302216, BioLegend), anti-CD5 (PE-labeled, UCHT2/300608, Biolegend). The analysis was performed on the CD5+CD19- cell fraction. (C) BH3-profiling in primary T-PLL samples treated with ibrutinib: cytochrome C release compared to control for overall mitochondrial priming and specific BCL2-dependence is shown for samples treated with either DMSO or ibrutinib 10 mM for 24 h (t-test). T-PLL: T-prolymphocytic leukemia; DMSO: dimethylsulfoxide; Ctrl. Control.

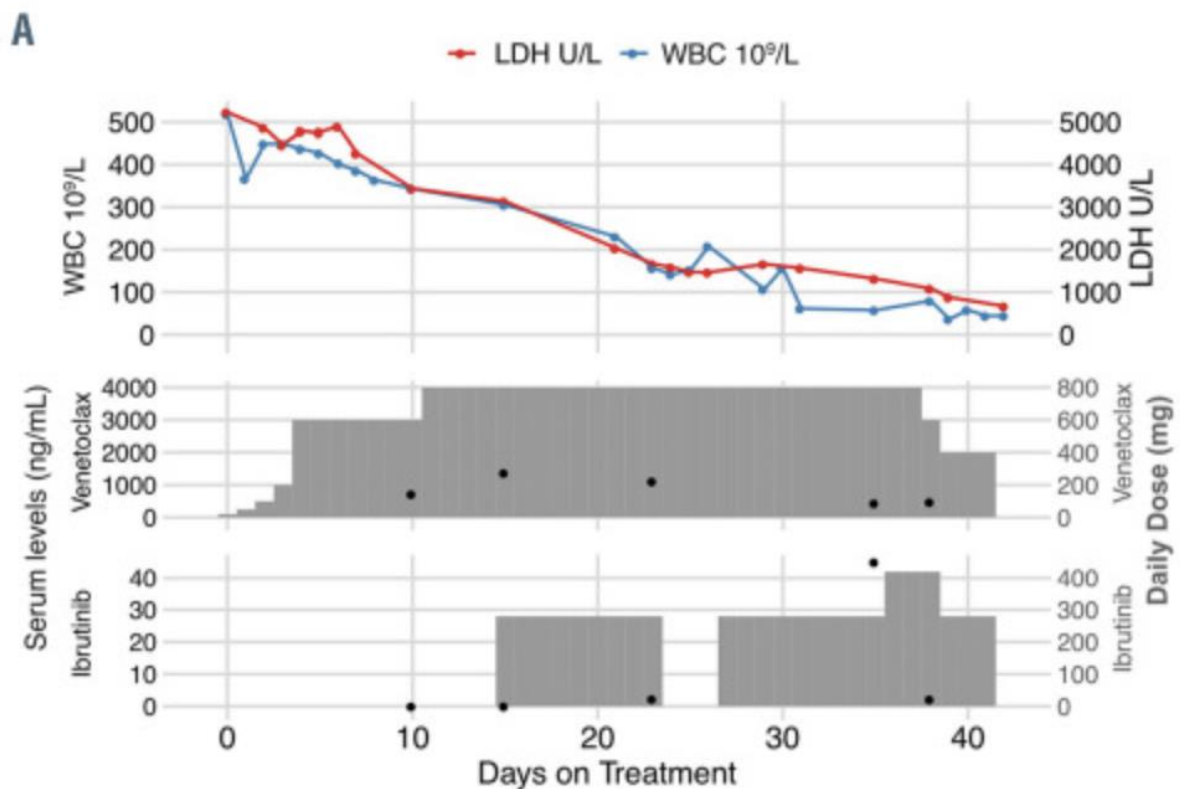


8.2. Co-Treatment of two patients with venetoclax and ibrutinib

Based on our in-vitro findings, we initiated combined treatment of venetoclax and ibrutinib in two alemtuzumab relapsed/refractory T-PLL patients. Both patients presented with active disease after multiple treatment lines and had no further treatment options available. Patient 1 (male aged 78) was admitted with relapsed T-PLL after three previous treatment lines (alemtuzumab monotherapy, alemtuzumab + FCM, re-challenged with alemtuzumab monotherapy) and presented with dyspnea, white blood cell count (WBC) at 519 G/L, elevated lactate dehydrogenase (LDH, 5230 U/L), fever and splenomegaly (diameter: 26cm). Venetoclax treatment was started with a daily ramp-up from 20 mg to 800mg, which was well tolerated. However, the clinical response was limited with WBC still above 300 G/L and LDH above 3000 U/L. When co-treatment with ibrutinib at a dose of 420mg was initiated both, WBC and LDH continued its regression (Figure 7 A). The overall clinical condition improved, and the spleen size decreased to 22cm after 20 days of treatment. Serum levels of venetoclax and ibrutinib were continuously monitored. The course of patient 1 was complicated by an influenza A infection and subsequent pneumonia requiring episodes of hospitalization, and mechanic respiratory support resulting in discontinuation of anti-T-PLL therapy. After the infectious episode, therapy was reinitiated, however treatment adherence dropped, and the patient was lost to follow-up.

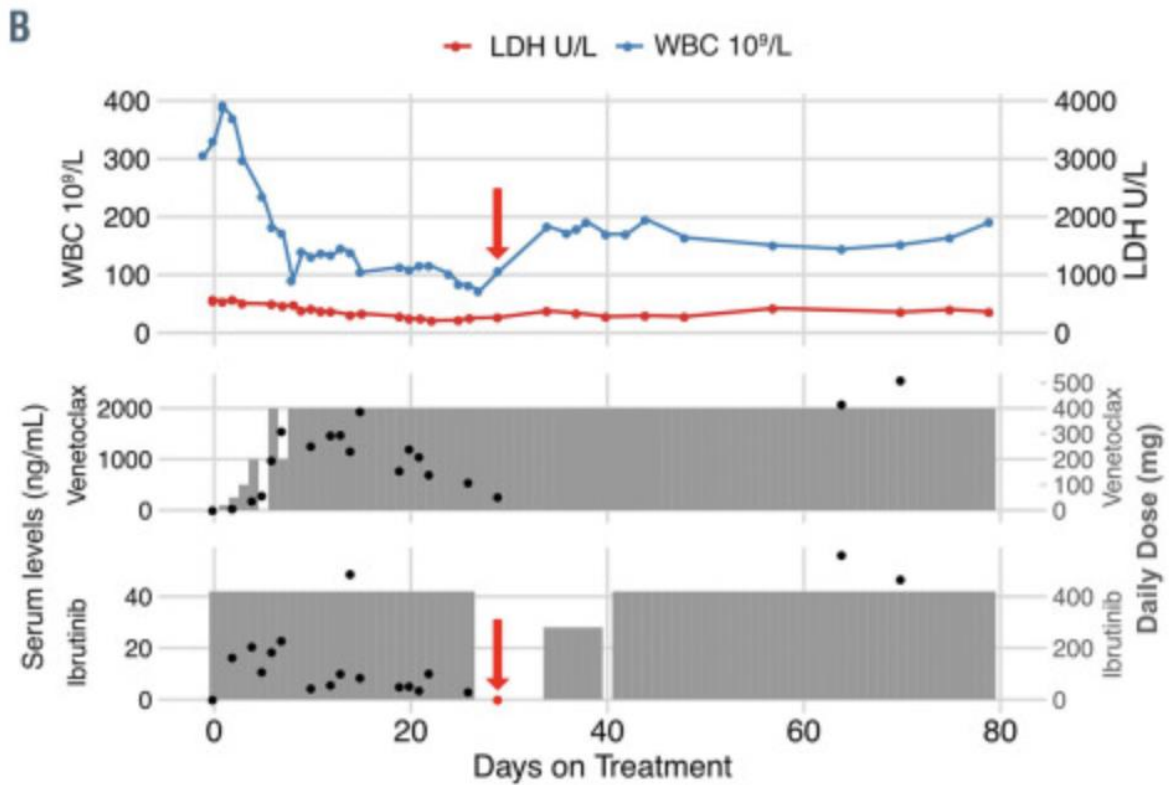
Figure 7 A and B: Clinical follow-up of two patients treated with the combination of ibrutinib and venetoclax. Patient A (A) and patient B (B). The WBC count and LDH concentration are plotted as blue and red lines, respectively. The lower part of each panel represents drug serum levels as black dots and drugs given as gray rectangles. Drug levels were determined by mass

spectrometry. The red arrow denotes the time point at which the serum ibrutinib concentration dropped below the level of detection with a concomitant rise of WBC. WBC: white blood cell; LDH: lactate dehydrogenase.



Patient 2 (female, aged 75) had a refractory T-PLL that was referred from another hospital where she previously was treated with CHOP, and was then re-challenged unsuccessfully with alemtuzumab. She clinically presented with dyspnea, pleural effusion, leukocytosis (WBC) of 300 G/L and elevated LDH. Ibrutinib was started at a dose of 420mg one day before venetoclax daily ramp-up from 20mg to 400mg. The combination of ibrutinib and venetoclax led to a rapid reduction of WBC, LDH and improvement of clinical status (Figure 7 B). After 3 weeks on treatment patient 2 experienced an intracranial hemorrhage leading to a pause of ibrutinib. Consequently, serum levels of ibrutinib dropped to undetectable levels

with concomitant increase of WBC. After the intracranial bleeding resolved without further intervention, ibrutinib was reinstated leading to stabilization of WBC. However, 3 weeks later patient 2 developed a respiratory infection and eventually succumbed to a pneumonia.

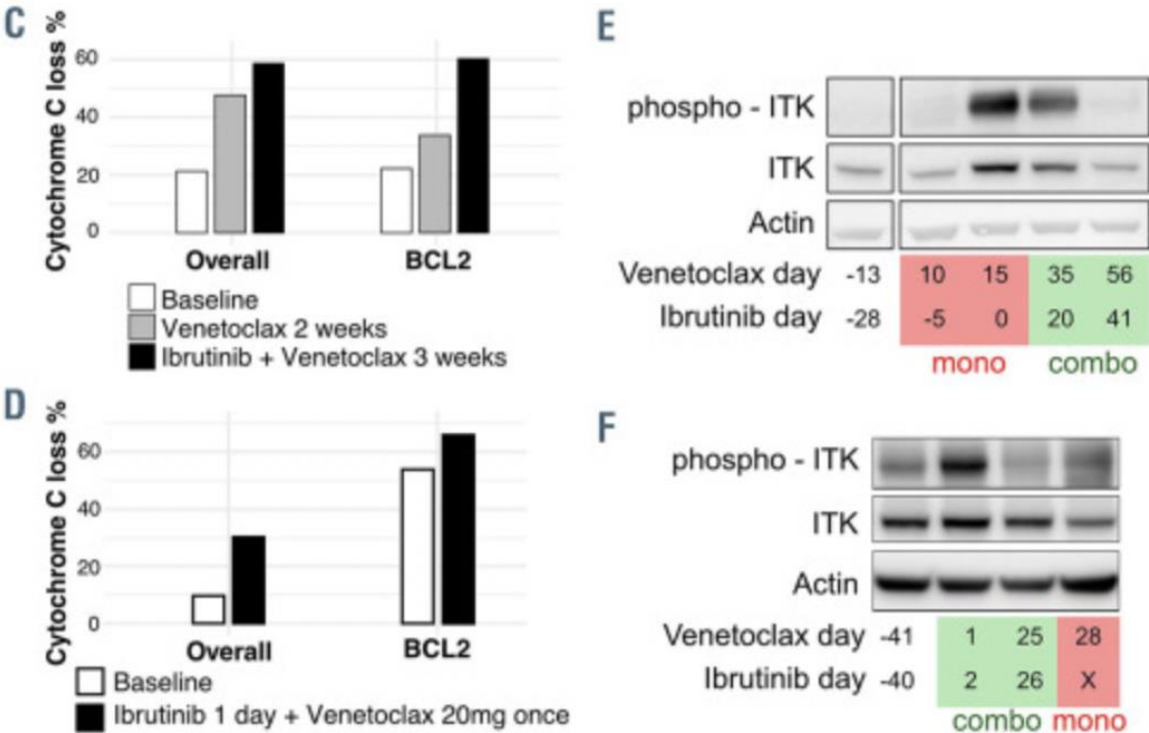


8.3. Ibrutinib is reducing ITK activity and enhancing BCL2 dependency in vivo

Dynamic BH3-profiling in vivo, that is of patient samples while on treatment, showed increased overall apoptotic priming by ibrutinib driven by an enhanced dependency on BCL2. This effect seems to be favored by venetoclax (Figure 7 C), which is in accordance with our ex-vivo data on T-PLL samples (Figure 6 B). Venetoclax treatment alone led to the induction of both, phosphorylated and total ITK. This effect could be abrogated by addition of ibrutinib (Figure 7 D). Intracellular TCR signaling via increased phospho-ITK expression was associated

with inferior clinical courses in T-neoplasms and ITK inhibition could prime apoptosis of malignant T-cells by downregulating anti-apoptotic proteins including BCL-2. (Liu *et al.*, 2019) Our data demonstrate that prolonged exposure to venetoclax led to BCL-2 upregulation and ITK activation, which resulted in loss of clinical response. Co-treatment with ibrutinib reduced ITK activity, increased BCL-2 dependent apoptotic priming, and restored the activity of venetoclax (Figure 7 E and F).

Figure 7 C to F: (C, D) In vivo BH3 profiling of primary patients' samples during co-treatment: patient A (C) and patient B (D). (E, F) Western blot analysis of primary cells showing changes in protein levels of ITK and phospho-ITK during co-treatment of patient A (E) and patient B (F).



These results prompted the initiation of the first international multicenter clinical study in T-PLL, the VIT-trial (NCT03873493) testing the combination of venetoclax and ibrutinib in r/r-T-PLL in a larger patient cohort. However, this trial was stopped prematurely due to lack of efficacy. We therefore wished to use another methodology to highlight T-PLL vulnerabilities.

8.4. T-PLL cells are relatively unprimed for apoptosis and have heterogeneous dependence on BCL-2 and MCL-1.

BH3 profiling has previously helped to characterize the BCL-2 family interactions of a variety of hematologic malignancies, for example in CLL, where relatively uniform BCL-2 dependence provided a strong rationale for exploring BCL-2 inhibition with venetoclax. (Del Gaizo Moore *et al.*, 2007; Davids *et al.*, 2012) To help identify potential pharmacologic vulnerabilities in T-PLL, we performed the first study of BH3 profiling in T-PLL utilizing primary samples collected from 24 patients. Patient characteristics are described in Table 2 (detailed cytogenetic and molecular data in Table 3).

Table 2: Mutational status of ATM and JAK/STAT associated with patient demographic and clinical diagnostic and prognostic information. Deletions or point mutations in the 11q23 locus or ATM gene, respectively, are indicated. For ATM, "*" indicates a variant of undetermined significance or a rare single-nucleotide polymorphism (SNP). Karyotypic or immunohistochemical evidence of rearrangements involving the TCL1A/B or MTCP1 loci are indicated. The presence of one or more mutations of genes in the JAK/STAT pathway are indicated. Patient #, patient number; F, female; M, male; PB, peripheral blood; abn, abnormality; chr, chromosome; "-", no chromosome abnormality detected; NA, not available.

Table 3: Detailed karyotypes and mutations of ATM and genes of the JAK/STAT pathway. For ATM, "*" indicates a variant of undetermined significance or a rare single-nucleotide polymorphism (SNP). NA, not available; abn, abnormality; chr, chromosome; "-", no chromosome abnormality detected; FISH, fluorescent in situ hybridization.

Patient	Sex	Age at diagnosis, y	PB lymph count at sample date, x10 ⁹ /L	Phenotype	14q11 abn or TCL1+	Iso(8)(q10)	ATM chr abn	ATM mutation	JAK-STAT mutated	Treatment-naive sample
1	M	80	11	CD4+CD8-	t(14;14)	N	Deletion	WT	JAK3	Yes
2	M	77	91	CD4+CD8+	inv(14)	Yes	—	K2413R*	STAT5B	Yes
3	M	86	54	CD4+CD8-	TCL1+	N	Deletion	K2700_D2703delinsN	STAT5B/JAK3	Yes
4	M	70	37	CD4+CD8-	NA	NA	NA	R3008C	STAT5B	Yes
5	F	70	54	CD4+CD8-	TCL1+	No	Deletion	G2765S*	STAT5B/JAK3	Yes
6	M	73	56	CD4+CD8-	inv(14)	No	Deletion	WT	JAK3	No
7	F	71	25	CD4+CD8-	TCL1+	No	—	WT	WT	Yes
8	F	65	82	CD4+CD8-	NA	NA	NA	WT	JAK3	Yes
9	M	64	14	CD4+CD8+	inv(14)	Yes	Deletion	R2032G	JAK3	Yes
10	M	53	179	CD4+CD8-	TCL1+	Yes	Deletion	L2633Ter	JAK3	Yes
11	M	68	300	CD4+CD8+	t(X;14)	No	—	WT	STAT5B/JAK3	Yes
12	M	69	17	CD4+CD8-	TCL1+	No	—	A3006V*	JAK3	Yes
13	F	66	5	CD4+CD8+	inv(14)	No	Deletion	WT	WT	Yes
14	M	65	16	CD4+CD8+	TCL1+	Yes	Deletion	L1328W*	WT	Yes
15	F	79	13	CD4+CD8-	inv(14)	No	Deletion	F2732_N2736del	JAK1	Yes
16	F	97	534	CD4+CD8+	NA	NA	NA	D148R	STAT5B/JAK3	Yes
17	F	67	14	CD4+CD8-	NA	NA	NA	T1029N	JAK3	Yes
18	F	59	130	CD4+CD8-	inv(14)	No	—	WT	JAK3	Yes
19	M	64	8	CD4+CD8-	TCL1+	No	—	WT	WT	Yes
20	M	74	348	CD4+CD8-	inv(14)	No	—	K1033T	WT	No
21	M	22	18	CD4+CD8-	inv(14)	Yes	—	T910Y	STAT5B	Yes
22	M	86	205	CD4+CD8+	TCL1+	Yes	Deletion	NA	STAT5B	Yes
23	F	63	12	CD4+CD8-	inv(14)	Yes	—	V2727G	JAK3	No
24	F	60	499	CD4+CD8+	t(14;14)	No	—	NA	JAK3	Yes

Patient #	Sex	TCL1 +	iso(8)(q10)	ATM chr abn	ATM mutation	JAK-STAT mutated	Detailed karyotype and FISH description
1	M	t(14;14)	no	deletion	wt	JAK3 M511I	44,XY,del(6)(q15q25),+6,add(10)(p12),del(11)(q13),t(14;14)(q11;q32),add(15)(p11),+20,-21,-22x2[3] / 44,idem,i(8)(q1.0)[6] / 46,XY [1]
2	M	inv(14)	yes	-	K2413R*	STAT5B N642H	complex karyotype with 10 to 13 abnormalities per cell including: i(8)(q10) and inv(14)(q11q32), full description not available
3	M	TCL1 +	no	deletion	K2700_D2703delinsN	STAT5B N642H; JAK3 M511I	44-46,Y,der(X)t(X;?)(q24;?),der(3)t(3;?)(p13;?)-5,-7,-11,der(11)t(8;11)(q21;p15)del(11)(q14q22),-14,-16,+3-5mar[cp20] ish 84% deletion of ATM-2 in 11q22; 88% trisomy cMyc in 8q24; 94% rearrangement of locus TRA/D in 14q11(chromosome 14 inversion)
4	M	NA	NA	NA	R3008C	STAT5B T628S	NA
5	F	TCL1 +	no	deletion	G2765S*	STAT5B Y665F; JAK3 A573V	46,XX,del(6)(q12q14),add(7)(q32),der(8)t(8;8)(p21;q13),del(11)(q14q25),-14,add(22)(q13),+mar[7]/46,sl,add(11)(p12),add(17)(p12)[2]/46,XX[1].ish add(7)(q32)(TCRB-),inv(14)(q11)(G36107+,G35927-)(q3?2)(G35927+)[20],add(17)(p12)(TP53+)[10]
6	M	inv(14)	no	deletion	wt	JAK3 M511I	47,XY,add(1)(p36),del(2)(q24q33),+3,der(7)add(7)(p15)add(7)(q31),del(11)(q21q23),inv(14)(q11q32),add(15)(p12),-20,-21,+ider(?),+mars[9]/47,s1,add(12)(p12)[3]
7	F	TCL1 +	no	-	wt	wt	46,XX[20]. nuc ish(TCRA/Dx2)(5'TCDRA/D sep 3'TCRA/Dx1)[110/200],(TCL1Ax2)(5'TCL1A sep 3'TCL1Ax1)[90/150],(D11Z1,ATM)x2[200]
8	F	NA	NA	NA	wt	JAK3 M511I	NA
9	M	inv(14)	yes	deletion	R2032G	JAK3 K563_M566 del	46~47,XY,add(2)(q33),-4,t(4;15)(q13;p13),i(8)(q10),+i(8)(q10),-11,del(11)(q13),-14,inv(14)(q11q32),-17,-22,+mar1,+mar1,+mar3[cp7]/46,XY[2]; FISH: nuc ish(TRD/TRAx2)(RP11-242H9 sep RP11-447G18x1)[90/200]

10	M	+	TCL1 yes	deleti on	L2633Ter	JAK3 A573V	45-46,X,- Y,i(8)(q10),add(10)t(10;14)(q24;q11),del(11)(q14),+12[5],add(12)(p11)[13],add(12)(q24) [5],-13,-14,add(17)(q25),-21,add(21)(p11),+2-3mar[cp18]/46,XY[2]. nuc ish(TCRA/Dx2)(5'TCDRA/D sep 3'TCRA/Dx1)[120/200],(TCL1Ax2)(5'TCL1A sep 3'TCL1Ax1)[100/150]
11	M	t(X; 14)	no	-	wt	STAT5B N642H; JAK3 M511I	42,t(X;14)(q28;q11),-Y,t(1;3)(p1?3;q2?4),-5,- 6,del(8)(p12),der(9)t(9;14)(q34;q11),add(11)(q?21),?dic(?6;12;?),-22[8]/46,XY[12] ish del17p[20]
12	M	+	TCL1 no	-	A3006V*	JAK3 M511I	46,XY,add(3)(q12),der(7)(15qter->15q12::?:7p15->7qter),add(15)(q11)[3]/46,XY,-8,- 13,-14,-14,-16,+5mar[3]/46,XY[14]
13	F	inv (14)	no	deleti on	wt	wt	44,X,add(X)(q27),add(3)(q21),der(5)(5pter->5q3 1::?:8q25->8q23::8q23- >8q25::?:14q11->14qter),-8,+add(11)(p13),del(11)(q12),r(11),-13,-14,i der(14)(q10)inv(14)(q11q32),-16,add(16)(q23),add(17)(q23),+mar[16] /46,XX [4].ish der(5)(MYC+,MYC+,TCRAD++,IGH+)[4],add(11)(D 1 1Z1+,ATM+),del(11)(D11Z1+,ATM- ,r(11)(D11Z1+,ATM-),i der(14)(IGH+,5' TCRAD+,3' TCRAD++,5' TCRAD+,IGH+),der(17)(TP53+,D17Z1+)
14	M	+	TCL1 yes	deleti on	L1328W*	wt	42,X,-Y,add(2)(q33),add(3)(q21),del(5)(p11),-6,del(7)(p21),i(8)(q10),-10,- 11,add(14)(q11),add(15)(p11),add(17)(p12),-18,-21,add(22)(q13),+3mar[10] nuc ish(TCRA/Dx2)(5'TCDRA/D sep 3'TCRA/Dx1)[90/200],(TCL1Ax2)(5'TCL1A sep 3'TCL1Ax1)[70/150]
15	F	inv (14)	no	deleti on	F2732_N2736d	JAK1 L653F	46,XY,der(2)t(2;22(p11)(q11) t(2;8),inv(14)(q11q32),del11(q13),der(22)t(2;22)
16	F	NA	NA	NA	D148R	STAT5B N642H; JAK3 A573V	NA
17	F	NA	NA	NA	T1029N	JAK3 M511I	NA

18	F	inv (14)	no	-	wt	JAK3 K563_C5 65 del	46,X,der(X)t(X;1)(p22;q21),add(7)(q34),der(14)add(14)(p11)inv(14)(q11q32), add(21)(p11)[7]/46,XX,der(8)t(8;8)(p23;q11),inv(14)(q11q32)[4]/46,XX[10]
19	M	TCL1 +	no	-	wt	wt	Del(6),add(16) [9/18] 82% rearrangement of locus TRA/D in 14q11(chromosome 14 inversion)
20	M	inv (14)	no	-	K1033T	wt	43~44,XY,add(1)(q21),add(4)(p15),-6,add(6)(q14),add(8)(p11),+add(8)(p11),- 9,add(11)(q13),add(12)(p12),-13,add(13)(q32),inv(14)(q11q32),-16,add(17)(q11),-18,- 20,-21,-22,+5~6mar,inc[cp19]/46,XY[1]
21	M	inv (14)	yes	-	T910Y	STAT5B N642H	46,XY,inv(14)(q11q32)[1]/44~45,sl,der(5)t(3;5)(p15;q21),i(6)(p10),+8,i(8)(q10), +i(8)(q10),-12,add(17)(q25),der(18)t(12;18)(q11;q23),-22,+mar[cp18]/46,XY[2]
22	M		yes	deleti on	NA	STAT5B N642H	41 -42,X,-Y,i(7)(q10),i(8)(q10),-11,-12,-13,-13,-14,-21,-22,+3-4mar,inc[cp20] 45, XX,+der(5)t(5;12)(p11;q11),t(6;17)(q25;q13),-6.i(8)(q10),-
23	F	inv (14)	yes	-	V2727G	JAK3 M511I	12,inv(14)(q11q32)[16]/46,XX ish.7p_del 6q_del 8q_amp 11q_amp 12p_del 13q14_del TCL1_translocation
24	F	t(14; 14)	no	-	NA	JAK3 Q507P	47,XY,t(4;20)(q31;p11),indic(8)(p11),+indic(8)(p11),der(9)t(p,14)(p24;q23),t(14;14)(q11; q32)

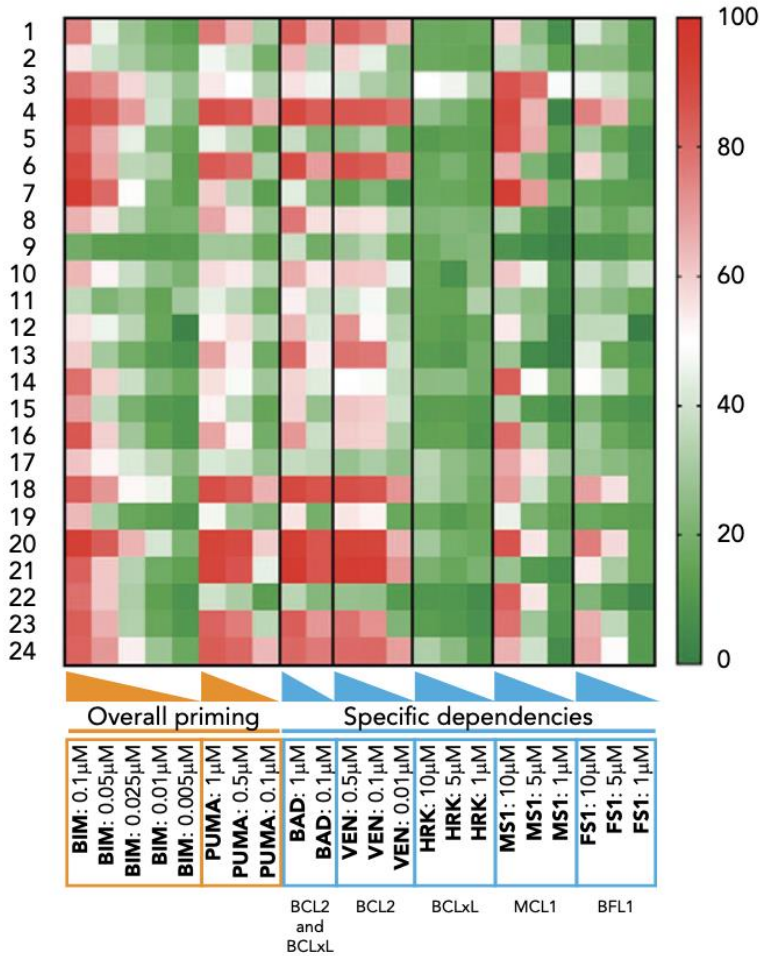
The baseline BH3 profiling was done right after thawing the tumor cells. A Trypan blue viability control was systematically performed, all samples with a viability below 50% were excluded (Table 4).

Table 4:

Final # (in the manuscript)	Initial patient #	Excluded samples	Viability after thawing (%)
1	1		79
2	2		72
3	3		84
4	4		60
5	5		64
6	6		76
7	7		84
8	8		65
9	9		70
	10	x	11
	11	x	19
	12	x	9
10	13		93
11	14		71
12	15		90
13	16		67
14	17		76
15	18		73
	19	x	20
16	20		81
17	21		67
18	22		82
19	23		85
20	24		90
21	25		87
22	26		73
23	27		90
24	28		83

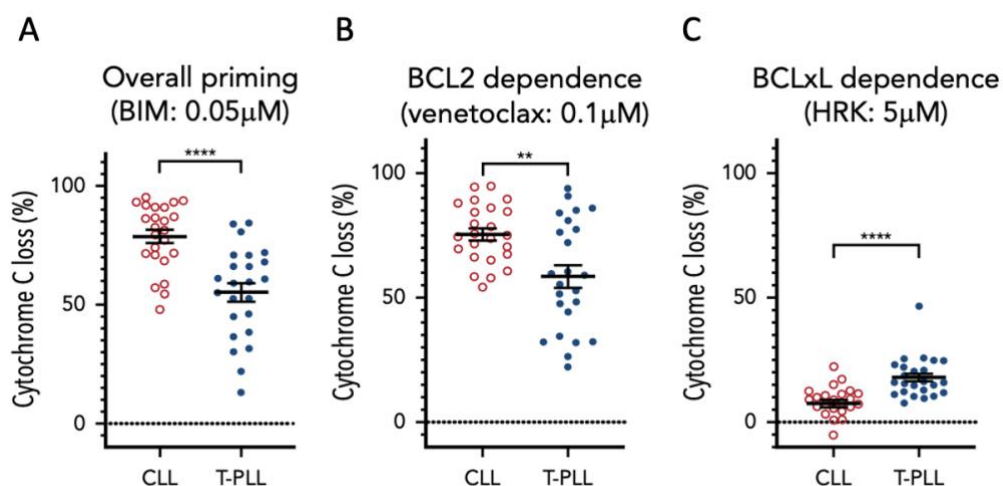
Significant heterogeneity was observed in the level of overall priming for apoptosis as well as in dependencies on individual anti-apoptotic proteins (Figure 8). Some T-PLL were mainly dependent on MCL-1 (e.g. T-PLL 3, 7 and 22), others were primarily dependent on BCL-2 (e.g. T-PLL 13, 15 and 21), and some were dependent on both MCL-1 and BCL-2 (e.g. T-PLL 4 and 20). No significant differences were observed between treatment naïve and relapsed samples, or between *JAK/STAT* mutated or unmutated samples (data not shown).

Figure 8: Heat map of the percentage of cyt c loss, as quantified by flow cytometry on 24 T-PLL patient samples at baseline. Each row is a sample, with the corresponding number, and each column refers to a BH3-only peptide or a tool compound with which the gently permeabilized cells were incubated for 60 minutes (green, lowest value; red, highest value).



Since the relative interactions of BH3 mimetics with the BCL-2 family are well characterized in CLL,(Davids *et al.*, 2012; Deng *et al.*, 2017b) (most notably venetoclax(Davids *et al.*, 2018)) we compared results from the T-PLL patients to an independent cohort of CLL samples, processed in the same conditions. Compared to primary CLL cells, T-PLL cells were less primed for apoptosis. The mean cytochrome c (cyt c) release with BIM BH3 peptide (which allows to measure overall apoptotic priming) was 55.2% for T-PLL vs 78.7% for CLL (Figure 9 A; $P < 0.0001$). Compared to CLL cells, T-PLL cells were less dependent on BCL-2 (Figure 9 B; average cyt c release with venetoclax 58.6% vs 75.4%; $P = 0.0019$), and more dependent on BCL-xL (Figure 9 C; average cyt c release with HRK 17.9% vs 7.5%; $P < 0.0001$). Dependence on MCL-1 or BFL-1 did not differ significantly between T-PLL and CLL (average cyt c release with; MS1 36.3% vs 37.5%, ns; FS1 28.4% vs 28.1%, ns). These data indicate that T-PLL cells are generally less primed for apoptosis than CLL cells, and depend on both BCL-2 and MCL-1.

Figure 9: Comparison with CLL. The percentage of cyt c loss for each of the 24 CLL (open circles) and 24 T-PLL (solid circles) samples. Unpaired Student *t* test; means \pm 6 standard error of the mean. The title of each panel denotes the parameter measured (overall priming and specific dependencies), as well as the peptide or tool compound used to probe it.

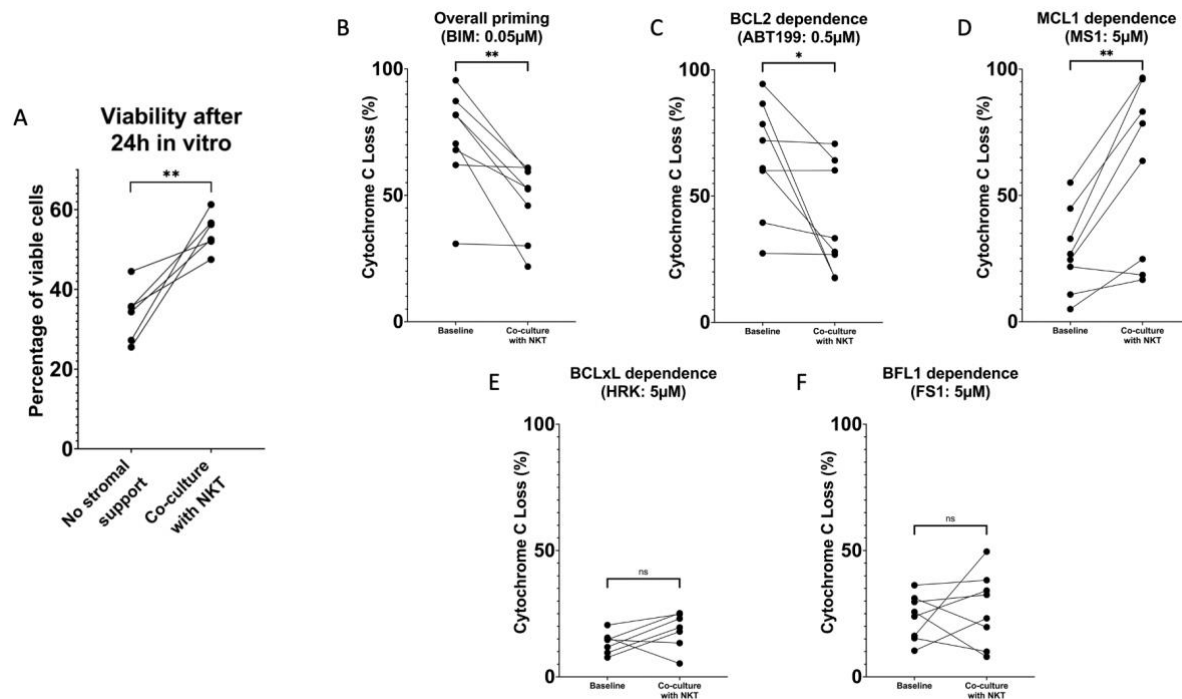


8.5. Stromal support promotes survival and reduces overall mitochondrial priming in vitro.

Preliminary assays of primary T-PLL cells *in vitro* without co-culture for 24 hours led to low cell viability making further analyses limited. Therefore, we explored co-culture with stromal cells to allow for increase *in vitro* T-PLL cell viability. As was previously demonstrated in CLL, we found that the survival of primary T-PLL cells *in vitro* also significantly increased with stromal co-culture, with a mean increase of 20.55% viability (Figure 10 A; P = 0.0047). Using the BIM BH3 peptide as a general measure of mitochondrial priming, stroma exposure induced decreased cytochrome C loss in T-PLL cells (n=8), with a mean decrease of 24.19% (Figure 10 B; P = 0.0054). This reduction appeared to be due primarily to a reduction in BCL-2 dependency, with a mean decrease between paired samples of 25.12% with venetoclax (Figure 10 C; P = 0.0384). Interestingly, MCL-1 dependency reciprocally increased, with a mean increase of 32.02% seen with MS1 peptide (Figure 10 D; P = 0.0053). No significant differences were observed with BCL-xL and BFL1 dependencies (Figure 10 E and 10 F; both ns). Given the robustness of T-PLL cell viability in these co-culture experiments, all further *ex vivo* experiments were performed with stromal support.

Figure 10: Stromal co-culture in vitro influence on viability and BH3 profiling. (A) Absolute viability values as a percentage of annexin V negative / Hoechst positive cells of 6 T-PLL samples after 24 hours in vitro in R10 with or without stromal support by co-culture with NKT. (B-F) Individual values of percentage cytochrome c loss for the 8 T-PLL samples. Each patient was profiled at baseline and after a 24h co-culture with NKT. The title of the panel gives the

measured parameter (overall priming and specific dependencies) as well as the peptide or tool drug used to measure it.



8.6. Pharmacological inhibition of BCL-2 and MCL-1 induces cell death

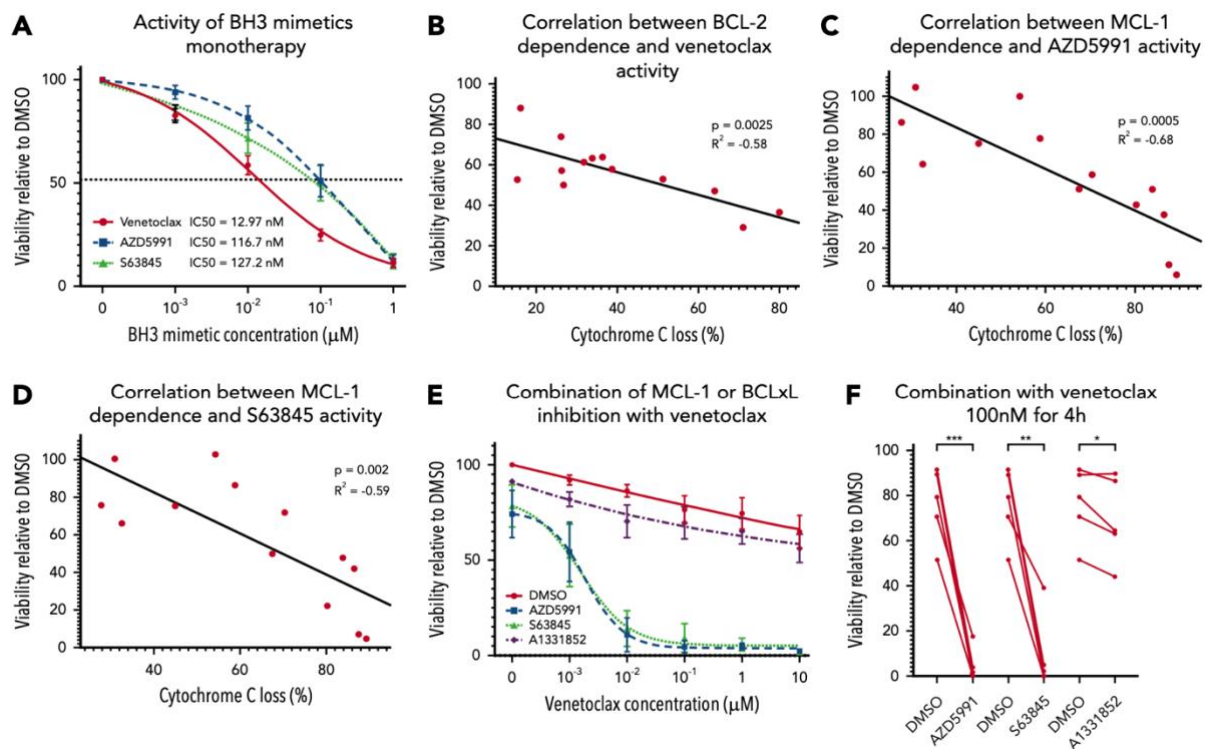
We next evaluated whether there is an association between anti-apoptotic dependencies in T-PLL cells and the efficacy of BH3 mimetic drugs selectively targeting BCL-2 and MCL-1. In the 13 primary T-PLL samples with sufficient cell count, 24h treatment with venetoclax or the MCL-1 inhibitors AZD5991 or S63845 was performed. Each inhibitor induced high levels of apoptotic cell death when utilized individually (Figure 11 A). Consistent with our BH3 profiling data, increased BCL-2 dependence was associated with increased apoptotic cell death induced by venetoclax (Figure 11 B; R^2 -0.58; P = 0.0025). Similarly, increased MCL-1 dependence was associated with increased apoptotic cell death induced by the MCL-1

inhibitor AZD5991 (Figure 11 C; R^2 -0.68; $P = 0.0005$) or S63845 (Figure 11 D; R^2 -0.68; $P = 0.002$).

Given predominant dependence on BCL-2 and MCL-1, we hypothesized that combining BH3 mimetic drugs targeting these two proteins could enhance cell death in T-PLL cells. Therefore, we treated cells for 24h with either DMSO (vehicle), AZD5991 100nM, S63845 100nM or the BCL-xL selective inhibitor A-1331852 1 μ M (as a control), and four hours prior to fixation, venetoclax was added at a range of doses from 1nM to 10 μ M. The addition of either AZD5991 or S63845 in combination with venetoclax led to markedly increased T-PLL cell death, whereas T-PLL cells were less sensitive to combination with A-1331852 (Figure 11 E). At an intermediate venetoclax dose of 100nM, combination with AZD5991 100nM reduced cell viability by a mean of 71.94% ($P = 0.001$; Figure 11 F). Likewise, pretreatment with S63845 (100nM) reduced viability by 67.28% ($P = 0.0037$), while A-1331852 1 μ M only modestly reduced cell viability by 6.91% ($P = 0.049$). The weak effect of A-1331852 drug treatment is consistent with the low mean cyt c release we observed with the HRK peptide at 5 μ M (17.9%, 95% CI 14.45-21.39) with BH3 profiling (Figure 9 C). Overall, these data indicate a good correlation of cell viability assays with baseline BH3 profiling and confirm BCL2 and MCL1 as molecular vulnerabilities in T-PLL.

Figure 11: Association between BH3 profiling and BH3 mimetic activity. (A) Induction of apoptosis shown as a percentage of viable (annexin V negative/Hoechst positive vs control) cells after 24-hour exposure to an increasing concentration of DMSO alone or a BH3 mimetic (1 nM, 10 nM, 100 nM, and 1 mM): venetoclax, AZD5991, or S63845 (n = 13; mean \pm standard error of the mean [SEM]). (B-D) Association between cyt c release induced by venetoclax at 0.1

mM (B) and MS1 peptide at 5 mM (C-D) with induction of apoptosis shown as a percentage of viable (annexin V negative/Hoechst positive) cells vs DMSO, after 24-hour exposure to venetoclax 10 nM (B), AZD5991 100 nM (C), or S63845 100 nM (D). Results show individual values for 13 different T-PLL samples and simple linear regression. (E) Induction of apoptosis shown as the percentage of viable (annexin V negative/Hoechst positive vs control) cells after 24-hour exposure to DMSO, AZD5991 100 nM, S63845 100 nM, or A-1331852 1 mM and 4-hour exposure to DMSO alone or an increasing concentration of venetoclax (1 nM, 10 nM, 100 nM, 1 mM, and 10 mM; $n = 5$; means \pm 6 SEM). (F) Same data set as in panel E, focused on venetoclax at 100 nM and showing individual values ($n = 5$; paired Student t test).



8.7. Belinostat and ruxolitinib selectively increase BCL-2 dependence

We next studied four inhibitors of candidate targets in T-PLL pathogenesis, ruxolitinib (JAK1/2i), ibrutinib (ITKi or other “off target”), PRN694 (ITKi), and belinostat (HDACi), as combination partners for BCL-2 or MCL-1 inhibitors. Even though IC50 of ibrutinib is higher than PRN694 on ITK, we included ibrutinib in our assays because its activity in T-PLL could be related to off target effects due to inhibition of other kinases. First, we have shown that ruxolitinib, PRN694 and belinostat were modulating their proposed targets in primary T-PLL samples (Supplemental Figure 12 and 13).

Figure 12: Effect of belinostat on proposed targets in primary T-PLL samples. (A) Densitometry analysis of the ratio of expression of Acetyl-Histone H3 to total Histone H3, in primary T-PLL samples. The samples were divided in two conditions, the first one exposed to the control (DMSO), the second one to belinostat 1 μ M for 4-hours (n=5; paired t-test). (B) Representative examples of the Western blot analysis of Acetyl-Histone H3 and total Histone H3 in 2 T-PLL samples (T-PLL 1 and 2) with and without treatment with belinostat 1 μ M, and without stromal support. β -Actin was used as the loading control. Molecular weights (in kDa) are indicated in the figure. Figures A and B show that treatment with belinostat significantly increases the level of acetylation of Histone H3 in T-PLL. (C) Densitometry analysis of the ratio of expression of acetyl-p53 (K382) to actin; as well as total p53 to actin, in primary T-PLL samples. The samples were divided in two conditions, the first one exposed to the control (DMSO), the second one to belinostat 1 μ M for 4-hours (n=7). (D) Western blot analysis of acetyl-p53 and total p53 in 7 T-PLL samples with and without treatment with belinostat 1 μ M, and without stromal support. β -Actin was used as the loading control. Molecular weights (in kDa) are indicated in the figure.

Figures C and D show that the HDACi belinostat significantly represses deacetylation of the tumor suppressor protein p53 in T-PLL. We also observed that this drug significantly increases total p53 expression levels, which could at least in part be explained by stabilization of p53 through its acetylation.

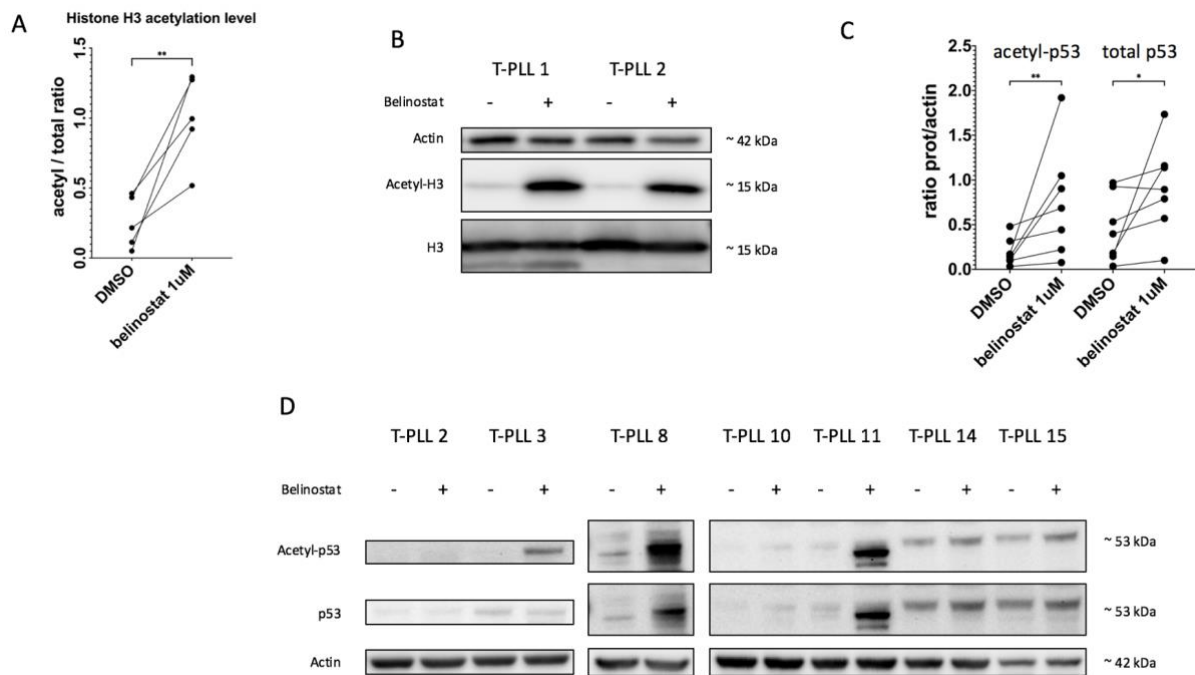
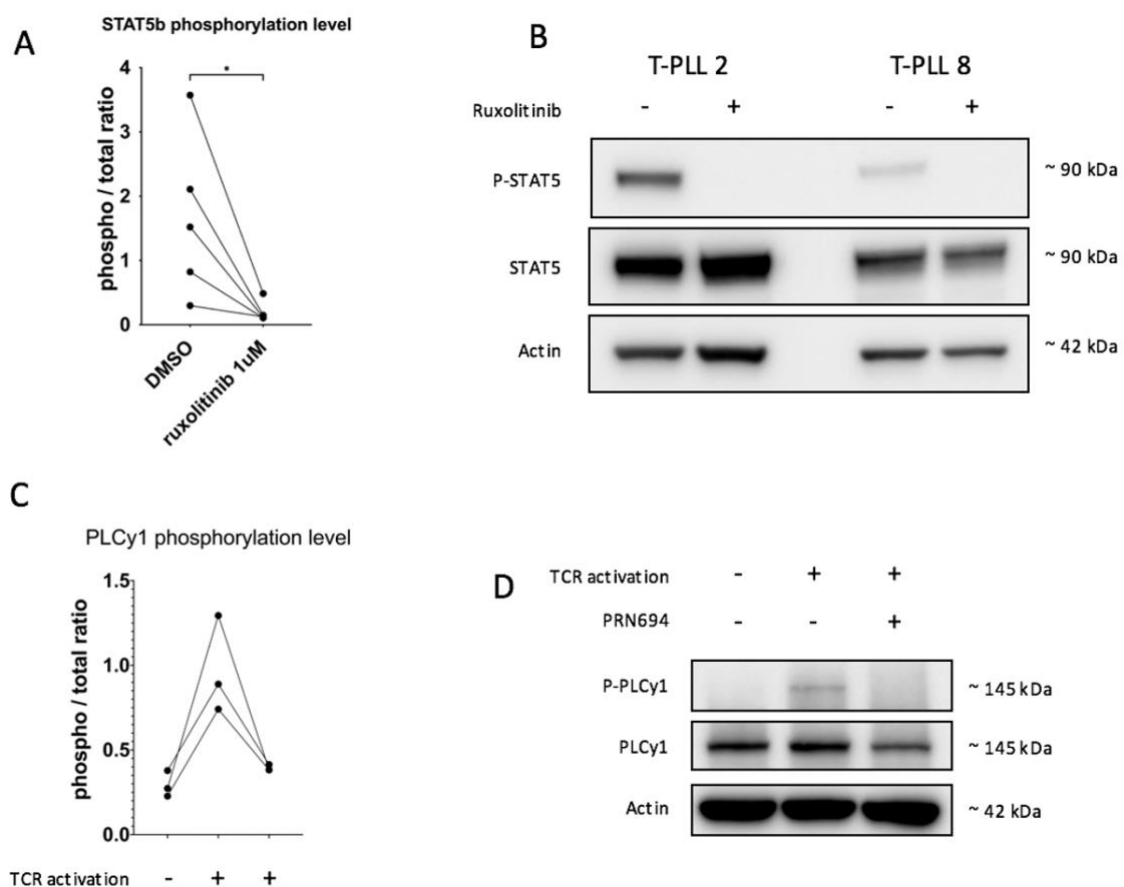


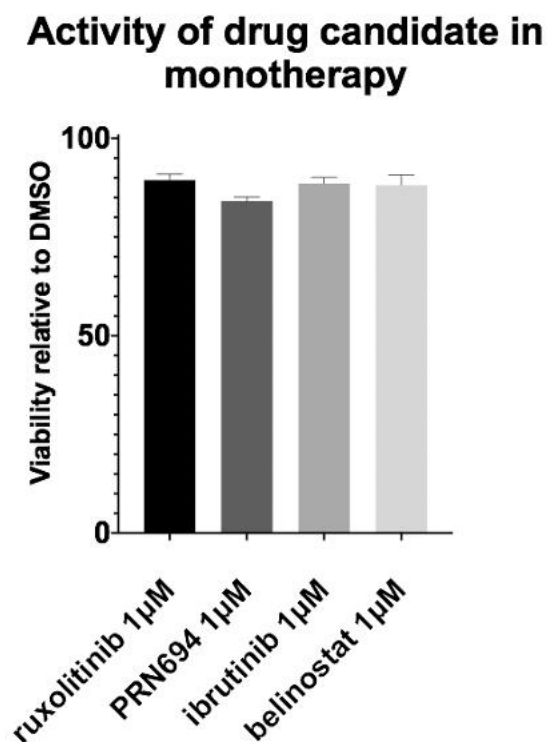
Figure 13: Effect of ruxolitinib and PRN694 on respective proposed target pathway in primary T-PLL samples. (A) Densitometry analysis of the ratio of expression of phospho-STAT5B to total STAT5B, in primary T-PLL samples. The samples were divided in two conditions, the first one exposed to DMSO, the second one to ruxolitinib 1 μ M for 4-hours (n=5; paired t-test). (B) Representative examples of the western blot analysis of phospho-STAT5 and total STAT5 in 2 T-PLL samples (T-PLL 2 and 8) with and without treatment with ruxolitinib 1 μ M, without stromal support. β -Actin was used as the loading control. Molecular weights (in kDa) are indicated in the figure. Figures A and B show a significant reduction of JAK/STAT pathway

baseline activation (measured on STAT5B phosphorylation level) under ruxolitinib treatment, in T-PLL harboring activating mutations of JAK3 or STAT5B. (C) Densitometry analysis of the ratio of expression of phospho-PLCy1 to total PLCy1, in primary T-PLL samples. The samples were divided in three conditions, the first one exposed to both control (saline and DMSO); the second one to TCR activation cocktail (anti-CD3, anti-CD28 and rabbit polyclonal antibody, the 3 compounds were used at 1 μ g/mL) and DMSO; the third one to TCR activation cocktail and PRN694 1 μ M, every condition for 4-hours without stromal support (n=3). (D) Representative example of the Western blot analysis of phospho-PLCy1 to total PLCy1 in a T-PLL sample (T-PLL 1) in the three described conditions. β -Actin was used as the loading control. Molecular weights (in kDa) are indicated in the figure. Figures C and D show that the ITKi PRN694 seems to inhibit the signal transduction of TCR activation (measured on PLCy1 phosphorylation level) in T-PLL.



However, unlike in prior studies where drugs (such as belinostat or ibrutinib) were used at higher doses of 10 μ M,(Andersson *et al.*, 2018) at the dose of 1 μ M in our co-culture model, none were cytotoxic to T-PLL cells as single agents (Figure 14).

Figure 14: drug candidate as single agent. Induction of apoptosis shown as percentage of viable (Annexin V negative / Hoechst positive, relative to control) cells after 24-hours exposure to ruxolitinib 1 μ M, belinostat 1 μ M, ibrutinib 1 μ M or PRN694 1 μ M in monotherapy (n = 24; mean with SEM).



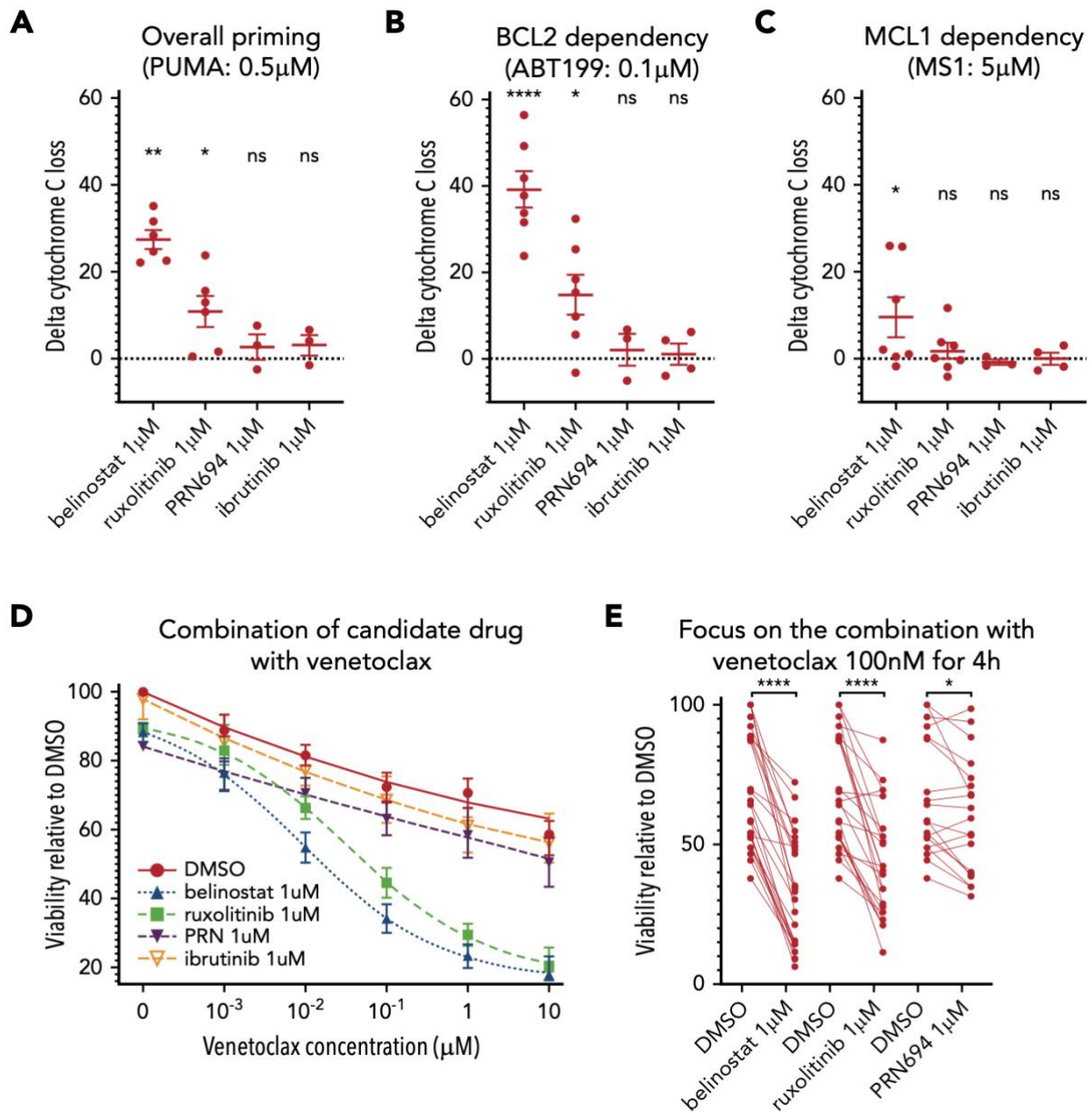
Nevertheless, given the importance of these pathways in T-PLL pathogenesis, we hypothesized that even if they did not induce frank cell death on their own, these drugs could augment mitochondrial priming through modulating anti-apoptotic protein dependence. To

evaluate this hypothesis, we performed dynamic BH3 profiling (DBP) after *ex vivo* treatment with each drug to assess the difference between the percentage of cyt c release with the control (DMSO) and each of the three drug candidates (“delta-priming”). Evaluating the overall priming with the PUMA peptide at 0.5 μ M (Figure 15 A), the mean delta-priming was 22.7% with belinostat (P = 0.0035), 8.48% with ruxolitinib (P = 0.019) and 2.72% with PRN694 (ns). Alteration of BCL-2 dependence was evaluated in the profile with venetoclax at 0.1 μ M (Figure 15 B), showing an increase in delta priming of 39.16% on average with belinostat (P <0.0001), 14.78% with ruxolitinib (P = 0.017) and 2.7% with PRN694 (ns). MCL-1 dependence was assessed with MS1 peptide at 0.5 μ M (Figure 15 C), showing an increase in delta priming by 11.04% with belinostat (P = 0.04), 1.74% with ruxolitinib (ns) and decreased by 0.82% with PRN694 (ns). We observed no significant effect of ibrutinib 1 μ M on overall priming or dependence on BCL-2 or MCL-1. Together, these data show that treatment with ruxolitinib or belinostat increases overall mitochondrial priming and BCL-2 dependence in T-PLL cells, but not MCL-1 dependence. No significant alteration of mitochondrial priming occurred with PRN694 or ibrutinib at the concentration of 1 μ M.

Next, we examined whether these findings with DBP could be corroborated with cell viability assays. Since DBP studies revealed stronger effects on BCL-2 dependence relative to MCL-1 dependence, we focused viability testing on venetoclax combinations. Primary samples were treated for 24h with either DMSO (vehicle), ruxolitinib 1 μ M, PRN694 1 μ M, or belinostat 1 μ M prior to fixation. Both ruxolitinib and belinostat were highly active in combination with venetoclax (Figure 15 D). Similar results were observed with an alternative HDACi (panobinostat; n=6; data not shown), whereas a minimal effect was observed with PRN694. Pretreatment with ruxolitinib 1 μ M in the presence of venetoclax 100nM reduced viability by

a mean of 25.8% ($P < 0.0001$; Figure 15 E). Pretreatment with belinostat $1\mu\text{M}$ reduced viability by 37.06% ($P < 0.0001$), whereas pretreatment with PRN694 $1\mu\text{M}$ reduced viability by 6.67% ($P = 0.01$). Consistent with our DBP data, pre-treatment with ibrutinib $1\mu\text{M}$ in the presence of venetoclax 100nM did not significantly reduce cell viability ($P = 0.35$). Collectively, the results of the viability studies are consistent with the DBP data, thus supporting that ruxolitinib and belinostat increase overall mitochondrial priming and BCL-2 dependence in T-PLL cells.

Figure 15: Influence of belinostat, ruxolitinib, PRN694, and ibrutinib on apoptotic priming and viability. (A-C) Impact of 24-hour exposure to $1\mu\text{M}$ belinostat, ruxolitinib, PRN694 or ibrutinib on BH3 profiling shown as delta percentage cyt c loss (delta = % loss T-PLL cells treated with drug – % loss T-PLL cells in DMSO). Results show individual delta values as well as means with SEM for 6 (belinostat), 7 (ruxolitinib), 3 (PRN694) and 4 (ibrutinib) different T-PLL samples (paired t-test). Overall priming was evaluated with the PUMA peptide at $0.5\mu\text{M}$ (A), BCL-2 dependency with venetoclax at $0.1\mu\text{M}$ (B) and BCL-2 dependency with MS1 peptide at $0.5\mu\text{M}$ (C). (D) Induction of apoptosis shown as percentage of viable (Annexin V negative / Hoechst positive, relative to control) cells after 24-hours exposure to DMSO (solid line), ruxolitinib $1\mu\text{M}$ (dashed line), belinostat $1\mu\text{M}$ (dotted line), PRN694 $1\mu\text{M}$ (dashed and dotted line) or ibrutinib $1\mu\text{M}$ (dashed and double dotted line) and 4-hour exposure to increasing concentrations of venetoclax (DMSO alone, 1nM , 10nM , 100nM , $1\mu\text{M}$ and $10\mu\text{M}$) ($n=24$; mean with SEM). (E) On the same dataset as panel D, focus on the venetoclax at 100nM , showing individual values of samples treated with ruxolitinib, belinostat and PRN694 ($n=24$; paired t-test).



8.8. Primary cells from JAK/STAT pathway mutated T-PLL are more sensitive to inhibition of JAK1 than of ITK

While no difference in the *ex vivo* activity of ruxolitinib, PRN694, ibrutinib or belinostat was observed according to *ATM* or *TP53* molecular status (data not shown), the activity of ruxolitinib in combination with venetoclax was significantly higher in the samples harboring

an activating mutation in the JAK/STAT pathway. The average ratio between viability with ruxolitinib plus venetoclax combination versus venetoclax monotherapy was 0.988 for the 5 patient samples without an activating mutation in the JAK/STAT pathway, and 0.483 for the 19 patient samples with a mutation ($P < 0.0001$; Figure 16 A). Activity of ruxolitinib in combination with venetoclax was significantly lower in samples with a downstream activating mutation of *STAT5B*. Pretreatment with ruxolitinib with venetoclax 100nM for 4h reduced viability by a mean of 23.82% in patient samples with a *STAT5B* mutation versus 42.90% in the patient samples with an isolated mutation of *JAK3* or *JAK1* ($P = 0.03$; Figure 16 B).

To better understand the mechanistic underpinnings of these differences, we measured the baseline activity of the JAK/STAT pathway by the level of phosphorylation of *STAT5B*. T-PLL cells harboring at least one JAK/STAT pathway mutation had a higher level of *STAT5B* phosphorylation compared to samples with no mutation ($n=7$ versus $n=2$ respectively; $P = 0.013$; protein quantification in Figure 16 C, representative examples in Figure 16 D and all 9 blots performed in Figure 17). No difference was observed according to *STAT5B* mutational status (data not shown). Conversely, the activity of PRN694 in combination with venetoclax was significantly higher in the samples without activating mutations in the JAK/STAT pathway, with a mean of 0.736 for the 5 patient samples without an activating mutation in the JAK/STAT pathway, and 0.956 for the 19 patient samples with a mutation ($P = 0.002$; Figure 16 E). No significant difference was seen in these subgroups with belinostat treatment (data not shown).

Figure 16: JAK/STAT molecular status influences efficacy of ruxolitinib and PRN694, as well as levels of *STAT5b* phosphorylation. (A) Induction of apoptosis shown as viability fold change.

Each point is one of the 24 T-PLL samples: 5 without any mutation in the JAK/STAT pathway, 19 with at least one mutation in this pathway. The values presented are the ratio between the viability (percentage relative to DMSO) with a combination treatment (ruxolitinib 1 μ M for 24h and venetoclax 100nM for 4h) versus the viability with monotherapy (venetoclax 100nM for 4h) (unpaired t-test; mean with SEM). (B) Induction of apoptosis shown as percentage of viable (Annexin V negative / Hoechst positive, relative to control) cells after 24-hours exposure to DMSO or ruxolitinib 1 μ M; and 4-hour exposure to venetoclax 100nM, showing individual paired values. The values on the left are those of the 8 samples presenting at least a mutation of STAT5B, the values on the right are those of the 11 samples presenting an isolated mutation of JAK3 or JAK1. The mean reduction of viability (measured as the delta viability between DMSO and ruxolitinib) is significantly larger in the 11 samples without STAT5B mutation (unpaired t-test). (C) Densitometry analysis of the ratio of expression of phospho-STAT5 to total STAT5, in 9 T-PLL samples (each point is labeled with the T-PLL #). The samples were divided in two groups, the first one included the 2 T-PLL without mutations in the JAK/STAT pathway genes, the second one included 7 T-PLL with at least one activating mutation in this pathway (unpaired t-test; mean with SEM). (D) Representative examples of Western blot analysis of phospho-STAT5 and total STAT5 in 4 T-PLL samples (T-PLL 3, 5 14 and 13) at baseline. β -Actin was used as the loading control. Molecular weights (in kDa) are indicated in the figure. (E) Induction of apoptosis shown as viability fold change, in the same 24 T-PLL samples. The values presented are the ratio between the viability (percentage relative to DMSO) with a combination treatment (PRN694 1 μ M for 24h and venetoclax 100nM for 4h) versus the viability with monotherapy (venetoclax 100nM for 4h) (unpaired t-test; mean with SEM).

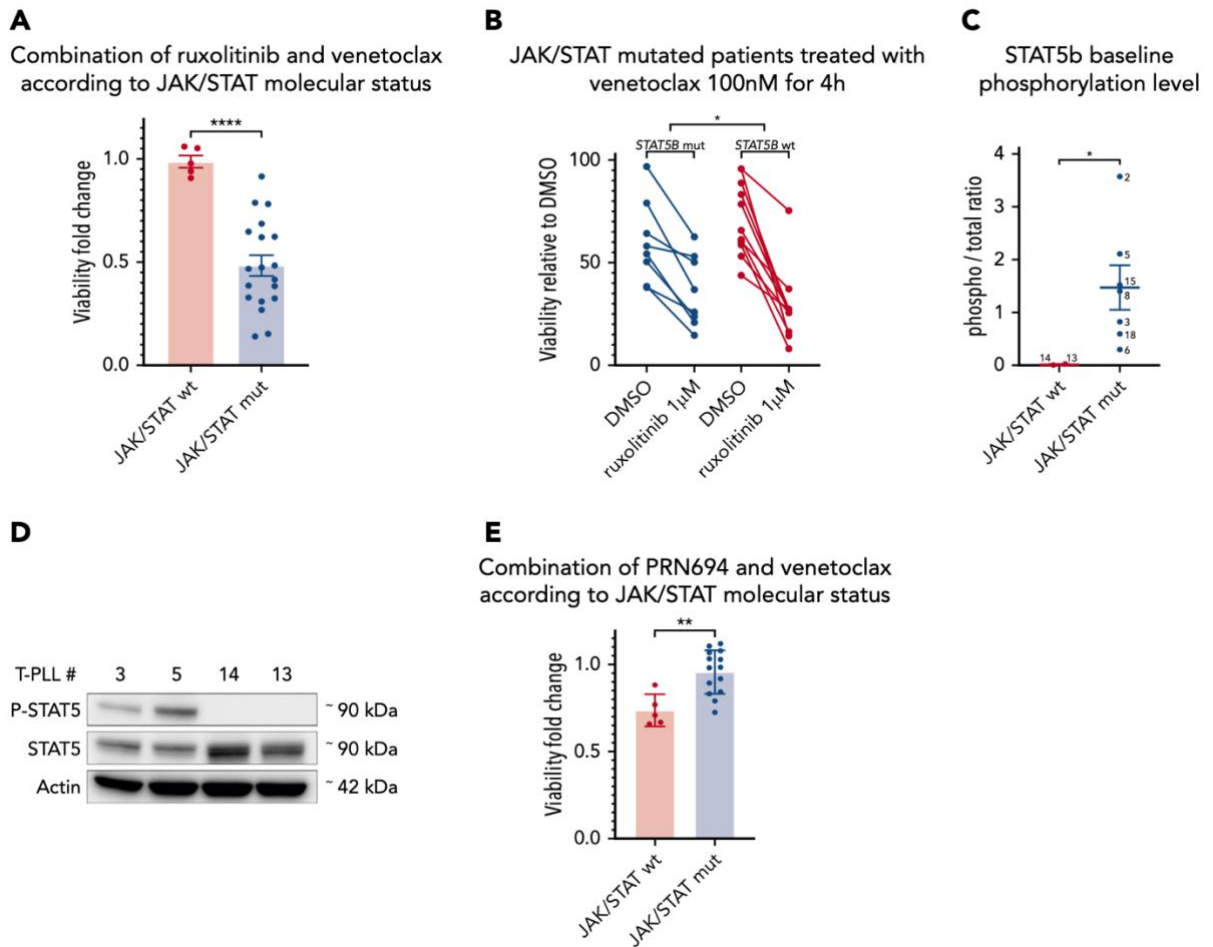
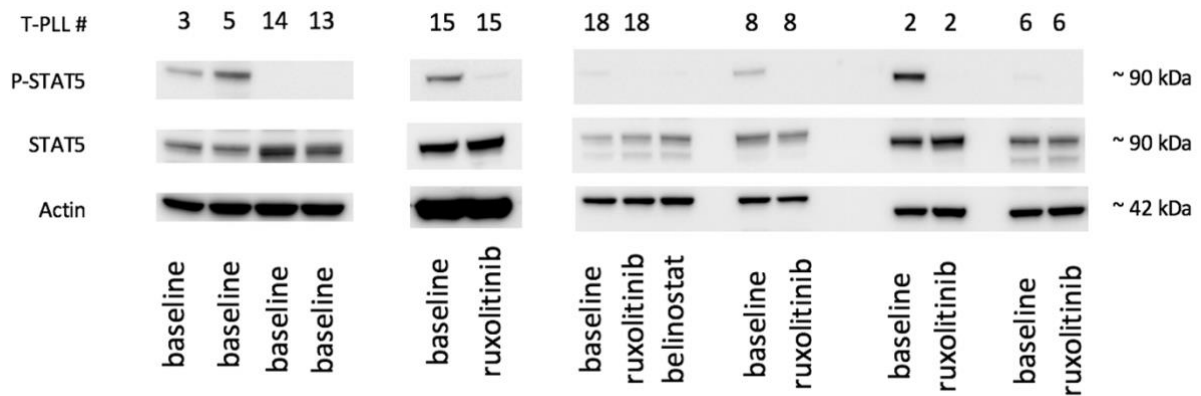


Figure 17: Baseline level of STAT5B phosphorylation. All performed Western blot analysis of phospho-STAT5 and total STAT5 in 9 T-PLL samples at baseline. β -Actin was used as the loading control. Molecular weights (in kDa) are indicated in the figure.



8.9. Venetoclax plus ruxolitinib was effective for two different refractory T-PLL patients

Based on our preclinical data, we treated two patients with refractory T-PLL for whom no standard treatment option was suitable with the combination of venetoclax and ruxolitinib. The patients' baseline characteristics and medical history are shown in Table 5.

Table 5: Medical history, diagnostic data and disease status of the 2 treated patients. Deletions or point mutations in the 11q23 locus or ATM gene, respectively, are indicated. F, female; M, male; abn, abnormality; chr, chromosome; “-”, no chromosome abnormality detected; FISH, fluorescent in situ hybridization.

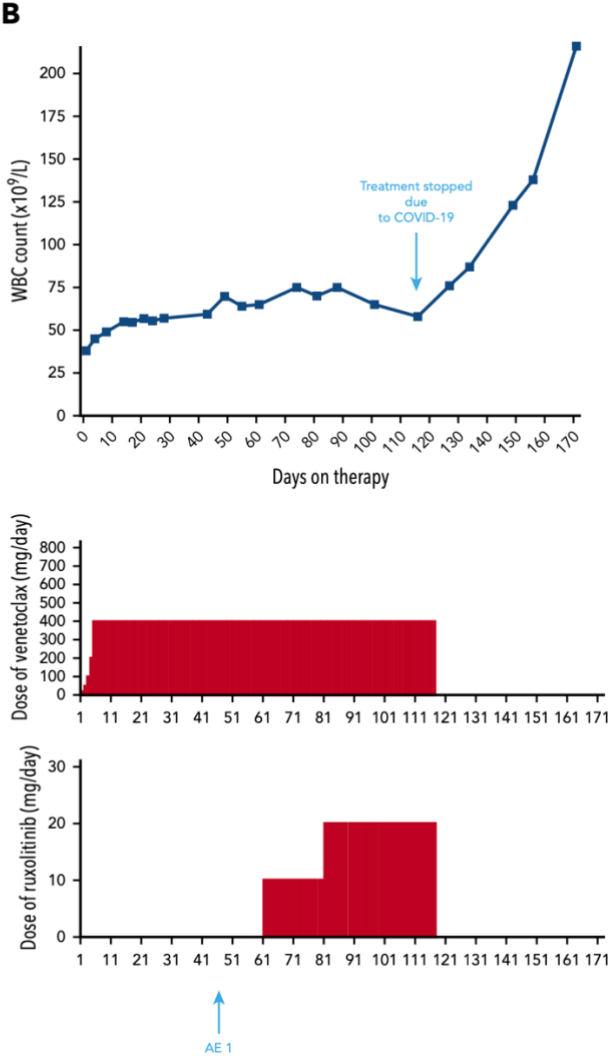
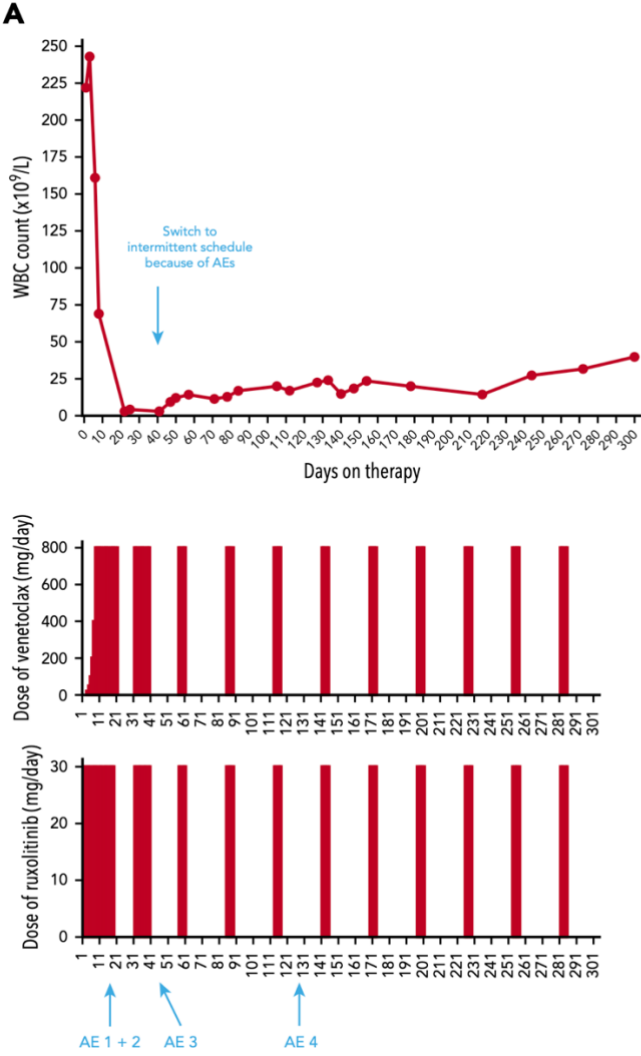
	Sex	Age at diag	Medical history	Phenotype	14q11 abn or TCL1+	ATM chr abn	ATM mut	JAK-STAT mut	Previous treatment status	Adverse events
Patient A (T-PLL 1 in Table 2)	M	80	· ischemic heart disease and anticoagulated atrial fibrillation, with recurrent cardiac decompensation	CD4+CD8-	t(14;14)	deletion	wt	JAK3	Bendamustine refractory	#1: Grade 3 klebsiella pneumoniae urinary infection (Day 18), resolved after IV antibiotics and withdrawal of ruxolitinib and venetoclax for 11 days
			· prostate cancer : cysto-prostastectomy						Alemtuzumab ineligible	#2: Grade 3 thrombocytopenia (Day 19), resolved after withdrawal of ruxolitinib and venetoclax for 11 days
			· stage IV chronic obstructive pulmonary disease (COPD) with repeated respiratory decompensation							#3: Grade 3 exacerbation of COPD (Day 40), resolved after IV antibiotics and withdrawal of ruxolitinib and venetoclax for 16 days ⇒ Decision to switch to an intermittent treatment schedule
			· mitral valvulopathy and tight aortic stenosis (TAVI)							#4: Grade 3 pneumonia (Day 117), resolved after IV antibiotics
		· type 2 diabetes								
		· sleep apnea with the use of a continuous positive airway pressure (CPAP) device								
Patient B	F	88	· high blood pressure	CD4+CD8-	t(14;14)	deletion	A3006T	wt	Bendamustine refractory	AE 1: Grade 2 thrombocytopenia (Day 50), resolved spontaneously under ruxolitinib, reappeared at grade 3 at day 130 during progression of the disease
									Alemtuzumab ineligible	

Patient C	F	56	None	CD4+CD8-	inv(14)	deletion	wt	wt	Bendamustine refractory	AE 1: Grade 4 thrombocytopenia from before the start of venetoclax to last follow-up, managed with transfusion support (every 2 or 3 weeks)
									Alemtuzumab refractory	AE 2: Grade 2 nausea (Day 41) following the first romidepsin injection

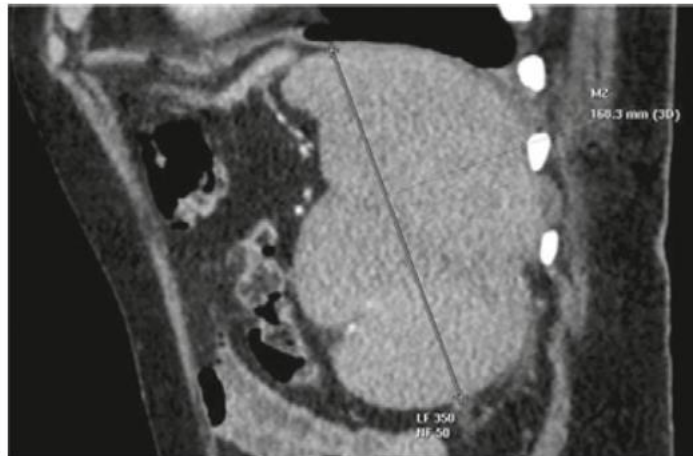
They provided informed consent to the therapeutic approach. The treatment schedules as well as WBC counts are presented in Figure 18 A and B. No patient developed tumor lysis syndrome on this combination. Repeat CT scans after 30 days of combination therapy for patient A showed resolution of splenomegaly (Figure 18 C). At latest follow-up, all consensus criteria (Staber *et al.*, 2019) for complete response were met except the circulating lymphocyte count of $23.6 \times 10^9/L$ (which was above the threshold of $4 \times 10^9/L$), classifying patient A in partial response (PR), now maintained for 10 months. Patient B had previously initiated venetoclax monotherapy, but began to have a slowly increasing lymphocyte count. The addition of ruxolitinib at day 61 led to stabilization of the disease. The combination was stopped because of the COVID-19 pandemic, as continuation of this off-label therapy was no longer possible in the patient's nursing facility during lockdown, and disease progression occurred off therapy at day 127. Patient B never resumed combination therapy and was lost to follow-up. Observed adverse events (AE), their timing and management are described in Table 5. Of note, T-PLL cells of patient A were *JAK3*-mutated and we did not find any mutation in the JAK/STAT pathway for patient B. Given the more robust clinical response of patient A, these clinical data are consistent with our previous preclinical finding that enhancement of BCL-2 dependence by JAK1 inhibition may be stronger in mutated T-PLL.

Figure 18: Two patients treated with the venetoclax + ruxolitinib combination. (A) Patient A: the top curve shows the evolution of WBC count ($\times 10^9/L$) during venetoclax and ruxolitinib combination. The two histogram graphs below show the daily doses of venetoclax and ruxolitinib received. The combination was started with ruxolitinib 15 mg twice daily, and venetoclax 2 days later with daily ramp-up from 20 mg to 800 mg over 6 days. The adverse events were: #1 grade 3 urinary infection; #2 grade 3 thrombocytopenia; #3 grade 3

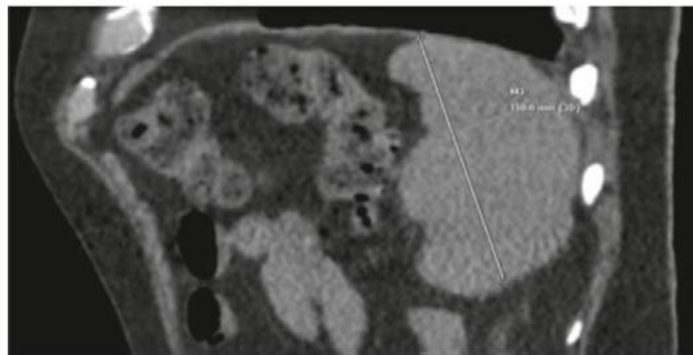
exacerbation of COPD; and #4 grade 3 pneumonia. Due to these repeated infectious AEs and to thrombocytopenia, the schedule was modified to an intermittent one, with ruxolitinib 15 mg twice daily given together with venetoclax 400 mg daily for 5 days out of every 4 weeks. (B) Same data for patient B. Venetoclax was started first with daily ramp-up from 20 mg to 800 mg over 6 days. After 2 months of slow progression, ruxolitinib was added at 10 mg/day and then increased to 10 mg twice daily. AE 1: grade 2 thrombocytopenia. (C) CT scan of patient A showing the spleen at baseline (largest dimension measured at 168.3mm) and one month after the beginning of the ruxolitinib and venetoclax combination (largest dimension measured at 110mm).



C



Day - 7

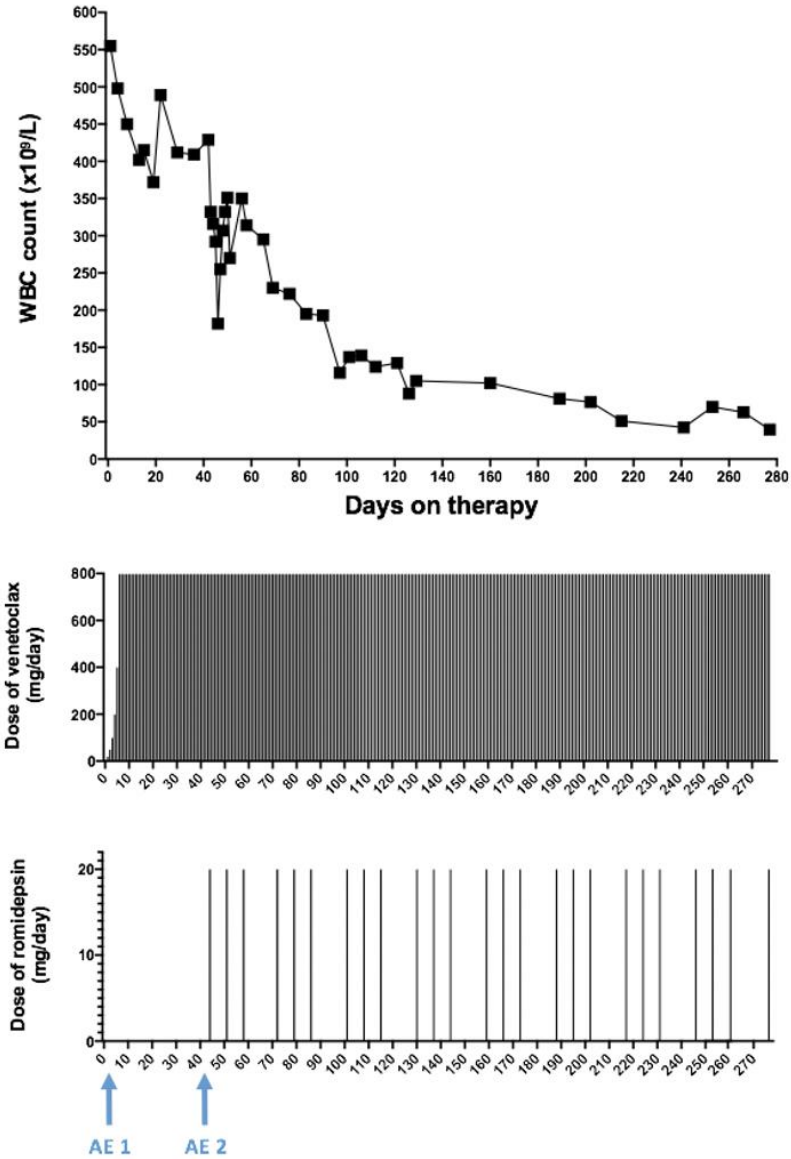


Day 30

8.10. Venetoclax plus romidepsin was effective for one refractory T-PLL patient

A patient ("patient C" described in Table 5 and Figure 19) was treated with the combination of venetoclax and the HDACi romidepsin (used instead of belinostat due to availability). This option was chosen because her disease was not mutated on the JAK/STAT pathway. She achieved a PR, currently ongoing after 9 months. With maximal venetoclax dosing (800mg/day) the lymphocyte count has stabilized around $40 \times 10^9/L$, with occasional need for platelet transfusion support.

Figure 19: Case report of venetoclax + HDACi combination. Patient C: the top curve shows the evolution of WBC count ($\times 10^9/L$) during venetoclax and romidepsin combination. The two histogram graphs below show the daily doses of venetoclax and romidepsin received. Venetoclax was started first with daily ramp-up from 20 mg to 800 mg over 6 days. After days of Stable Disease, romidepsin was added IV at 20 mg/day on days 1, 8, and 15 of 28-days cycle. The adverse events are described in Table 5.

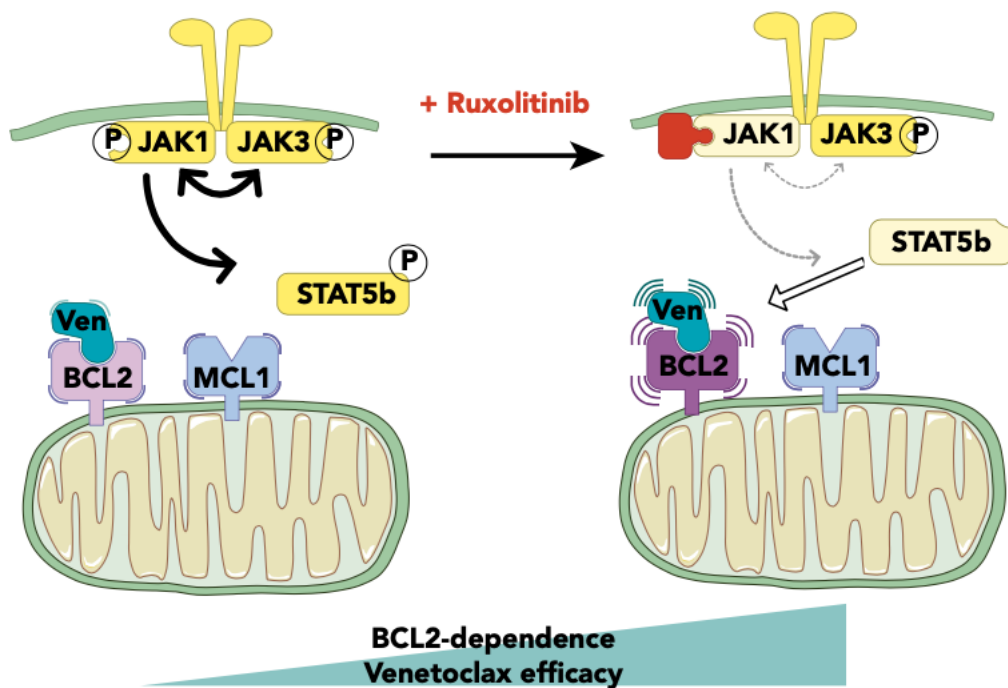


9. Discussion

Recent international collaborations (Staber *et al.*, 2019) have begun to promote translational science that may bring the benefits of novel agent based therapies to T-PLL. Much of this initial preclinical work has focused on the genetics of T-PLL, and how that might influence susceptibility to various targeted treatments (Braun *et al.*, 2020). Here, we have first performed a drug screening using CTG without the support of stromal cells. Ibrutinib and venetoclax were identified as potential efficient partners, and we described the *in vivo* effect of ibrutinib on the TCR pathway. These data led to the treatment of 2 refractory patients with ibrutinib and venetoclax, with limited efficacy, and to the initiation of a prospective clinical trial that was unfortunately not successful. Then, we report for the first time a functional precision medicine approach, using BH3 profiling to dissect T-PLL biology and to identify novel combination approaches to therapy. We found that – relative to CLL – T-PLL cells are less primed to undergo apoptosis. Unlike CLL cells, which depend primarily on BCL-2 for survival, T-PLL cells are heterogeneous and may commonly also depend on MCL-1. Through a stromal co-culture system, we modeled the T-PLL microenvironment and found that this made the malignant cells even less primed for apoptosis and less dependent on BCL-2, with increased MCL-1 dependence. Dual inhibition of BCL-2 and MCL-1 potently induced cell death in our model. Moreover, JAK/STAT pathway inhibition with ruxolitinib, and HDAC inhibition with belinostat, selectively increase BCL-2 dependence, thereby sensitizing T-PLL cells to venetoclax. A model of these interactions is summarized in Figure 20. We began to explore the combination of venetoclax plus ruxolitinib *in vivo* by treating two patients with refractory T-PLL, and we observed a deep response, which is ongoing after 5 months in the *JAK3*-mutated

T-PLL, as well as a stabilization of the disease in a patient for whom no mutation was found on the JAK/STAT pathway of tumor cells.

Figure 20: Proposed mechanism underlying our main findings. At baseline, BCL-2 and MCL-1 are molecular vulnerabilities in T-PLL. JAK/STAT pathway inhibition through JAK1 inhibition selectively increases BCL-2 dependent apoptotic priming and increases the activity of venetoclax.



Several recent studies have evaluated targeted therapies in T-PLL cells through analysis of isolated primary T-PLL cells derived from the peripheral blood;(Boidol, Kornauth, Kouwe, *et al.*, 2017; Kornauth *et al.*, 2019; Smith *et al.*, 2020) however, the microenvironment likely modulates intracellular survival signaling in T-PLL. One group used stromal support (NKT) and found that SNS-032, a cyclin-dependent kinase inhibitor, overcame the stroma-mediated

protective effect.(Andersson *et al.*, 2018) In another study, IL-2, IL-4, and CD40L stimulation was used to mimic the effects of the lymph node microenvironment, which led to resistance to inhibition of both BCL-2 and MCL-1.(Smith *et al.*, 2020) We utilized the NKT stromal co-culture system, which is known to generate media enriched with IL-6 and CXCL10,(Manshour *et al.*, 2011) and also promotes malignant cell survival through direct cell-cell interactions. This robust simulation of the microenvironment may more closely mimic what is occurring *in vivo* as T-PLL cells circulate through the marrow, spleen, and lymph nodes. Our data also suggest that NKT may decrease sensitivity to BCL-2 inhibition, which may at least in part explain the limited benefit of venetoclax monotherapy in T-PLL. In other words, although an initial response is achieved by decreasing the more susceptible cells circulating in the peripheral blood, a reservoir of resistant T-PLL cells in the microenvironment may then allow for subsequent clinical disease progression. Our data suggest that the microenvironment may also increase dependence on MCL-1, suggesting a possible benefit to combining MCL-1 inhibition with BCL-2 inhibition in T-PLL. The use of this co-culture model may at least in part explain the lower activity of the drugs used in monotherapy in our study in comparison to the CTG drug screening.(Andersson *et al.*, 2018) An advantage of this model is that it allowed us to confirm, under different conditions, the synergy between BCL-2 and MCL-1 inhibition in T-PLL which was also suggested by a recent study.(Smith *et al.*, 2020) Although this promising approach is now under evaluation in other hematologic malignancies, theoretical concerns about the potential for hematologic and cardiac toxicities suggest that we should also investigate other venetoclax-combination strategies given the possibility that a BCL-2 plus MCL-1 inhibitor combination is not feasible from a safety perspective.

To explore other potential combination partners for venetoclax, we focused on targeting other pathways crucial to the pathophysiology of T-PLL: JAK/STAT, histone acetylation, and the TCR pathway. In a meta-analysis that included sequence information on *JAK* or *STAT* gene loci in 275 T-PLL patients, a cumulative rate of 62.1% of cases with mutated *JAK* or *STAT* genes were found. Functionally, it has been shown that *IL2RG-JAK1-JAK3-STAT5B* mutations led to STAT5 hyperactivation that transformed Ba/F3 cells, resulting in cytokine-independent growth, and/or enhanced colony formation in Jurkat T cells.(Kiel *et al.*, 2014b) Prior work had also suggested that pharmacologic inhibition of the JAK/STAT pathway with the phospho-STAT5 inhibitor tool compound pimozide led to decreased T-PLL cell viability and diminished phospho-STAT5 levels.(Kiel *et al.*, 2014b) Basal STAT5B phosphorylation level in T-PLL cells was evaluated in two studies(Schrader *et al.*, 2018b; Wahnschaffe *et al.*, 2019), and a common finding was noticeable basal phosphorylation of STAT5B in several T-PLL samples, which could be explained by *IL2RG-JAK1-JAK3-STAT5B* mutations or by genomic losses of hypothetical negative regulators of STAT5B(Wahnschaffe *et al.*, 2019). In both studies, the amount of STAT5B phosphorylation was heterogeneous and was higher in cases with mutated *JAK1*, *JAK3* or *STAT5B*, consistent with our findings.

Previous work has shown that JAK3, even when constitutively active, does not mediate STAT5 phosphorylation without JAK1; and that JAK1 phosphorylates JAK3 and STAT5, while JAK3 phosphorylates and fully activates JAK1, but not STAT5.(Haan *et al.*, 2011, p. 1) Our results are consistent with these data, since we found that JAK1 inhibition with ruxolitinib (IC50: 3.3nM) enhances BCL-2 dependence and venetoclax activity, while JAK3 inhibition with PRN694 (IC50: 30nM) does not. Moreover, the growth-promoting activity of mutated STAT5B can be partially abrogated by a JAK1 inhibitor.(Küçük *et al.*, 2015, p. 5) To some extent, even

mutated *STAT5B* needs some phosphorylated JAK1 to transduce signal, consistent with our data showing that ruxolitinib has a preserved (but less pronounced) effect on *STAT5B* mutated T-PLL cells. Finally, an influence of phosphorylated *STAT5B* on BCL-2-family proteins in T cells is described (Lord *et al.*, 2000; Burchill *et al.*, 2003; Tripathi *et al.*, 2010), but further work will be needed to explore this in T-PLL.

In addition to JAK/STAT dysregulation, T-PLL is characterized by dysregulation of histone acetylation, which can be targeted by HDACi. (Schrader *et al.*, 2018b) We showed a significant increase in overall priming after treatment with belinostat, which may help explain the reported synergy of HDACi with chemotherapy and alemtuzumab. (Hasanali *et al.*, 2015) Likewise, it has been proposed that p53 activation – by re-acetylation through HDAC inhibition – can influence BCL-2 family proteins, particularly BCL-2 and BCL-xL. (Schrader, Braun and Herling, 2019) Our finding that belinostat increases BCL-2 dependence is consistent with that hypothesis. Finally, our results also shed light on how targeting the TCR pathway could be effective in T-PLL. Although not as pronounced as the effects we saw with JAK/STAT or HDAC inhibitors, we do see a modest effect on viability with TCR pathway inhibition through the selective ITK inhibitor PRN694 when combined with venetoclax. This effect was not significant with ibrutinib at the dose of 1 μ M in coculture conditions. This is consistent with our previous data, where ibrutinib was used at a higher dose of 10 μ M that allows it to more potently inhibit ITK. (Kornauth *et al.*, 2019) Interestingly, the effect of PRN694 was primarily seen in T-PLL cells without activating mutations in the JAK/STAT pathway, suggesting that the pathophysiology in this subset of T-PLL patients may rely more on the proximal TCR signalosome.

Our preclinical data on venetoclax with ruxolitinib led to the initial exploration of this combination in two patients with refractory T-PLL. One *JAK3*-mutated experienced a deep partial response, which has now been sustained for 10 months with an intermittent treatment strategy. The second patient (without JAK-STAT pathway mutation detected in tumor cells) experienced disease stabilization. These results, along with our preclinical data, strongly support the development of a prospective clinical trial to evaluate the safety and efficacy of this combination in T-PLL. Finally, the partial response of patient C (without a JAK-STAT pathway mutation detected in tumor cells and treated with venetoclax and romidepsin), which has now been sustained for 9 months, supports further evaluation of venetoclax + HDACi in T-PLL, especially in patients without a JAK/STAT pathway mutation in their T-PLL cells.

10. Perspective

Directly based on those results, 15 patients from the French Innovative Leukemia Organization (FILO) network were treated with ruxolitinib and venetoclax oral combination for T-PLL. All patients were refractory to, or ineligible for alemtuzumab, the principal therapeutic option to date. In this multicenter retrospective study, all patients were informed about the off-label use of this combination and provided informed consent. Patients received a maximum dose of ruxolitinib 15 mg twice daily, and venetoclax 800 mg daily. Venetoclax was started with daily ramp-up from 20 mg to 800 mg over 6 days, with tumor lysis syndrome prophylaxis (rasburicase and IV hydration). Responses were assessed by consensus criteria. We performed Next Generation Sequencing (NGS) using a custom-designed panel of 33 genes, including among others: *ATM*, *TP53*, *IL2R*, *JAK1*, *JAK3*, and *STAT5B*. CytoScan HD microarray (Affymetrix) were used to study copy number variation and or uniparental disomy. We also performed an in vivo dynamic BH3 profiling (DBP) on samples obtained from two patients on treatment. Preliminary results of this project will be presented as a poster at American Society of Hematology annual congress this December 2021.

In our team in Montpellier at Institute of Human Genetics (IGH in French), we are currently working on another project, to better understand the response profiles and the adaptation of the cells to the therapeutic pressure exerted by ruxolitinib and venetoclax. The technology of single-cell RNA sequencing (scRNA-Seq) enables robust as well as simple access to the transcriptome of tumor cells at single cell level. This modern technique will also allow us to study the molecular dynamics of the different subclones at different times after diagnosis. It will also help us in revealing dynamic changes in cell fate as well as mapping

differential tumor subclonal trajectories. We recently obtained a grant that will allow to evaluate 4 pairs of samples. Cell isolation and library preparation will be completed using 10X single-cell analysis system available in the laboratory. Quality control will be assessed by flow cytometry before library preparation. Single-cell multiplexing will be used on tumor cells followed by cell count and viability measurement before loading the microwell cartridge. Cell capture and library for sc-RNA-seq will be prepared with the 10X single-cell analysis system. Libraries will be sequenced using NovaSeq 6000 system (Illumina) on the MGX platform (Montpellier GenomiX platform (<https://www.mgx.cnrs.fr/?lang=fr>)) at a sequencing depth of 50 000 reads per cells (1500 to 2000 sequenced cells per sample). Sc-RNA-seq data will be analyzed using Seurat R package and SeqGeq software.

A third and broader project stems from this work. We wish to use the same methodology to find new therapeutic options in other, more frequent T hematologic malignancies, T non-Hodgkin lymphomas. There is a clear unmet medical need in this class of cancer. For this purpose, we are developing a BH3 tool kit in our team at the IGH. As explained above, this method has the advantage of being easier to perform and more robust. Our experimental plan is described below:

Aim 1: baseline BH3 profiling of T cell lymphomas

- Identification of functional subgroups of T cell lymphomas with BH3 tool kit on primary samples from CALYM biobank
 - BH3 tool kit uses well known BH3 mimetics, as venetoclax

- But also BH3 mimetics in development, as those from AZ, as well as CDK9 inhibitors
- Identification of genomic subgroups of T cell lymphomas with targeted NGS panel
- Correlation between functional and genomic subgroups

Aim 2: increase baseline BH3 dependencies with other inhibitors

- Treating primary cells with known targeted therapies tailored to genomic subgroups
 - TFH lymphomas with epigenetic drugs, JAK/STAT pathway dependent lymphomas with JAK inhibitors, TCR pathway dependent lymphoma with TCR pathway inhibitors, etc
 - Dynamic BH3 profiling to measure the impact of these inhibitions to BH3 dependencies
- Confirm the suspected synergies with viability assays combining pathway inhibitors and BH3 mimetics

11. Acknowledgements

The authors thank the patients and their families.

C.H. was supported by Lille University School of Medicine (France), Fondation Monahan, Fulbright *Commission Franco-Américaine*, SiLLC (*association de Soutien et d'Information à la LLC*) and the Pan Massachusetts Challenge Team FLAMES. M.S.D. is a Scholar in Clinical Research from the Leukemia & Lymphoma Society.

The authors thank the French Innovative Leukemia Organization for support and bio banking, as well as Christophe Roumier and Lille Hospital Tumor Bank, for handling, conditioning, and storing patient samples. The authors also thank Nathalie Helevaut for her excellent technical help.

Lille Hospital Tumor Bank: *Tumorotheque du C2RC Lille, Centre de Biologie Pathologie Pôle de Pathologie Tumorotheque du Centre Régional de Référence en Cancérologie de Lille. 2 Avenue Oscar LAMBRET, 59037 LILLE, certification NF 96900-2014/65453-1, Centre Hospitalier Régional Universitaire de Lille.*

12. Publications and co-authors

Most of this work has been published in two papers. Charles Herbaux is first author of the main manuscript published as a full research paper in *Blood* on 2021 February 17th. He is co-first author of the second one, published as a letter in *Haematologica* on 2021 February 25th. The two full references are stated below, with the list of the co-authors. The contribution of each co-author can be found in details in the publications.

Herbaux C, Kornauth C, Poulain S, Chong SJF, Collins MC, Valentin R, Hackett L, Tournilhac O, Lemonnier F, Dupuis J, Daniel A, Tomowiak C, Laribi K, Renaud L, Roos-Weil D, Rossi C, Van Den Neste EW, Leyronnas C, Merabet F, Malfuson JV, Tiab M, Ysebaert L, Ng SY, Morschhauser F, Staber PB, Davids MS. BH3 profiling identifies ruxolitinib as a promising partner for venetoclax to treat T-cell prolymphocytic leukemia. **Blood**. 2021 Feb 17:blood.2020007303. doi:10.1182/blood.2020007303. PMID: 33598678.

Kornauth C, **Herbaux C**, Boidol B, Guillemette C, Caron P, Mayerhöfer ME, Poulain S, Tournilhac O, Pemovska T, Chong SJF, Van der Kouwe E, Kazianka L, Hopfinger G, Heintel D, Jäger R, Raderer M, Jäger U, Simonitsch-Klupp I, Sperr WR, Kubicek S, Davids MS, Staber PB. Rationale for the combination of venetoclax and ibrutinib in T-prolymphocytic leukemia. **Haematologica**. 2021 Feb 25. doi:10.3324/haematol.2020.271304. PMID: 33626863.

13. References

1. Anderson, M.A. *et al.* (2016) 'The BCL2 selective inhibitor venetoclax induces rapid onset apoptosis of CLL cells in patients via a TP53-independent mechanism', *Blood*, 127(25), pp. 3215–3224. doi:10.1182/blood-2016-01-688796.
2. Andersson, E.I. *et al.* (2018) 'Discovery of novel drug sensitivities in T-PLL by high-throughput ex vivo drug testing and mutation profiling', *Leukemia*, 32(3), pp. 774–787. doi:10.1038/leu.2017.252.
3. Ashkenazi, A. *et al.* (2017) 'From basic apoptosis discoveries to advanced selective BCL-2 family inhibitors', *Nature Reviews. Drug Discovery*, 16(4), pp. 273–284. doi:10.1038/nrd.2016.253.
4. Bellanger, D. *et al.* (2014) 'Recurrent JAK1 and JAK3 somatic mutations in T-cell prolymphocytic leukemia', *Leukemia*, 28(2), pp. 417–419. doi:10.1038/leu.2013.271.
5. Berg, L.J. *et al.* (2005) 'Tec family kinases in T lymphocyte development and function', *Annual Review of Immunology*, 23, pp. 549–600. doi:10.1146/annurev.immunol.22.012703.104743.
6. Boidol, B., Kornauth, C., Kouwe, E. van der, *et al.* (2017) 'First in human response of BCL-2 inhibitor venetoclax in T-cell prolymphocytic leukemia', *Blood*, p. blood-2017-05-785683. doi:10.1182/blood-2017-05-785683.
7. Boise, L.H. *et al.* (1993) 'bcl-x, a bcl-2-related gene that functions as a dominant regulator of apoptotic cell death', *Cell*, 74(4), pp. 597–608. doi:10.1016/0092-8674(93)90508-N.
8. Braun, T. *et al.* (2020) 'Advances and Perspectives in the Treatment of T-PLL', *Current Hematologic Malignancy Reports* [Preprint]. doi:10.1007/s11899-020-00566-5.
9. Burchill, M.A. *et al.* (2003) 'Distinct Effects of STAT5 Activation on CD4+ and CD8+ T Cell Homeostasis: Development of CD4+CD25+ Regulatory T Cells versus CD8+ Memory T Cells', *The Journal of Immunology*, 171(11), pp. 5853–5864. doi:10.4049/jimmunol.171.11.5853.
10. Catovsky, D. *et al.* (1973) 'Prolymphocytic leukaemia of B and T cell type', *Lancet (London, England)*, 2(7823), pp. 232–234. doi:10.1016/s0140-6736(73)93135-8.
11. Catovsky, D. (1982) 'Prolymphocytic leukaemia', *Nouvelle Revue Francaise D'hematologie*, 24(6), pp. 343–347.
12. Chen, L. *et al.* (2005) 'Differential targeting of prosurvival Bcl-2 proteins by their BH3-only ligands allows complementary apoptotic function', *Molecular Cell*, 17(3), pp. 393–403. doi:10.1016/j.molcel.2004.12.030.
13. Cheson, B.D. *et al.* (1988) 'Guidelines for clinical protocols for chronic lymphocytic leukemia: recommendations of the National Cancer Institute-sponsored working group', *American Journal of Hematology*, 29(3), pp. 152–163. doi:10.1002/ajh.2830290307.
14. Cheson, B.D. *et al.* (1996) 'National Cancer Institute-sponsored Working Group guidelines for chronic lymphocytic leukemia: revised guidelines for diagnosis and treatment', *Blood*, 87(12), pp. 4990–4997.
15. Cimmino, A. *et al.* (2005) 'miR-15 and miR-16 induce apoptosis by targeting BCL2', *Proceedings of the National Academy of Sciences of the United States of America*, 102(39), pp. 13944–13949. doi:10.1073/pnas.0506654102.

16. Cleary, M.L., Smith, S.D. and Sklar, J. (1986) 'Cloning and structural analysis of cDNAs for bcl-2 and a hybrid bcl-2/immunoglobulin transcript resulting from the t(14;18) translocation', *Cell*, 47(1), pp. 19–28. doi:10.1016/0092-8674(86)90362-4.
17. Croce, C.M. *et al.* (1985) 'Gene for alpha-chain of human T-cell receptor: location on chromosome 14 region involved in T-cell neoplasms', *Science*, 227(4690), pp. 1044–1047. doi:10.1126/science.3919442.
18. Cross, M.J. *et al.* (2019) 'No Improvement in Survival for T-PLL Patients over the Last Two Decades', *Blood*, 134(Supplement_1), pp. 1552–1552. doi:10.1182/blood-2019-122094.
19. Czabotar, P.E. *et al.* (2013) 'Bax crystal structures reveal how BH3 domains activate Bax and nucleate its oligomerization to induce apoptosis', *Cell*, 152(3), pp. 519–531. doi:10.1016/j.cell.2012.12.031.
20. Davids, M.S. *et al.* (2012) 'Decreased mitochondrial apoptotic priming underlies stroma-mediated treatment resistance in chronic lymphocytic leukemia', *Blood*, 120(17), pp. 3501–3509. doi:10.1182/blood-2012-02-414060.
21. Davids, M.S. *et al.* (2018) 'Comprehensive Safety Analysis of Venetoclax Monotherapy for Patients with Relapsed/Refractory Chronic Lymphocytic Leukemia', *Clinical Cancer Research: An Official Journal of the American Association for Cancer Research*, 24(18), pp. 4371–4379. doi:10.1158/1078-0432.CCR-17-3761.
22. Dearden, C. (2015) 'Management of prolymphocytic leukemia', *Hematology. American Society of Hematology. Education Program*, 2015, pp. 361–367. doi:10.1182/asheducation-2015.1.361.
23. Dearden, C.E. *et al.* (2001) 'High remission rate in T-cell prolymphocytic leukemia with CAMPATH-1H', *Blood*, 98(6), pp. 1721–1726.
24. Dearden, C.E. *et al.* (2011) 'Alemtuzumab therapy in T-cell prolymphocytic leukemia: comparing efficacy in a series treated intravenously and a study piloting the subcutaneous route', *Blood*, 118(22), pp. 5799–5802. doi:10.1182/blood-2011-08-372854.
25. Del Gaizo Moore, V. *et al.* (2007) 'Chronic lymphocytic leukemia requires BCL2 to sequester prodeath BIM, explaining sensitivity to BCL2 antagonist ABT-737', *The Journal of Clinical Investigation*, 117(1), pp. 112–121. doi:10.1172/JCI28281.
26. Deng, J. *et al.* (2017) 'Bruton's tyrosine kinase inhibition increases BCL-2 dependence and enhances sensitivity to venetoclax in chronic lymphocytic leukemia', *Leukemia*, 31(10), pp. 2075–2084. doi:10.1038/leu.2017.32.
27. Dondorf, S., Schrader, A. and Herling, M. (2015) 'Interleukin-2-inducible T-cell Kinase (ITK) Targeting by BMS-509744 Does Not Affect Cell Viability in T-cell Prolymphocytic Leukemia (T-PLL)', *The Journal of Biological Chemistry*, 290(16), pp. 10568–10569. doi:10.1074/jbc.L115.644641.
28. Dürig, J. *et al.* (2007) 'Combined single nucleotide polymorphism-based genomic mapping and global gene expression profiling identifies novel chromosomal imbalances, mechanisms and candidate genes important in the pathogenesis of T-cell prolymphocytic leukemia with inv(14)(q11q32)', *Leukemia*, 21(10), pp. 2153–2163. doi:10.1038/sj.leu.2404877.
29. Gandhi, V. *et al.* (2008) 'Phase I trial of nelarabine in indolent leukemias', *Journal of Clinical Oncology: Official Journal of the American Society of Clinical Oncology*, 26(7), pp. 1098–1105. doi:10.1200/JCO.2007.14.1986.
30. Garand, R. *et al.* (1998) 'Indolent course as a relatively frequent presentation in T-

- prolymphocytic leukaemia. Groupe Français d'Hématologie Cellulaire', *British Journal of Haematology*, 103(2), pp. 488–494. doi:10.1046/j.1365-2141.1998.00977.x.
31. Ghia, P. *et al.* (1998) 'Unbalanced expression of bcl-2 family proteins in follicular lymphoma: contribution of CD40 signaling in promoting survival', *Blood*, 91(1), pp. 244–251.
 32. Gomez-Arteaga, A. *et al.* (2019) 'Combined use of tofacitinib (pan-JAK inhibitor) and ruxolitinib (a JAK1/2 inhibitor) for refractory T-cell prolymphocytic leukemia (T-PLL) with a JAK3 mutation', *Leukemia & Lymphoma*, 60(7), pp. 1626–1631. doi:10.1080/10428194.2019.1594220.
 33. Gomez-Bougie, P. *et al.* (2018) 'BH3-mimetic toolkit guides the respective use of BCL2 and MCL1 BH3-mimetics in myeloma treatment', *Blood*, 132(25), pp. 2656–2669. doi:10.1182/blood-2018-03-836718.
 34. Guillaume, T. *et al.* (2015) 'Allogeneic hematopoietic stem cell transplantation for T-prolymphocytic leukemia: a report from the French society for stem cell transplantation (SFGM-TC)', *European Journal of Haematology*, 94(3), pp. 265–269. doi:10.1111/ejh.12430.
 35. Haan, C. *et al.* (2011) 'Jak1 Has a Dominant Role over Jak3 in Signal Transduction through γ -Containing Cytokine Receptors', *Chemistry & Biology*, 18(3), pp. 314–323. doi:10.1016/j.chembiol.2011.01.012.
 36. Hallas, C. *et al.* (1999) 'Genomic analysis of human and mouse TCL1 loci reveals a complex of tightly clustered genes', *Proceedings of the National Academy of Sciences*, 96(25), pp. 14418–14423. doi:10.1073/pnas.96.25.14418.
 37. Hallek, M. *et al.* (2008) 'Guidelines for the diagnosis and treatment of chronic lymphocytic leukemia: a report from the International Workshop on Chronic Lymphocytic Leukemia updating the National Cancer Institute-Working Group 1996 guidelines', *Blood*, 111(12), pp. 5446–5456. doi:10.1182/blood-2007-06-093906.
 38. Hallek, M. *et al.* (2018) 'iwCLL guidelines for diagnosis, indications for treatment, response assessment, and supportive management of CLL', *Blood*, 131(25), pp. 2745–2760. doi:10.1182/blood-2017-09-806398.
 39. Hanahan, D. and Weinberg, R.A. (2011) 'Hallmarks of cancer: the next generation', *Cell*, 144(5), pp. 646–674. doi:10.1016/j.cell.2011.02.013.
 40. Hasanali, Z.S. *et al.* (2015) 'Epigenetic therapy overcomes treatment resistance in T cell prolymphocytic leukemia', *Science Translational Medicine*, 7(293), p. 293ra102. doi:10.1126/scitranslmed.aaa5079.
 41. He, L. *et al.* (2018) 'Methods for High-throughput Drug Combination Screening and Synergy Scoring', *Methods in Molecular Biology (Clifton, N.J.)*, 1711, pp. 351–398. doi:10.1007/978-1-4939-7493-1_17.
 42. Herbaux, C. *et al.* (2015) 'Bendamustine is effective in T-cell prolymphocytic leukaemia', *British Journal of Haematology*, 168(6), pp. 916–919. doi:10.1111/bjh.13175.
 43. Herishanu, Y. *et al.* (2011) 'Activation of CD44, a receptor for extracellular matrix components, protects chronic lymphocytic leukemia cells from spontaneous and drug induced apoptosis through MCL-1', *Leukemia & Lymphoma*, 52(9), pp. 1758–1769. doi:10.3109/10428194.2011.569962.
 44. Herling, M. *et al.* (2004) 'A systematic approach to diagnosis of mature T-cell leukemias reveals heterogeneity among WHO categories', *Blood*, 104(2), pp. 328–335. doi:10.1182/blood-2004-01-0002.

45. Herling, M. *et al.* (2008) 'High TCL1 expression and intact T-cell receptor signaling define a hyperproliferative subset of T-cell prolymphocytic leukemia', *Blood*, 111(1), pp. 328–337. doi:10.1182/blood-2007-07-101519.
46. Hopfinger, G. *et al.* (2013) 'Sequential chemoimmunotherapy of fludarabine, mitoxantrone, and cyclophosphamide induction followed by alemtuzumab consolidation is effective in T-cell prolymphocytic leukemia', *Cancer*, 119(12), pp. 2258–2267. doi:10.1002/cncr.27972.
47. Jain, P. *et al.* (2017) 'Characteristics, outcomes, prognostic factors and treatment of patients with T-cell prolymphocytic leukemia (T-PLL)', *Annals of Oncology: Official Journal of the European Society for Medical Oncology*, 28(7), pp. 1554–1559. doi:10.1093/annonc/mdx163.
48. Kaufmann, S.H. *et al.* (1998) 'Elevated expression of the apoptotic regulator Mcl-1 at the time of leukemic relapse', *Blood*, 91(3), pp. 991–1000.
49. Kerr, J.F., Wyllie, A.H. and Currie, A.R. (1972) 'Apoptosis: a basic biological phenomenon with wide-ranging implications in tissue kinetics', *British Journal of Cancer*, 26(4), pp. 239–257. doi:10.1038/bjc.1972.33.
50. Kiel, M.J. *et al.* (2014) 'Integrated genomic sequencing reveals mutational landscape of T-cell prolymphocytic leukemia', *Blood*, 124(9), pp. 1460–1472. doi:10.1182/blood-2014-03-559542.
51. Kornauth, C. *et al.* (2019) 'Combination of Venetoclax and Ibrutinib Increases bcl2-Dependent Apoptotic Priming, Reduces ITK-Phosphorylation and Is Clinically Promising in Relapsed/Refractory T-Prolymphocytic Leukemia', *Blood*, 134(Supplement_1), pp. 3965–3965. doi:10.1182/blood-2019-124392.
52. Kotrova, M. *et al.* (2018) 'Next-generation amplicon TRB locus sequencing can overcome limitations of flow-cytometric V β expression analysis and confirms clonality in all T-cell prolymphocytic leukemia cases', *Cytometry. Part A: The Journal of the International Society for Analytical Cytology*, 93(11), pp. 1118–1124. doi:10.1002/cyto.a.23604.
53. Kozopas, K.M. *et al.* (1993) 'MCL1, a gene expressed in programmed myeloid cell differentiation, has sequence similarity to BCL2', *Proceedings of the National Academy of Sciences of the United States of America*, 90(8), pp. 3516–3520. doi:10.1073/pnas.90.8.3516.
54. Krishnan, B. *et al.* (2010) 'Stem cell transplantation after alemtuzumab in T-cell prolymphocytic leukaemia results in longer survival than after alemtuzumab alone: a multicentre retrospective study', *British Journal of Haematology*, 149(6), pp. 907–910. doi:10.1111/j.1365-2141.2010.08134.x.
55. Küçük, C. *et al.* (2015) 'Activating mutations of STAT5B and STAT3 in lymphomas derived from $\gamma\delta$ -T or NK cells', *Nature Communications*, 6(1), pp. 1–12. doi:10.1038/ncomms7025.
56. Kurtova, A.V. *et al.* (2009) 'Diverse marrow stromal cells protect CLL cells from spontaneous and drug-induced apoptosis: development of a reliable and reproducible system to assess stromal cell adhesion-mediated drug resistance', *Blood*, 114(20), pp. 4441–4450. doi:10.1182/blood-2009-07-233718.
57. Liu, X. *et al.* (1996) 'Induction of apoptotic program in cell-free extracts: requirement for dATP and cytochrome c', *Cell*, 86(1), pp. 147–157. doi:10.1016/s0092-8674(00)80085-9.
58. Liu, Y. *et al.* (2019) 'ITK inhibition induced in vitro and in vivo anti-tumor activity

- through downregulating TCR signaling pathway in malignant T cell lymphoma', *Cancer Cell International*, 19(1), p. 32. doi:10.1186/s12935-019-0754-9.
59. Lord, J.D. *et al.* (2000) 'The IL-2 receptor promotes lymphocyte proliferation and induction of the c-myc, bcl-2, and bcl-x genes through the trans-activation domain of Stat5', *Journal of Immunology (Baltimore, Md.: 1950)*, 164(5), pp. 2533–2541. doi:10.4049/jimmunol.164.5.2533.
 60. Manshouri, T. *et al.* (2011) 'Bone marrow stroma-secreted cytokines protect JAK2(V617F)-mutated cells from the effects of a JAK2 inhibitor', *Cancer Research*, 71(11), pp. 3831–3840. doi:10.1158/0008-5472.CAN-10-4002.
 61. Matutes, E. *et al.* (1991) 'Clinical and laboratory features of 78 cases of T-prolymphocytic leukemia', *Blood*, 78(12), pp. 3269–3274.
 62. Mercieca, J. *et al.* (1994) 'The role of pentostatin in the treatment of T-cell malignancies: analysis of response rate in 145 patients according to disease subtype', *Journal of Clinical Oncology: Official Journal of the American Society of Clinical Oncology*, 12(12), pp. 2588–2593. doi:10.1200/JCO.1994.12.12.2588.
 63. Montero, J. *et al.* (2015) 'Drug-induced death signaling strategy rapidly predicts cancer response to chemotherapy', *Cell*, 160(5), pp. 977–989. doi:10.1016/j.cell.2015.01.042.
 64. Oberbeck, S. *et al.* (2020) 'Noncanonical effector functions of the T-memory-like T-PLL cell are shaped by cooperative TCL1A and TCR signaling', *Blood*, 136(24), pp. 2786–2802. doi:10.1182/blood.2019003348.
 65. Pawson, R. *et al.* (1997) 'Treatment of T-cell prolymphocytic leukemia with human CD52 antibody', *Journal of Clinical Oncology: Official Journal of the American Society of Clinical Oncology*, 15(7), pp. 2667–2672. doi:10.1200/JCO.1997.15.7.2667.
 66. Pekarsky, Y. *et al.* (2000) 'Tcl1 enhances Akt kinase activity and mediates its nuclear translocation', *Proceedings of the National Academy of Sciences*, 97(7), pp. 3028–3033. doi:10.1073/pnas.97.7.3028.
 67. Pekarsky, Y., Hallas, C. and Croce, C.M. (2001) 'Molecular basis of mature T-cell leukemia', *JAMA*, 286(18), pp. 2308–2314. doi:10.1001/jama.286.18.2308.
 68. Pflug, N. *et al.* (2019) 'New lessons learned in T-PLL: results from a prospective phase-II trial with fludarabine-mitoxantrone-cyclophosphamide-alemtuzumab induction followed by alemtuzumab maintenance', *Leukemia & Lymphoma*, 60(3), pp. 649–657. doi:10.1080/10428194.2018.1488253.
 69. Punnoose, E.A. *et al.* (2016) 'Expression Profile of BCL-2, BCL-XL, and MCL-1 Predicts Pharmacological Response to the BCL-2 Selective Antagonist Venetoclax in Multiple Myeloma Models', *Molecular Cancer Therapeutics*, 15(5), pp. 1132–1144. doi:10.1158/1535-7163.MCT-15-0730.
 70. Pützer, S. *et al.* (2020) 'Reinstated p53 response and high anti-T-cell leukemia activity by the novel alkylating deacetylase inhibitor tinostamustine', *Leukemia*, pp. 1–6. doi:10.1038/s41375-020-0772-6.
 71. Ravandi, F. and O'Brien, S. (2005) 'Chronic lymphoid leukemias other than chronic lymphocytic leukemia: diagnosis and treatment', *Mayo Clinic Proceedings*, 80(12), pp. 1660–1674. doi:10.4065/80.12.1660.
 72. Roberts, A.W. *et al.* (2012) 'Substantial susceptibility of chronic lymphocytic leukemia to BCL2 inhibition: results of a phase I study of navitoclax in patients with relapsed or refractory disease', *Journal of Clinical Oncology: Official Journal of the American Society of Clinical Oncology*, 30(5), pp. 488–496. doi:10.1200/JCO.2011.34.7898.

73. Ryan, J. *et al.* (2016) 'iBH3: simple, fixable BH3 profiling to determine apoptotic priming in primary tissue by flow cytometry', *Biological Chemistry*, 397(7), pp. 671–678. doi:10.1515/hsz-2016-0107.
74. Schrader, A. *et al.* (2018) 'Actionable perturbations of damage responses by TCL1/ATM and epigenetic lesions form the basis of T-PLL', *Nature Communications*, 9(1), p. 697. doi:10.1038/s41467-017-02688-6.
75. Schrader, A., Braun, T. and Herling, M. (2019) 'The dawn of a new era in treating T-PLL', *Oncotarget*, 10(6), pp. 626–628. doi:10.18632/oncotarget.26595.
76. Silva, M. *et al.* (1998) 'Expression of Bcl-x in erythroid precursors from patients with polycythemia vera', *The New England Journal of Medicine*, 338(9), pp. 564–571. doi:10.1056/NEJM199802263380902.
77. Smith, V.M. *et al.* (2020) 'Dual dependence on BCL2 and MCL1 in T-cell prolymphocytic leukemia', *Blood Advances*, 4(3), pp. 525–529. doi:10.1182/bloodadvances.2019000917.
78. Souers, A.J. *et al.* (2013) 'ABT-199, a potent and selective BCL-2 inhibitor, achieves antitumor activity while sparing platelets', *Nature Medicine*, 19(2), pp. 202–208. doi:10.1038/nm.3048.
79. Staber, P.B. *et al.* (2019) 'Consensus criteria for diagnosis, staging, and treatment response assessment of T-cell prolymphocytic leukemia', *Blood*, 134(14), pp. 1132–1143. doi:10.1182/blood.2019000402.
80. Stengel, A. *et al.* (2016) 'Genetic characterization of T-PLL reveals two major biologic subgroups and JAK3 mutations as prognostic marker', *Genes, Chromosomes & Cancer*, 55(1), pp. 82–94. doi:10.1002/gcc.22313.
81. Stilgenbauer, S. *et al.* (1997) 'Biallelic mutations in the ATM gene in T-prolymphocytic leukemia', *Nature Medicine*, 3(10), pp. 1155–1159. doi:10.1038/nm1097-1155.
82. Sun, Y. *et al.* (2018) 'Comparison of karyotyping, TCL1 fluorescence in situ hybridisation and TCL1 immunohistochemistry in T cell prolymphocytic leukaemia', *Journal of Clinical Pathology*, 71(4), pp. 309–315. doi:10.1136/jclinpath-2017-204616.
83. Swerdlow, S.H. *et al.* (2016) 'The 2016 revision of the World Health Organization classification of lymphoid neoplasms', *Blood*, 127(20), pp. 2375–2390. doi:10.1182/blood-2016-01-643569.
84. Ten Hacken, E. *et al.* (2018) 'Splicing modulation sensitizes chronic lymphocytic leukemia cells to venetoclax by remodeling mitochondrial apoptotic dependencies', *JCI insight*, 3(19). doi:10.1172/jci.insight.121438.
85. Touzeau, C. *et al.* (2016) 'BH3 profiling identifies heterogeneous dependency on Bcl-2 family members in multiple myeloma and predicts sensitivity to BH3 mimetics', *Leukemia*, 30(3), pp. 761–764. doi:10.1038/leu.2015.184.
86. Tripathi, P. *et al.* (2010) 'STAT5 is critical to maintain effector CD8+ T cell responses', *Journal of Immunology (Baltimore, Md.: 1950)*, 185(4), pp. 2116–2124. doi:10.4049/jimmunol.1000842.
87. Tsujimoto, Y., Ikegaki, N. and Croce, C.M. (1987) 'Characterization of the protein product of bcl-2, the gene involved in human follicular lymphoma', *Oncogene*, 2(1), pp. 3–7.
88. Valentin, R., Grabow, S. and Davids, M.S. (2018) 'The rise of apoptosis: targeting apoptosis in hematologic malignancies', *Blood*, 132(12), pp. 1248–1264. doi:10.1182/blood-2018-02-791350.
89. Vorechovský, I. *et al.* (1997) 'Clustering of missense mutations in the ataxia-

- telangiectasia gene in a sporadic T-cell leukaemia', *Nature Genetics*, 17(1), pp. 96–99. doi:10.1038/ng0997-96.
90. Wahnschaffe, L. *et al.* (2019) 'JAK/STAT-Activating Genomic Alterations Are a Hallmark of T-PLL', *Cancers*, 11(12). doi:10.3390/cancers11121833.
91. Wiktor-Jedrzejczak, W. *et al.* (2019) 'EBMT prospective observational study on allogeneic hematopoietic stem cell transplantation in T-prolymphocytic leukemia (T-PLL)', *Bone Marrow Transplantation*, 54(9), pp. 1391–1398. doi:10.1038/s41409-019-0448-x.
92. Willis, S.N. *et al.* (2007) 'Apoptosis initiated when BH3 ligands engage multiple Bcl-2 homologs, not Bax or Bak', *Science (New York, N.Y.)*, 315(5813), pp. 856–859. doi:10.1126/science.1133289.
93. Yamasaki, S. *et al.* (2019) 'Effect of allogeneic hematopoietic cell transplantation for patients with T-prolymphocytic leukemia: a retrospective study from the Adult Lymphoma Working Group of the Japan Society for hematopoietic cell transplantation', *Annals of Hematology*, 98(9), pp. 2213–2220. doi:10.1007/s00277-019-03759-y.
94. Zhong, Y. *et al.* (2015) 'Targeting interleukin-2-inducible T-cell kinase (ITK) and resting lymphocyte kinase (RLK) using a novel covalent inhibitor PRN694', *The Journal of Biological Chemistry*, 290(10), pp. 5960–5978. doi:10.1074/jbc.M114.614891.

BH3 profiling allows to functionally characterize T-cell prolymphocytic leukemia and to identify innovative therapeutic options.

Caractérisation fonctionnelle par profilage BH3 de la leucémie prolymphocytaire T et appliquée à la recherche de nouvelles options thérapeutiques.

Abstract:

Conventional therapies for patients with T-cell prolymphocytic leukemia (T-PLL), such as cytotoxic chemotherapy and alemtuzumab, have limited efficacy and considerable toxicity. Several novel agent classes have demonstrated preclinical activity in T-PLL, including inhibitors of the JAK/STAT and T-cell receptor pathways, as well as histone deacetylase (HDAC) inhibitors. Recently, the BCL-2 inhibitor venetoclax also showed some clinical activity in T-PLL. A first step was to perform a conventional drug screening with a measure of the metabolism of the cells with CellTiter-Glo. Venetoclax was used in pairwise combination with 25 selected drugs. This assay revealed ibrutinib as the most potent partner in primary T-PLL samples. Two patients were treated with this combination, with only a transient response to therapy. Then we sought to characterize functional apoptotic dependencies in T-PLL to identify a novel combination therapy in this disease. Twenty-four samples from patients with primary T-PLL were studied by using BH3 profiling, a functional assay to assess the propensity of a cell to undergo apoptosis (priming) and the relative dependence of a cell on different antiapoptotic proteins.

Primary T-PLL cells had a relatively low level of priming for apoptosis and predominantly depended on BCL-2 and MCL-1 proteins for survival. Selective pharmacologic inhibition of BCL-2 or MCL-1 induced cell death in primary T-PLL cells. Targeting the JAK/STAT pathway with the JAK1/2 inhibitor ruxolitinib or HDAC with belinostat both independently increased dependence on BCL-2 but not MCL-1, thereby sensitizing T-PLL cells to venetoclax. Based on these results, we treated 2 patients with refractory T-PLL with a combination of venetoclax and ruxolitinib. We observed a deep response in JAK3-mutated T-PLL and a stabilization of the nonmutated disease.

Our functional, precision-medicine-based approach identified inhibitors of HDAC and the JAK/STAT pathway as promising combination partners for venetoclax, warranting a clinical exploration of such combinations in T-PLL.

Thèse de Science soutenue par Charles Herbaux le 01 décembre 2021